Supporting information

Cost-efficient and user-friendly $^{17}O/^{18}O$ labeling procedures of fatty acids using mechanochemistry

J. Špačková, C. Fabra, G. Cazals, M. Hubert-Roux, I. Schmitz-Afonso, I. Goldberga,

D. Berthomieu, A. Lebrun, T.-X. Métro*, D. Laurencin*

TABLE OF CONTENTS

A) MATERIALS AND METHODS

A1) Reagents

The following reagents were used as received: stearic acid ($C_{18}H_{36}O_2$, Sigma-Aldrich, 95%, noted here SA), palmitic acid ($C_{16}H_{32}O_2$, Sigma, ≥ 99%, noted here PA), myristic acid ($C_{14}H_{28}O_2$, Sigma, ≥ 99%, noted here MA), lauric acid ($C_{12}H_{24}O_2$, Acros Organics, 99%, noted here LauA), linoleic acid ($C_{18}H_{32}O_2$, Sigma, ≥ 99%, noted here LA), α-linolenic acid ($C_{18}H_{30}O_2$, Sigma, ≥ 99%, noted here ALA), arachidonic acid ($C_{20}H_{32}O_2$, Sigma, > 95%, noted here AA), ethyl-linolenate ($C_{20}H_{34}O_2$, Sigma, ≥ 98%), 1,1'-carbonyldiimidazole ($C_7H_6N_4O$, TCI, > 97%, noted here CDI), potassium carbonate anhydrous (K_2CO_3, Alfa Aesar, 99%), sodium ethanolate (C_2H_5ONa, Sigma-Aldrich, 95%). Ethyl-eicosapentaeonate ($C_{22}H_{34}O_2$) and ethyl-docosahexaeonate ($C_{24}H_{36}O_2$) were kindly offered by Dr Céline Crauste (IBMM, Montpellier). Reagent grade solvents were used in all purification protocols.

^{17}O-labeled water with ~ 90% ^{17}O-enrichment was purchased from CortecNet.

^{18}O-labeled water was purchased from Eurisotop (its isotopic composition, as indicated in the certificate of analysis, is 97.1 % ^{18}O, 1.1 % ^{17}O, 1.8 % ^{16}O) or CortecNet (its isotopic composition, as indicated in the certificate of analysis, is 97.1 % ^{18}O, 1.4 % ^{17}O, 1.5 % ^{16}O).

A2) Synthetic equipment

Milling treatments were carried out in a Retsch Mixer Mill 400 apparatus, using 10 mL or 5 mL screw-type stainless steel grinding jars, containing 10 mm or 7 mm diameter stainless steel beads or in a Fritsch mini-mill Pulverisette 23 apparatus, using 5 mL screw-type Teflon jar containing one 10 mm diameter Teflon-coated bead. All protocols were first tested using non-labeled water and then optimized using ^{18}O-labeled water, before performing experiments with ^{17}O-labeled H_2O.

Zirconia milling jars and beads were not employed in the enrichment protocols of saturated fatty acids described below. Indeed, zirconia being a less dense material than stainless steel, longer milling times would probably be required to complete hydrolysis, during which more debris could shed off the milling equipment. This could imply a simultaneous loss of enrichment in the final material, because we have shown that zirconia particles can be labeled in ^{17}O using mechanochemistry.[1]

A3) Characterization protocols

Infrared (IR) spectra were recorded on a Perkin Elmer Spectrum 2 FT-IR instrument. The attenuated total reflectance (ATR) measurement mode was used (diamond crystal), and measurements were performed in the 400-4000 cm^{-1} range.

Powder XRD analyses were carried out on a X'Pert MPD diffractometer using Cu $K_{\alpha 1}$ radiation (λ = 1.5406 Å) with the operation voltage and current maintained at 40 kV and 25 mA, respectively. Diffractograms were recorded between 5°and 60° in 2θ, with step size of 0.017°, and a time per step of 40 s.

Melting points were measured on BÜCHI Melting Point B-540 instrument with temperature gradient 2 °C/1 min.

EDXS analyses were carried out on a Zeiss Evo HD15 scanning electron microscope equipped with an Oxford Instruments X-MaxN SDD 50 mm2 EDX detector. Powdered samples were deposited on double sided conducting carbon tape.

Mass spectrometry (MS) analyses were performed on a Waters Synapt G2-S apparatus, using electrospray ionization in negative or positive mode in a range of 50-1500 Da. Capillary and cone voltage were 2000 V and 30 V, respectively. The source temperature was 100 °C and desolvation

temperature was set to 50°C. Data were processed by MassLynxV4.1 software. For each product three solutions were prepared (in acetonitrile or methanol, depending on the solubility), which were analyzed five-times by ESI-MS.

The ^{18}O-enrichement levels (EL) were estimated based on the calculation of an apparent average atomic weight for oxygen in the isolated phase, from which enrichment level per carboxylic oxygen was subsequently derived using ^{18}O enrichment and $^{18}O/^{17}O$ isotopic ratio of the labeled water. Reported error bars for ^{18}O labeling correspond to the standard deviation between different synthetic batches, each batch having been analyzed 5 times. Error bars for ^{17}O labeling were estimated to ~1-3%.

Enrichment yields (EY) correspond to the ratio between the average enrichment level per carboxylic oxygen determined by MS and the maximum average enrichment level per carboxylic oxygen which could have been obtained, considering the composition of enriched water used for the hydrolysis, and assuming that each carboxylic group is enriched on one of the 2 oxygen atoms (based on the hydrolysis of the acyl-imidazole intermediate, or the saponification of the ester).

LC-MS (liquid chromatography-mass spectrometry) analyses were done using an Acquity H-Class (Waters) system equipped with a Kinetex EVO C18 column (1.7 µm particle size, 50 x 2.1 mm, Phenomenex). Mobile phase A consisted of water while mobile phase B was acetonitrile, both containing 0.1% formic acid. The gradient started at 50% mobile phase B and increased to 100% mobile phase B over 5 min. After holding for 2 min the gradient returned to 50% B before re-equilibration for 3 min, to give a total run time of 10 min. The flow rate was 0.2 mL/min and the eluent was directed to the atmospheric pressure ionization source of a Synapt G2-S (Waters) operating under the conditions described above.

Ultra-high resolution mass spectrometry analyses were carried out on a FTICR instrument (SolariX XR FTMS, Bruker Daltonics) equipped with a 12 Tesla superconducting magnet and a dynamically harmonized ICR cell. The instrument is equipped with an electrospray (ESI) ionization source. Each sample was diluted in methanol, introduced in the ESI source at 200 µL/hr and analyzed in negative ion mode. Source parameters were as follows: nebulizer gas: 1 bar, dry gas 3 L/min and dry temperature 200 °C. Acquisition was realized with a 1.4 s transient length, with an accumulation time of 0.02 s and 50 scans accumulation. Resolution was 500 000 at *m/z* 277. FTICR-MS data were treated with Data Analysis 5.0 (Bruker). Molecular formulae were attributed considering $[M–H]^-$ deprotonated molecules. Isotopic fine structures were deciphered including ^{13}C and ^{18}O isotopes.

^1H and ^{13}C solution NMR spectra were recorded on an Avance III Bruker 600 MHz NMR spectrometer equipped with a TCI Prodigy cryoprobe or on an Avance III Bruker 500 MHz NMR spectrometer equipped with a BBO Helium cryoprobe, using DMSO-d_6 as a solvent. Chemical shifts were referenced to the residual solvent peaks at 2.50 ppm (^1H NMR spectra) and 39.52 ppm (^{13}C NMR spectra).

^{17}O solid state NMR experiments were performed on a VNMRS 600 MHz (14.1 T) NMR spectrometer, using a 3.2 mm probe tuned to ^1H (599.82 MHz) and ^{17}O (81.31 MHz). Two types of probes were used, depending on the availability of the equipment: a 3.2 mm Varian HX probe, or a 3.2 mm Varian HXY probe equipped with a 3.2 mm probe head. Spectra were recorded under MAS (Magic Angle Spinning) conditions, using a spinning frequency 16 kHz. ^{17}O NMR experiments were recorded using DFS (Double Frequency Sweep)[2] excitation scheme followed by a rotor-synchronized echo (one rotor period, 62.5 µs delay) to enhance the ^{17}O signal. The parameters were as following: DFS pulse of 500 µs, with sweep between 200 and 80 kHz, followed by a 90° ”solid” pulse of 2 µs and a 180° pulse of 4 µs. ^1H decoupling (RF ~62.5 kHz) (SPINAL-64) was applied during acquisition. More details on acquisition conditions are reported in Table A1. ^{17}O chemical shifts were referenced to D_2O at -2.7 ppm (which corresponds to tap-water at 0 ppm).

Table A1: ^{17}O solid state NMR acquisition parameters.

Sample	Figure	MAS frequency [kHz]	Temp. reg. [°C]	Recycle delay (D1) [s]	Acq. time [ms]	Number of scans (NS)	Exp. time
Lauric acid							
LauA	B1-13	16	5 °C	0.8	6	1850	~ 0h30
Myristic acid							
MA	B2-13	16	5 °C	0.8	6	6950	~ 1h30
Palmitic acid							
PA	B3-13	16	5 °C	0.8	20	6950	~ 1h30

B) SYNTHESES AND CHARACTERIZATIONS OF ^{17}O AND ^{18}O-LABELED COMPOUNDS PREPARED VIA CDI-ACTIVATION/HYDROLYSIS PROCEDURE

B1) Lauric acid (LauA, $C_{12}H_{24}O_2$)

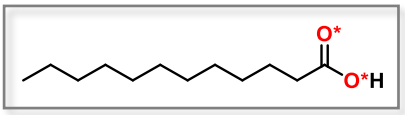

B1-a) Optimized labeling protocol

Lauric acid (79.4 mg, 0.40 mmol, 1.0 eq) and CDI (70.7 mg, 0.44 mmol, 1.1 eq) were introduced into the stainless-steel grinding jar (10 mL inner volume) containing two stainless-steel balls (10 mm diameter). The jar was closed and subjected to grinding for 30 minutes in the MM400 mixer mill operated at 25 Hz. ^{18}O-labeled water (97.1%, 21.5 µL, 1.2 mmol, 3.0 eq) was then added into the jar, and the mixture was subjected to further grinding for 120 minutes at 25 Hz. To help recover the product, non-labeled water (1 mL) was added into the jar, and the content was subjected to grinding for 2 minutes at 25 Hz. Then, the medium ("milky" solution with a foam on top) was transferred to a beaker (together with sufficient amount of non-labeled water (10 mL) used here to rinse the jar). The medium was acidified to pH ~ 1 with an aqueous solution of HCl (6M, 12 drops) and extracted with ethyl acetate (1x20 mL, 3x10 mL). Combined organic phases were dried over Na_2SO_4 and filtered. Solvent was evaporated giving white solid, which was re-dissolved in diethyl ether and finally dried under vacuum to yield the product as white microcrystalline solid. Average yield (n = 3): 64 ± 10 mg, 80 ± 12 %, m. p. 43.7-45.7 °C.

For the ^{17}O-labeling, exactly the same reaction/work-up conditions as for ^{18}O-labeling were employed with 90% ^{17}O-enriched water (21.5 µL, 3.0 eq.) used at the hydrolysis step. After addition of ^{17}O-labeled water, the mixture was subjected to grinding for 150 min at 25 Hz. Yield (n = 1): 68 mg, 85 %.

Figure B1-1: ATR-IR analysis of the starting material, reaction intermediates, and final products. The dashed line shows that the C=O stretching frequency of $^{18}O/^{17}O$-enriched product is shifted to lower wavenumbers in comparison with non-labeled precursor.

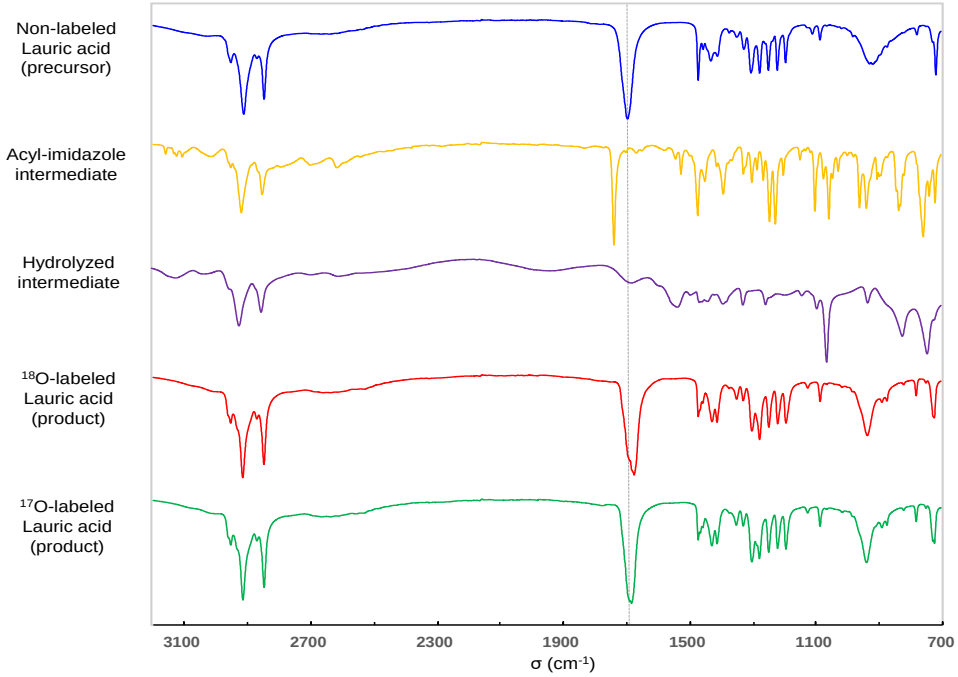

B1-b) Characterization of the ^{18}O-labeled LauA

Figure B1-2: MS analyses of the non-labeled precursor in comparison to the ^{18}O-enriched product. Average enrichment per carboxylic oxygen determined by MS: 46.9 ± 0.5 % (n = 3), enrichment yield: ~ 96 %.

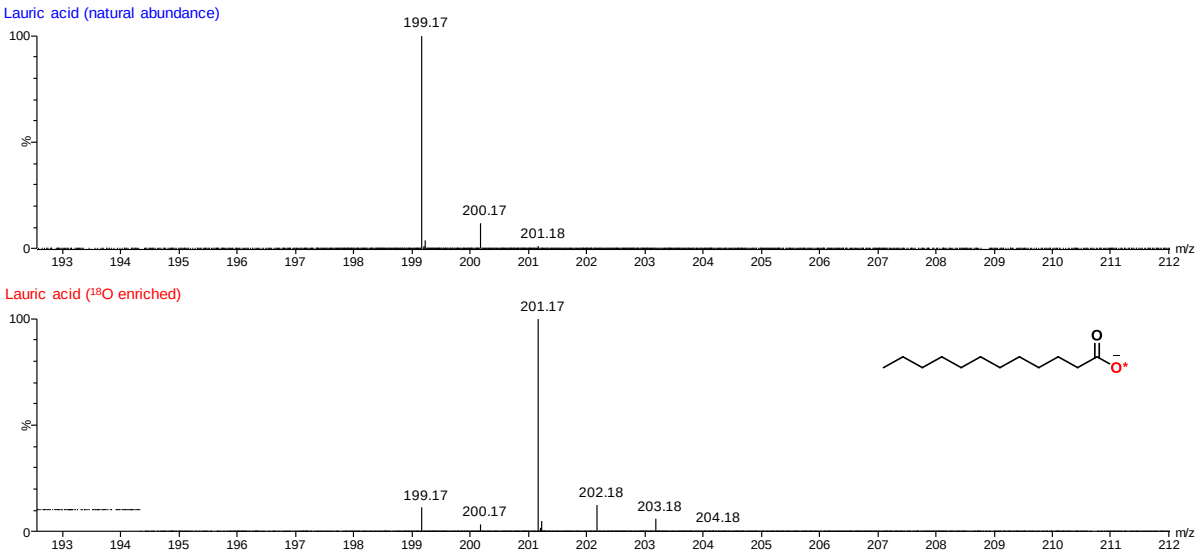

Figure B1-3: LC analyses of the non-labeled precursor in comparison to the ^{18}O-enriched product.

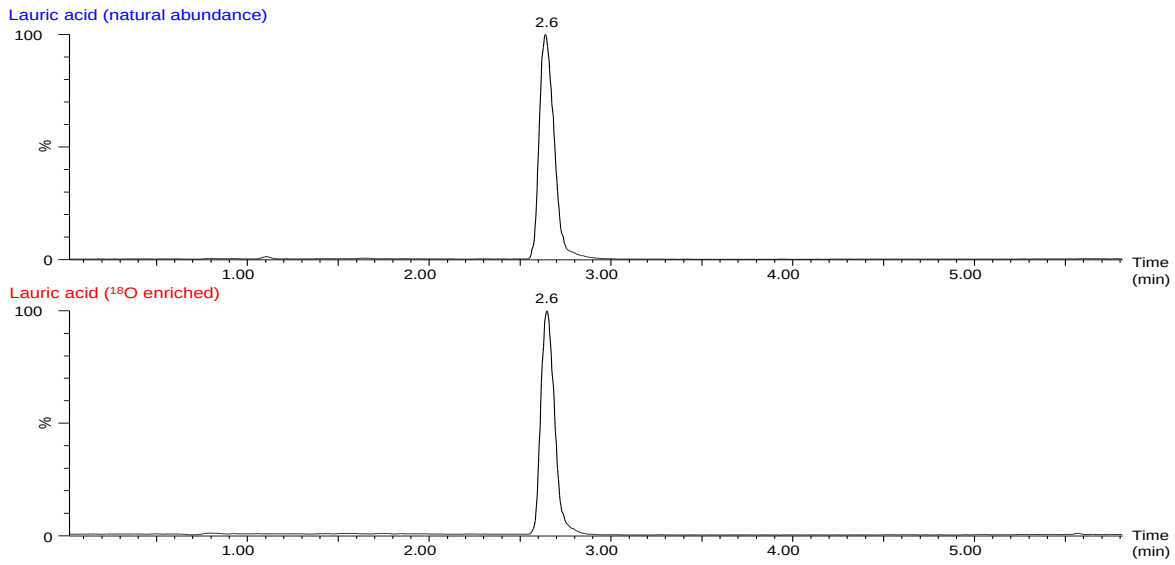

Figure B1-4: ^{1}H NMR spectra of the non-labeled precursor in comparison to the ^{18}O-enriched product (DMSO-d_6, 600 MHz; solvent peaks crossed out).

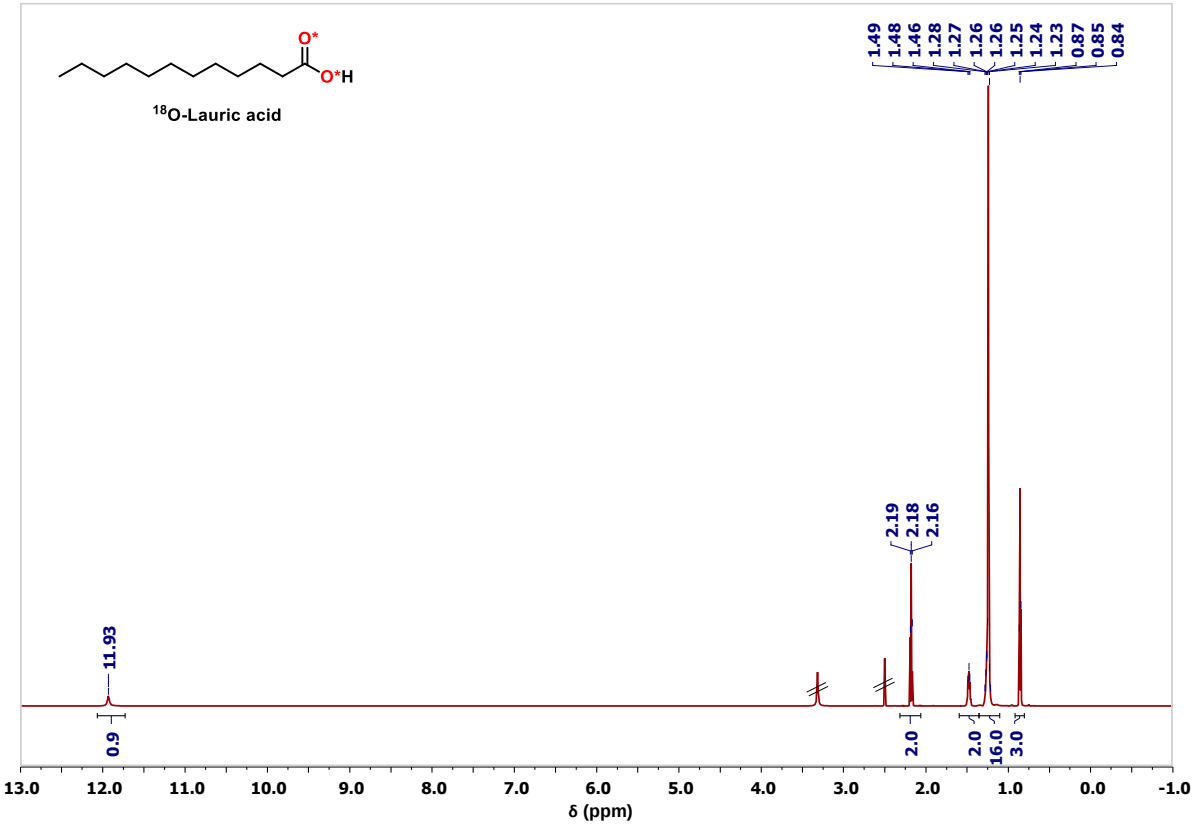

Figure B1-5: ^{13}C NMR spectra of the non-labeled precursor in comparison to the ^{18}O-enriched product (DMSO-d_6, 600 MHz; solvent peaks crossed out).

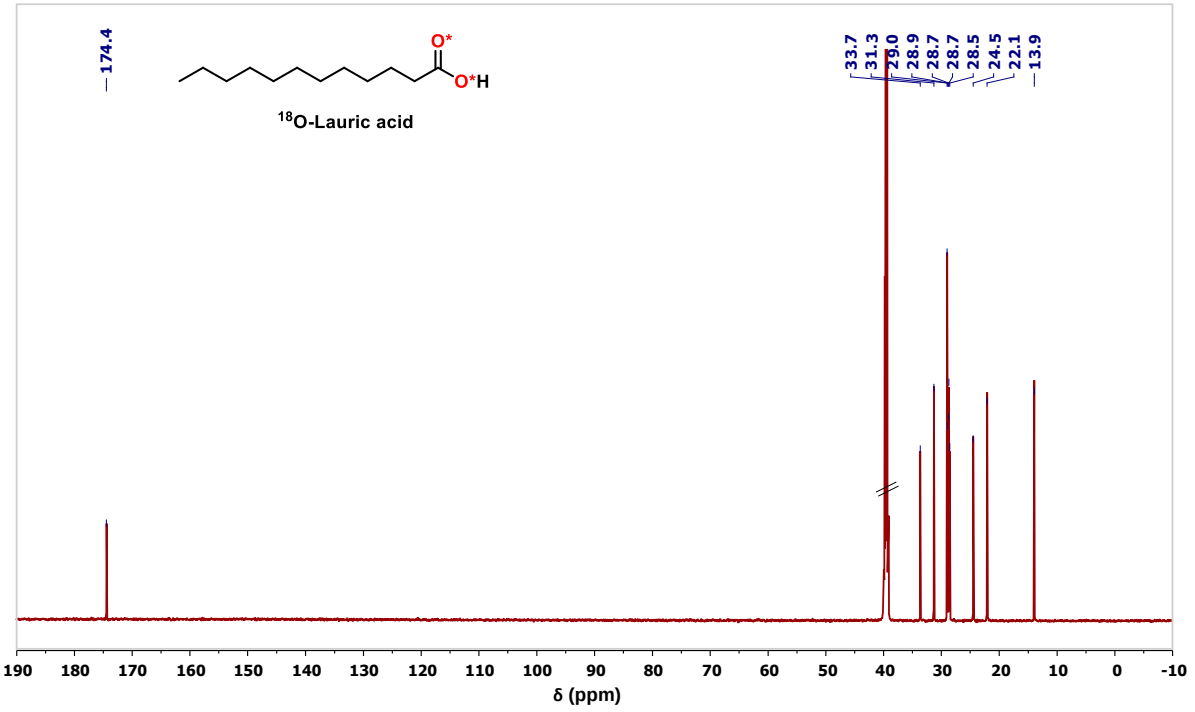

Figure B1-6: XRD powder pattern of the ^{18}O-enriched product in comparison to the simulated powder pattern of lauric acid (CSD-LAURAC05). Experimentally, we have crystallized lauric acid in a form more similar to that of other FAs (e.g. myristic acid), rather than in the one found reported in the CSD database.

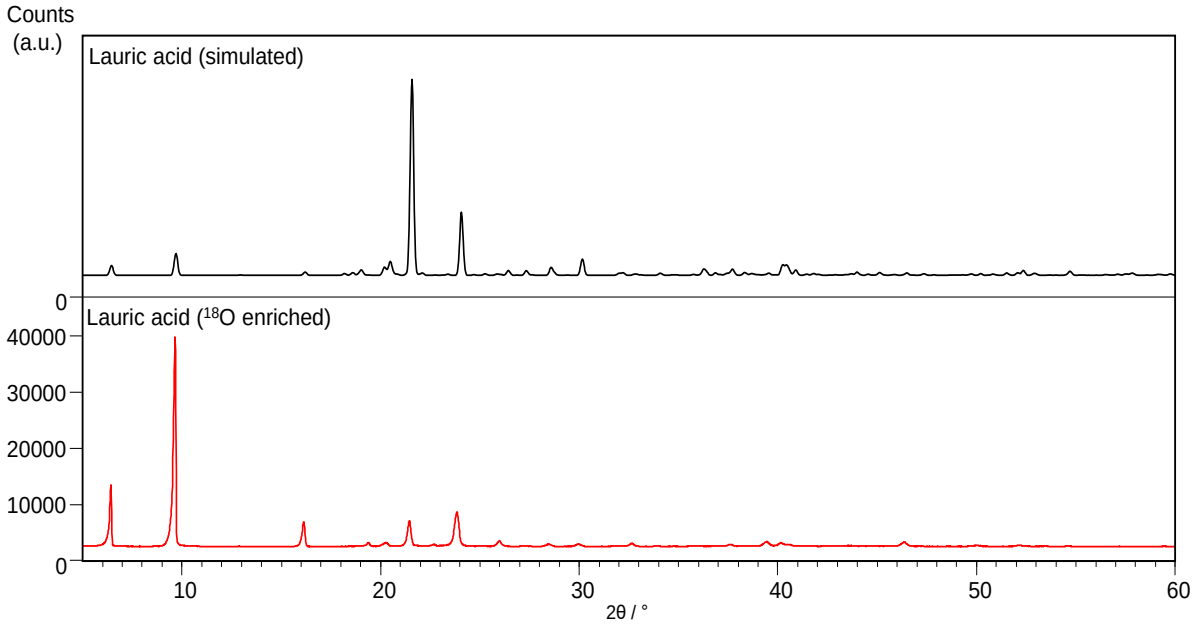

Figure B1-7: ^{13}C NMR study of ^{18}O-isotope effect on the ^{13}C-carboxylic resonance in solution NMR. The non-labeled precursor is compared to the ^{18}O-enriched product, both having been mixed in different ratios, as indicated above each spectrum (DMSO-d_6, 600 MHz).

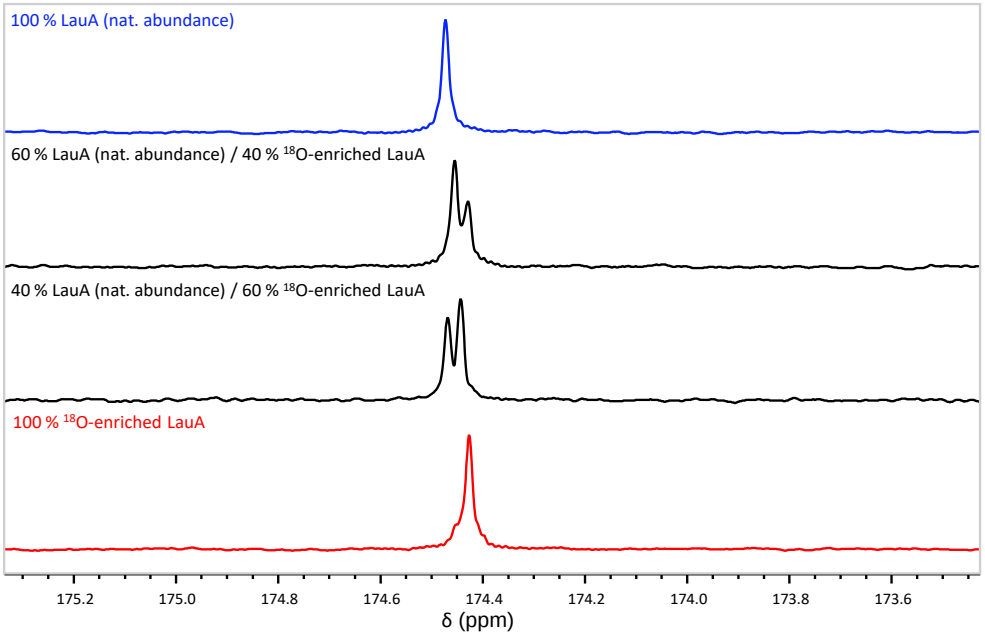

B1-c) Characterization of the ^{17}O-labeled LauA

Figure B1-8: MS analyses of the non-labeled precursor in comparison to the ^{17}O-enriched product. Average enrichment per carboxylic oxygen determined by MS: 44 % (n = 1).

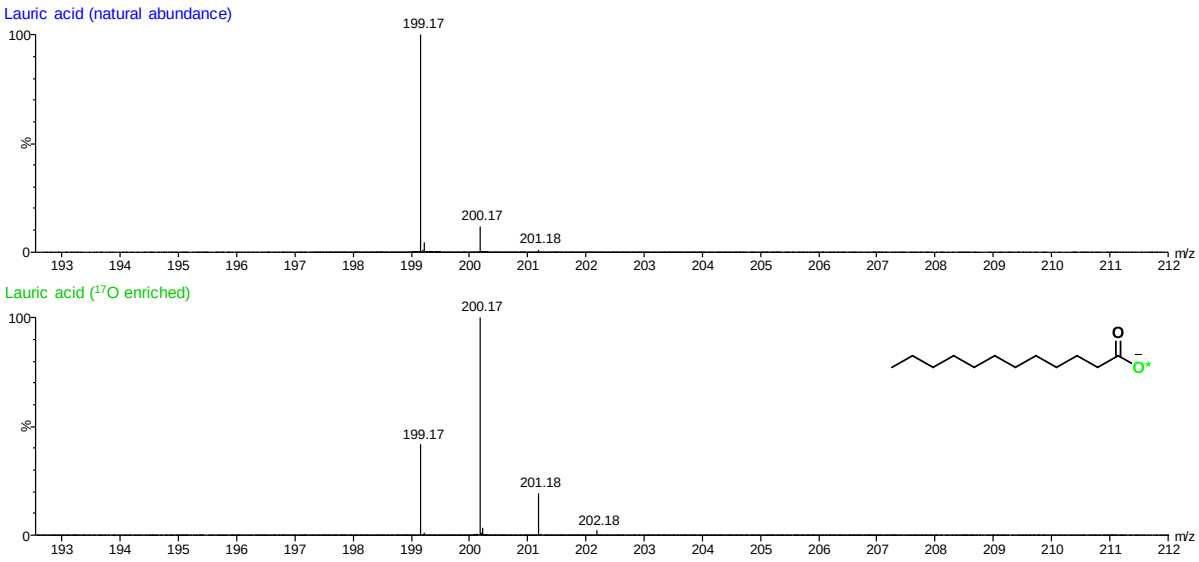

Figure B1-9: LC analyses of the non-labeled precursor in comparison to the ^{17}O-enriched product.

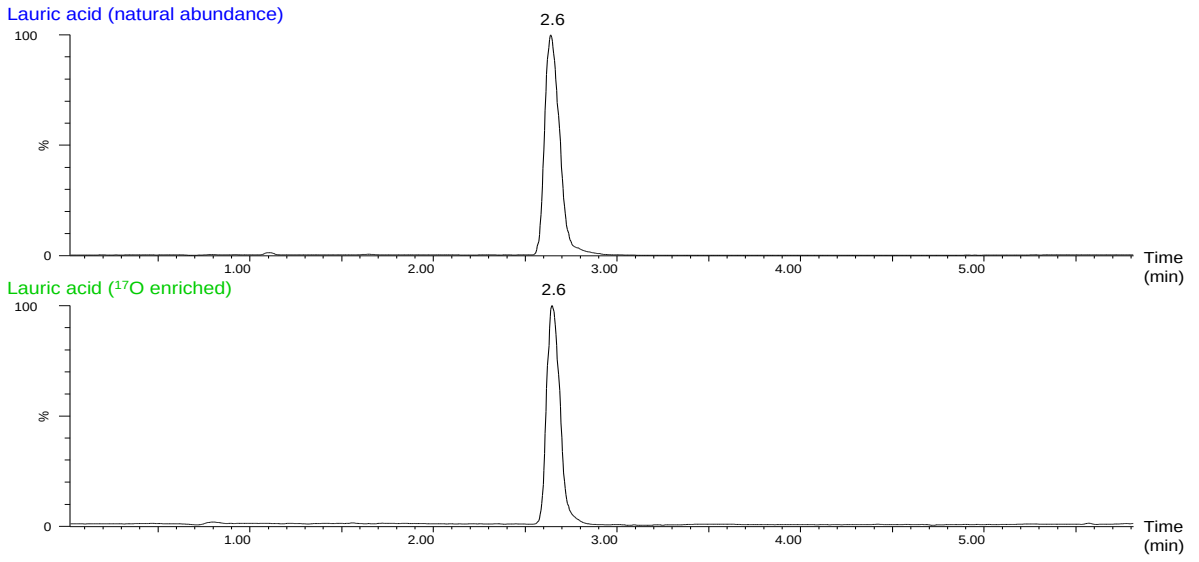

Figure B1-10: ^{1}H NMR spectra of the non-labeled precursor in comparison to the ^{17}O-enriched product (DMSO-d_6, 600 MHz; solvent peaks are crossed out).

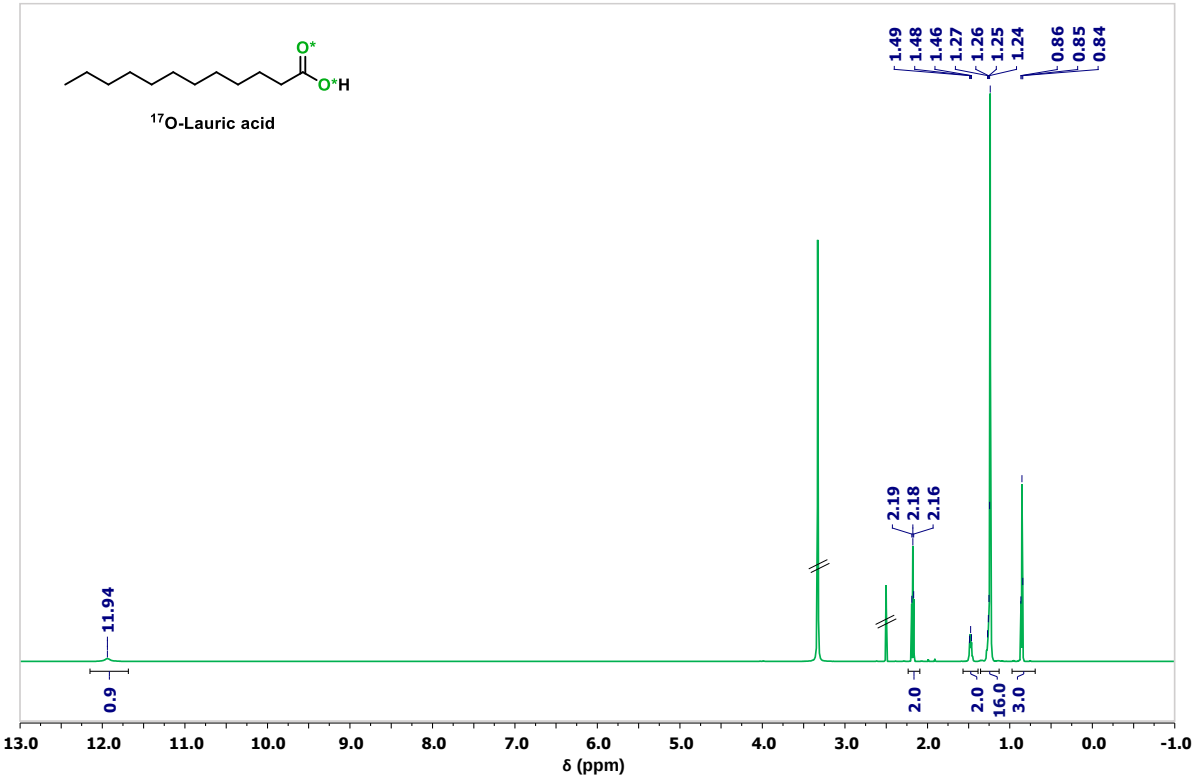

Figure B1-11: ^{13}C NMR spectra of the non-labeled precursor in comparison to the ^{17}O-enriched product (DMSO-d_6, 600 MHz; solvent peaks are crossed out).

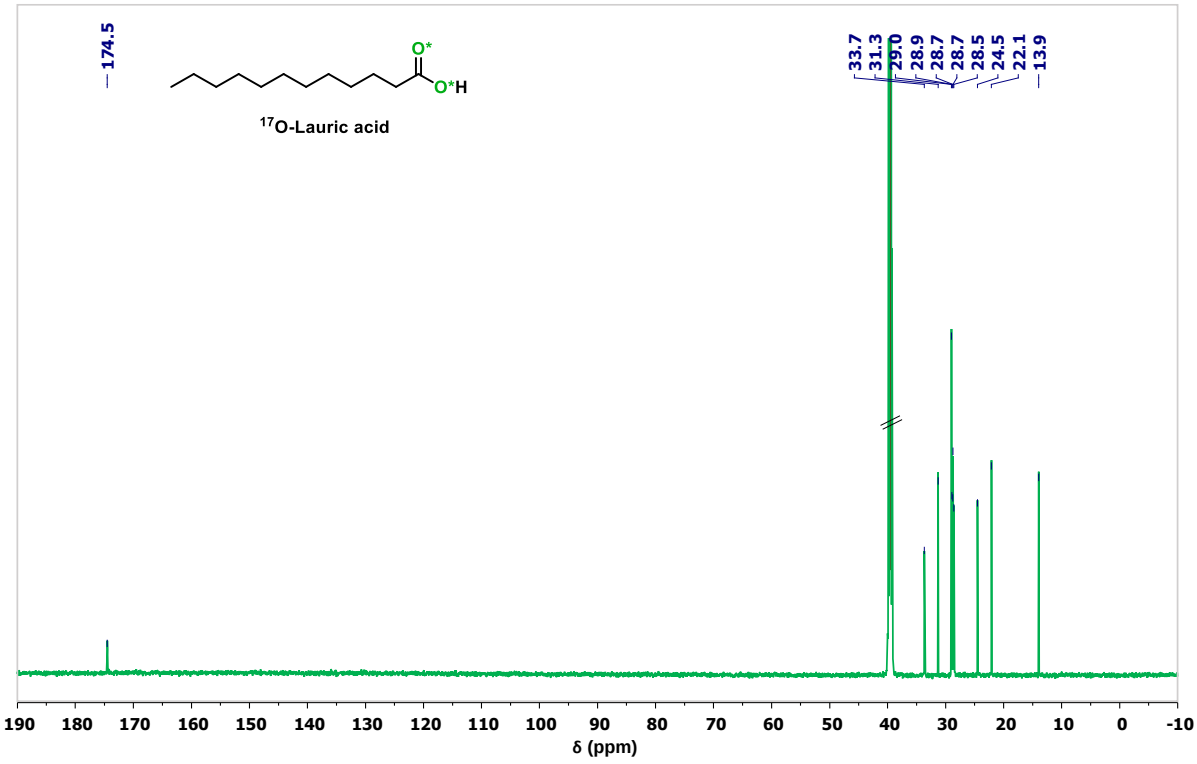

Figure B1-12: XRD powder pattern of the ^{17}O-enriched product in comparison to the simulated powder pattern of lauric acid (CSD-LAURAC05). Experimentally, we have crystallized lauric acid in a form more similar to that of other FAs (e.g. myristic acid), rather than in the one found reported in the CSD database.

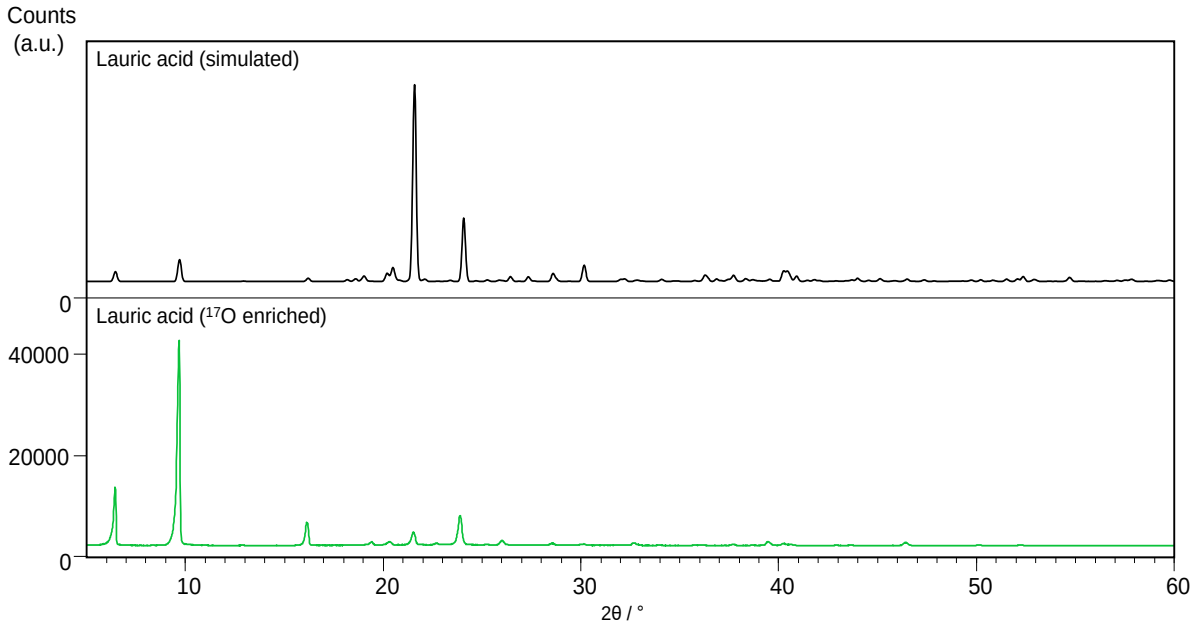

Figure B1-13: ^{17}O MAS NMR spectrum of ^{17}O-labeled LauA (black) and its fit (dashed red line), considering the presence of C=O (green) and C-OH (purple) contributions.

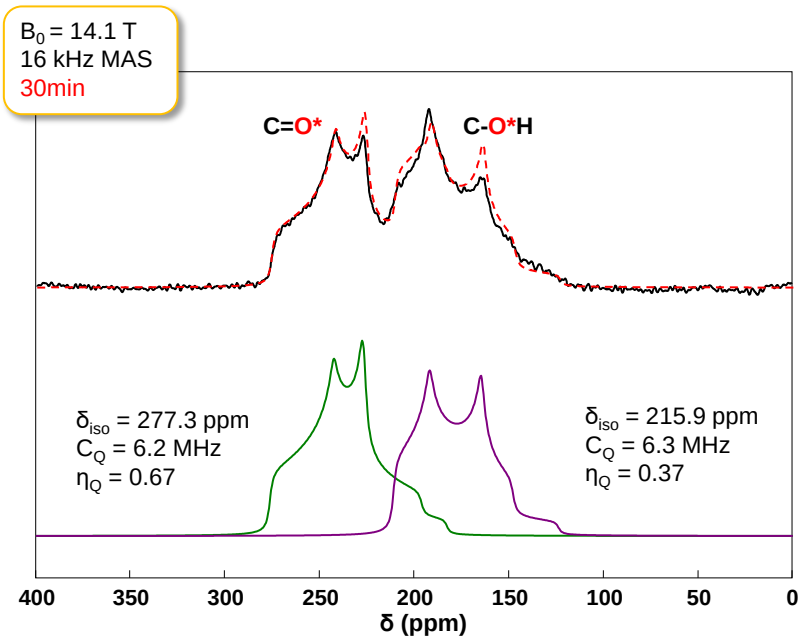

B2) Myristic acid (MA, $C_{14}H_{28}O_2$)

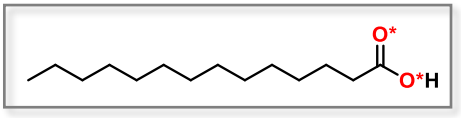

B2-a) Optimized labeling protocol

Myristic acid (84.2 mg, 0.37 mmol, 1.0 eq) and CDI (65.8 mg, 0.41 mmol, 1.1 eq) were introduced into the stainless-steel grinding jar (10 mL inner volume) containing two stainless-steel balls (10 mm diameter). The jar was closed and subjected to grinding for 30 minutes in the MM400 mixer mill operated at 25 Hz. ^{18}O-labeled water (97.1%, 20 µL, 1.1 mmol, 3.0 eq) was then added into the jar, and the mixture was subjected to further grinding for 150 minutes at 30 Hz. To help recover the product, non-labeled water (1 mL) was added into the jar, and the content was subjected to grinding for 2 minutes at 25 Hz. Then, the medium ("milky" solution with a foam on top) was transferred to a beaker (together with sufficient amount of non-labeled water (10-12 mL) used here to rinse the jar). The medium was acidified to pH ~ 1 with an aqueous solution of HCl (6M, 10 drops) and extracted with ethyl acetate (1x20 mL, 3x10 mL). Combined organic phases were washed with HCl (1M, 15 mL), dried over Na_2SO_4 and filtered. Solvent was evaporated giving white solid, which was re-dissolved in diethyl ether and finally dried under vacuum to yield the product as white microcrystalline solid. Average yield (n = 3): 70 ± 4 mg, 82 ± 5 %, m .p. 53.1-55.6 °C.

For the ^{17}O-labeling, exactly the same reaction/work-up conditions as for ^{18}O-labeling were employed with 90% ^{17}O-enriched water (20 µL, 3.0 eq.) used at the hydrolysis step. Yield (n = 1): 63 mg, 75 %.

Figure B2-1: ATR-IR analysis of the starting material, reaction intermediates, and final products. The dashed line shows that the C=O stretching frequency of ^{18}O/^{17}O-enriched product is shifted to lower wavenumbers in comparison with non-labeled precursor.

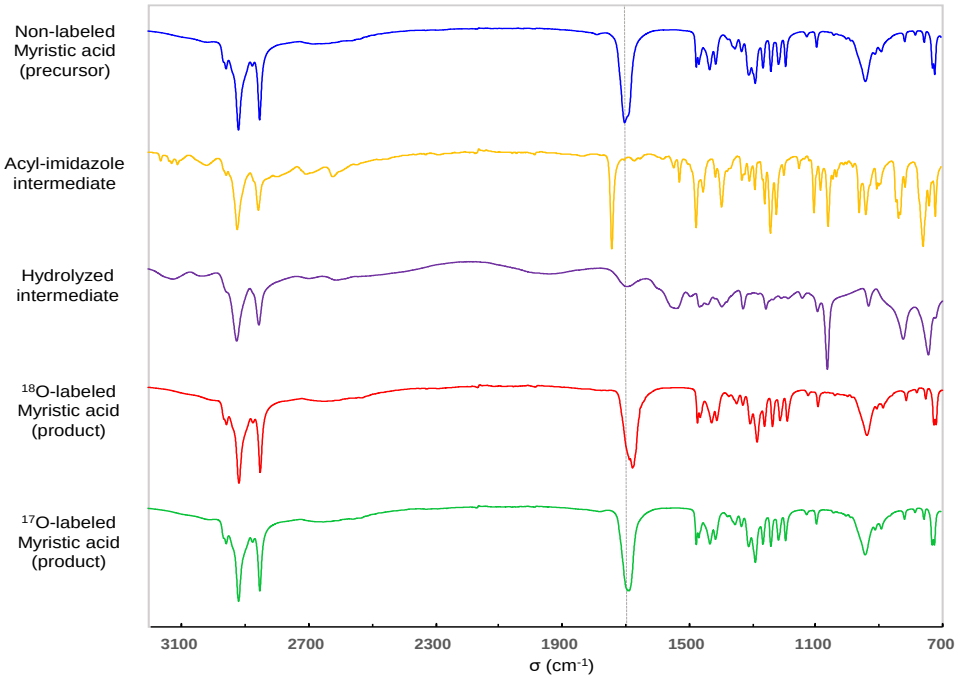

B2-b) Characterization of the ^{18}O-labeled MA

Figure B2-2: MS analyses of the non-labeled precursor in comparison to the ^{18}O-enriched product. Average enrichment per carboxylic oxygen determined by MS: 46.4 ± 0.8 % (n = 3), enrichment yield: ~ 97 %.

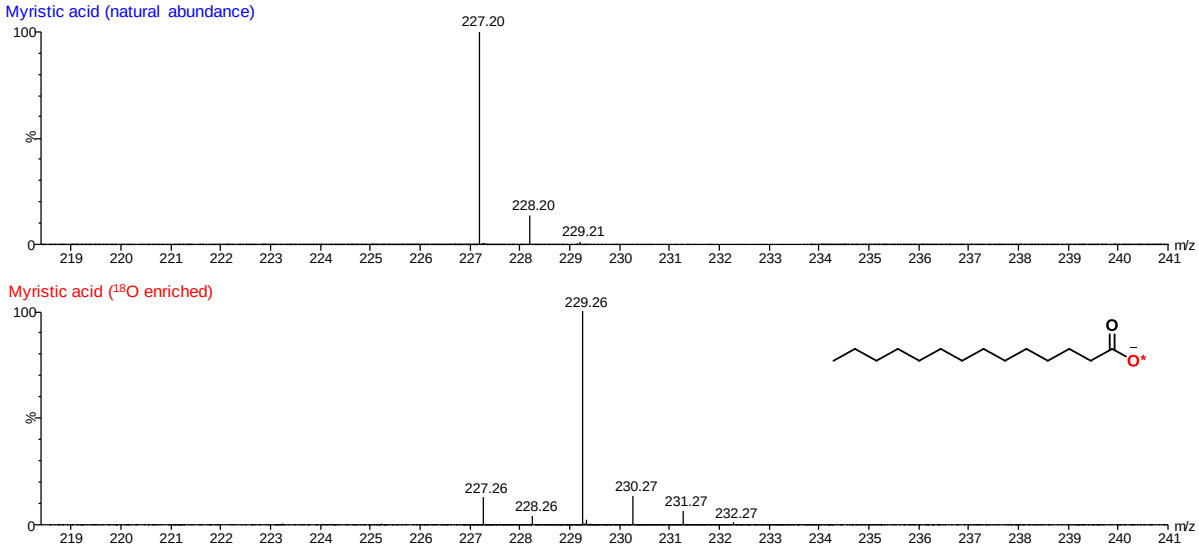

Figure B2-3: LC analyses of the non-labeled precursor in comparison to the ^{18}O-enriched product.

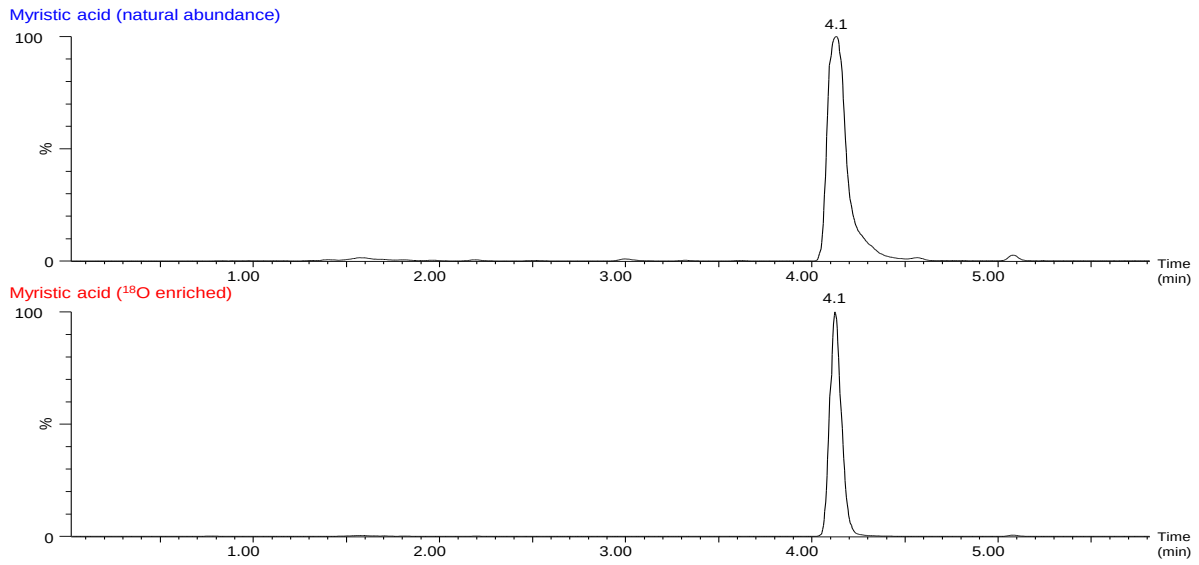

Figure B2-4: ^{1}H NMR spectra of the non-labeled precursor in comparison to the ^{18}O-enriched product (DMSO-d_6, 600 MHz; solvent peaks are crossed out).

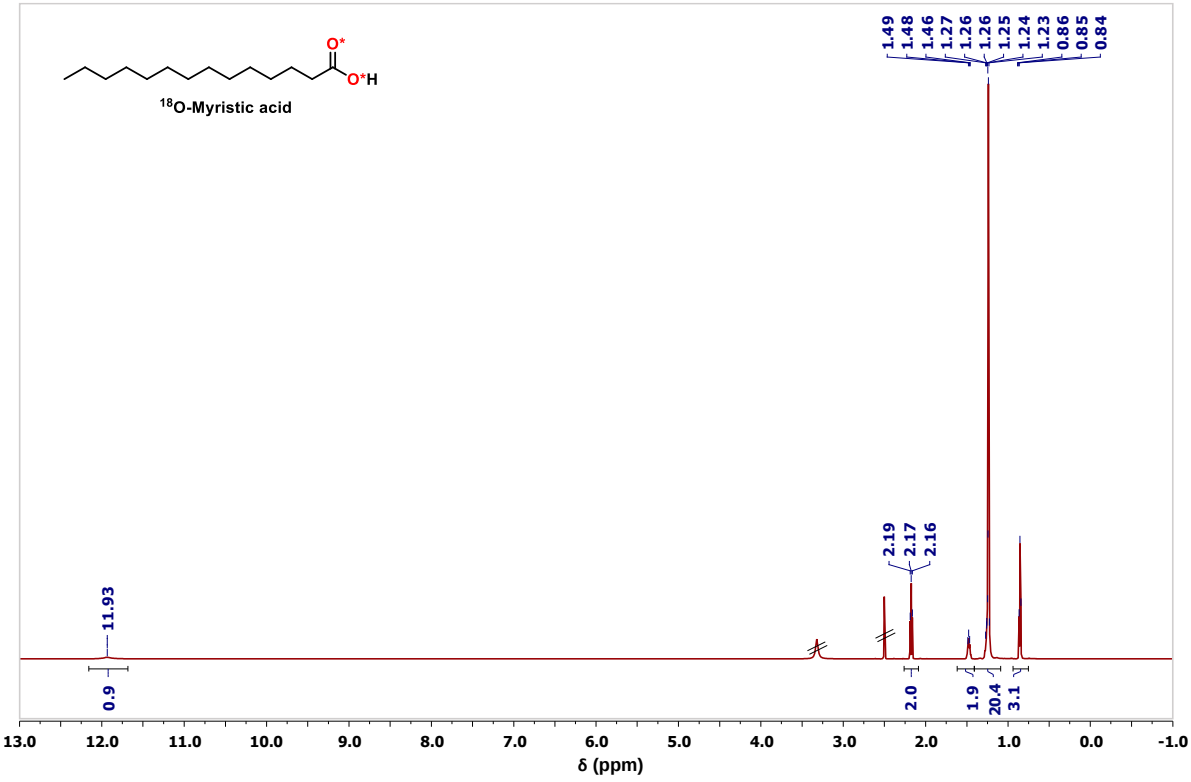

Figure B2-5: ^{13}C NMR spectra of the non-labeled precursor in comparison to the ^{18}O-enriched product (DMSO-d_6, 600 MHz; solvent peaks are crossed out).

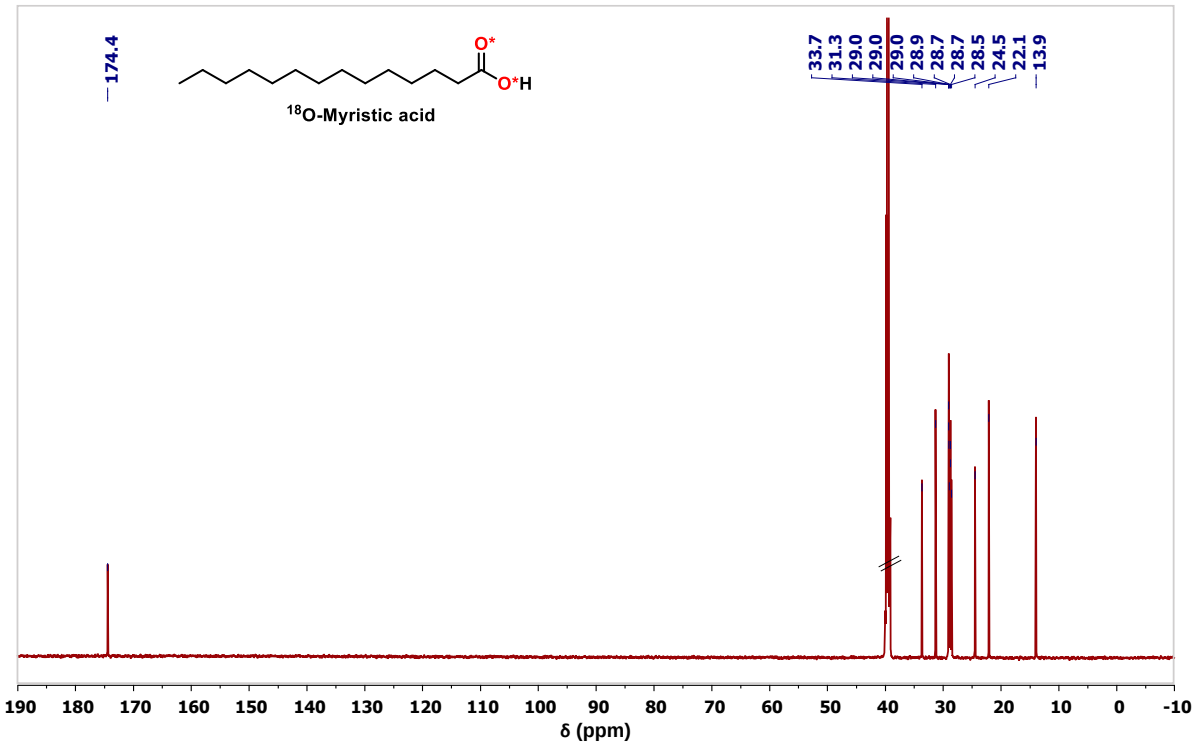

Figure B2-6: XRD powder pattern of the non-labeled precursor in comparison to the ^{18}O-enriched product.

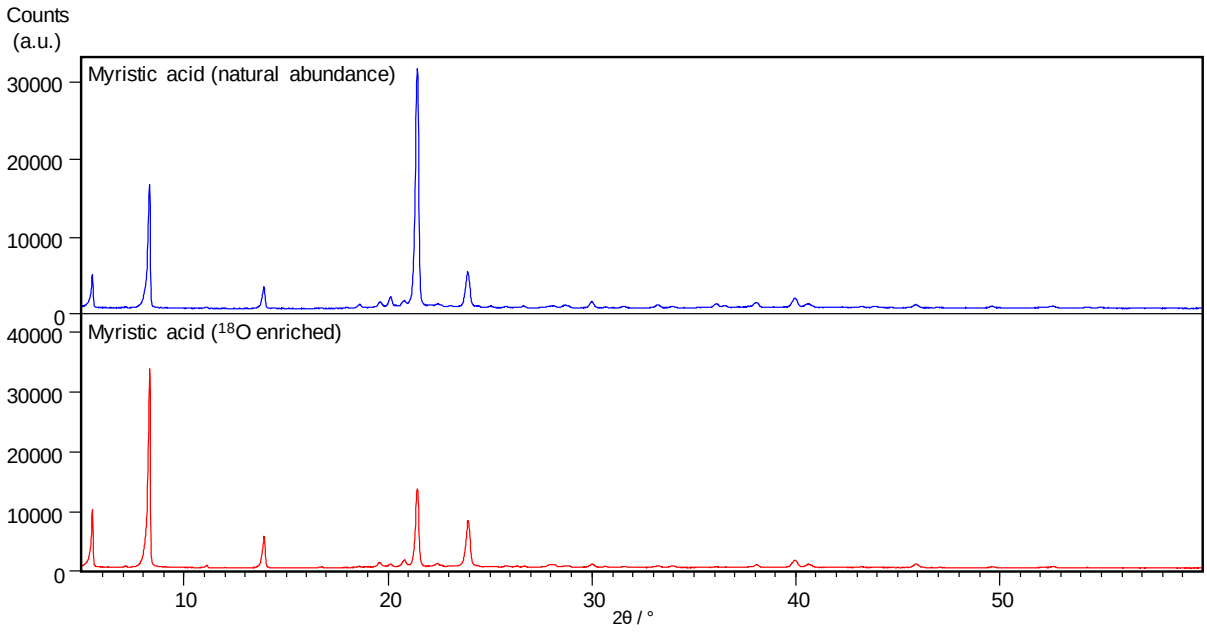

Figure B2-7: ^{13}C NMR study of ^{18}O-isotope effect on the ^{13}C-carboxylic resonance in solution NMR. The non-labeled precursor is compared to the ^{18}O-enriched product, both having been mixed in different ratios, as indicated above each spectrum (DMSO-d_6, 600 MHz).

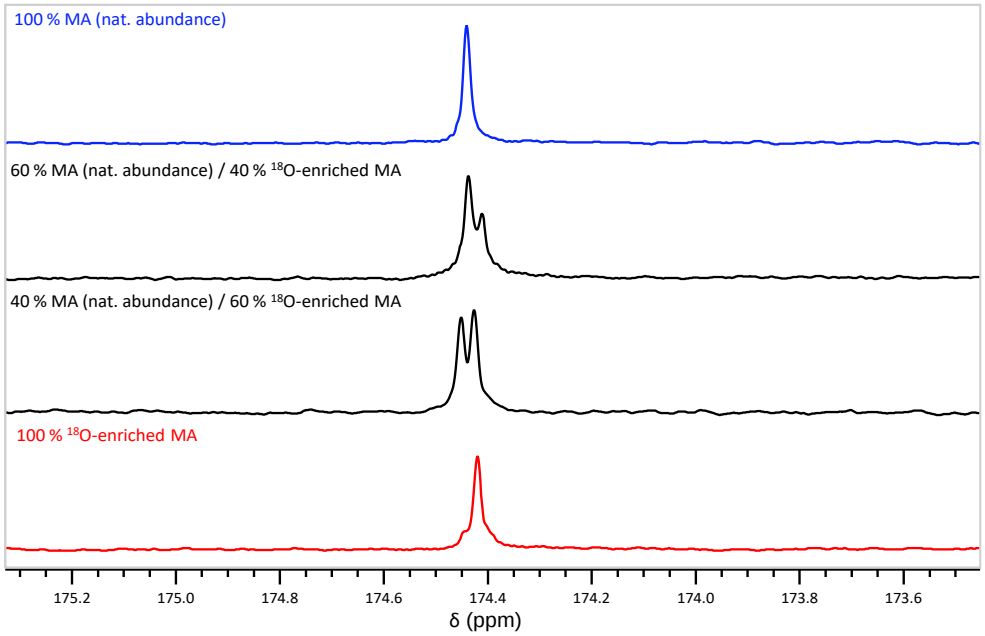

B2-c) Characterization of the ^{17}O-labeled MA

Figure B2-8: MS analyses of the non-labeled precursor in comparison to the ^{17}O-enriched product. Average enrichment per carboxylic oxygen determined by MS: 44 % (n = 1).

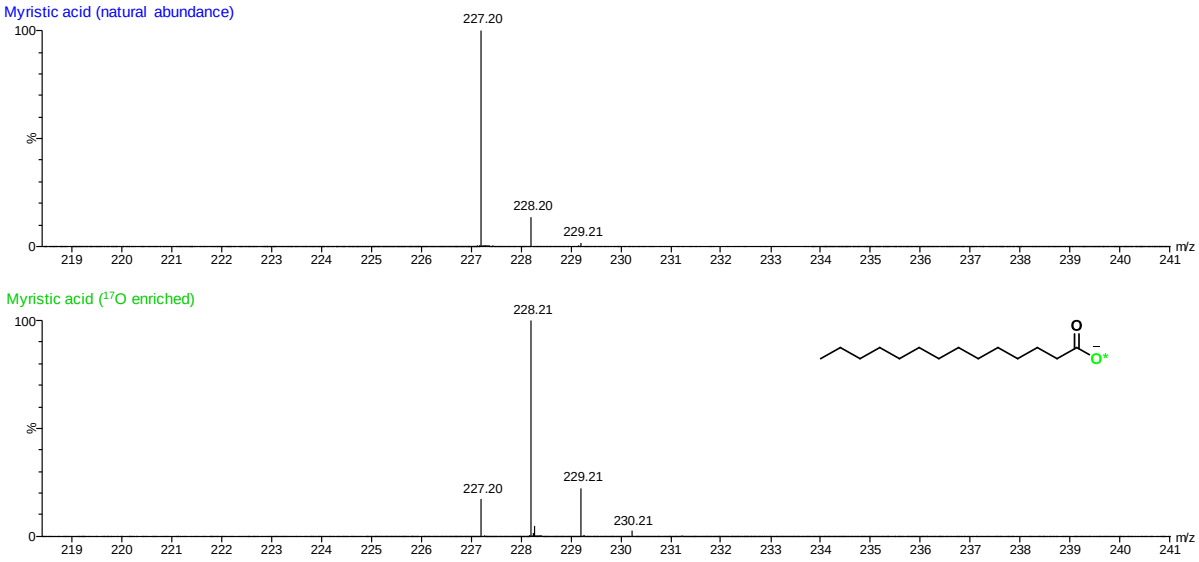

Figure B2-9: LC analyses of the non-labeled precursor in comparison to the ^{17}O-enriched product.

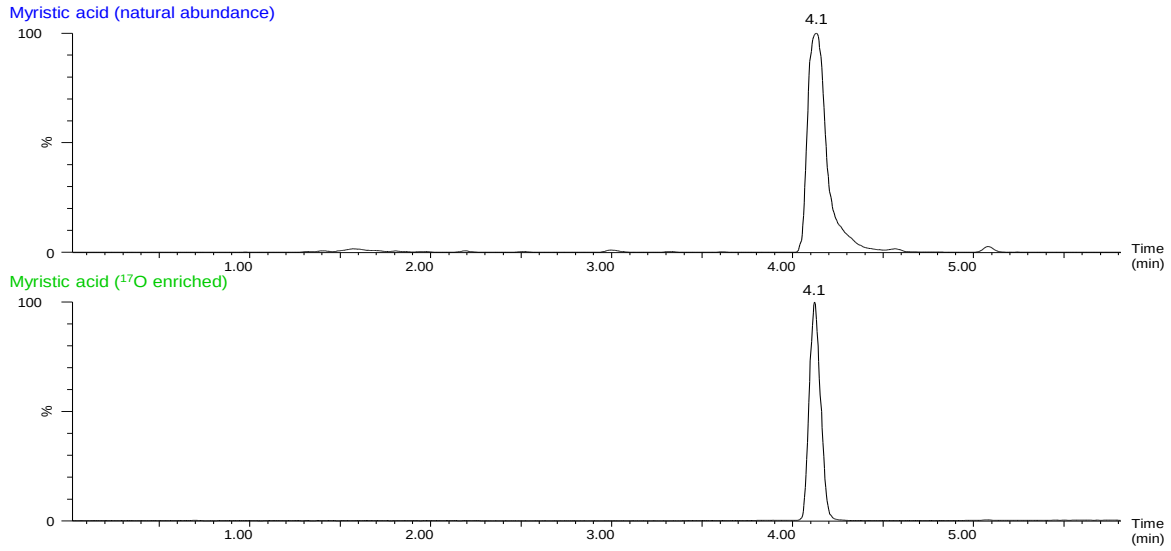

Figure B2-10: ^{1}H NMR spectra of the non-labeled precursor in comparison to the ^{17}O-enriched product (DMSO-d_6, 600 MHz; solvent peaks are crossed out).

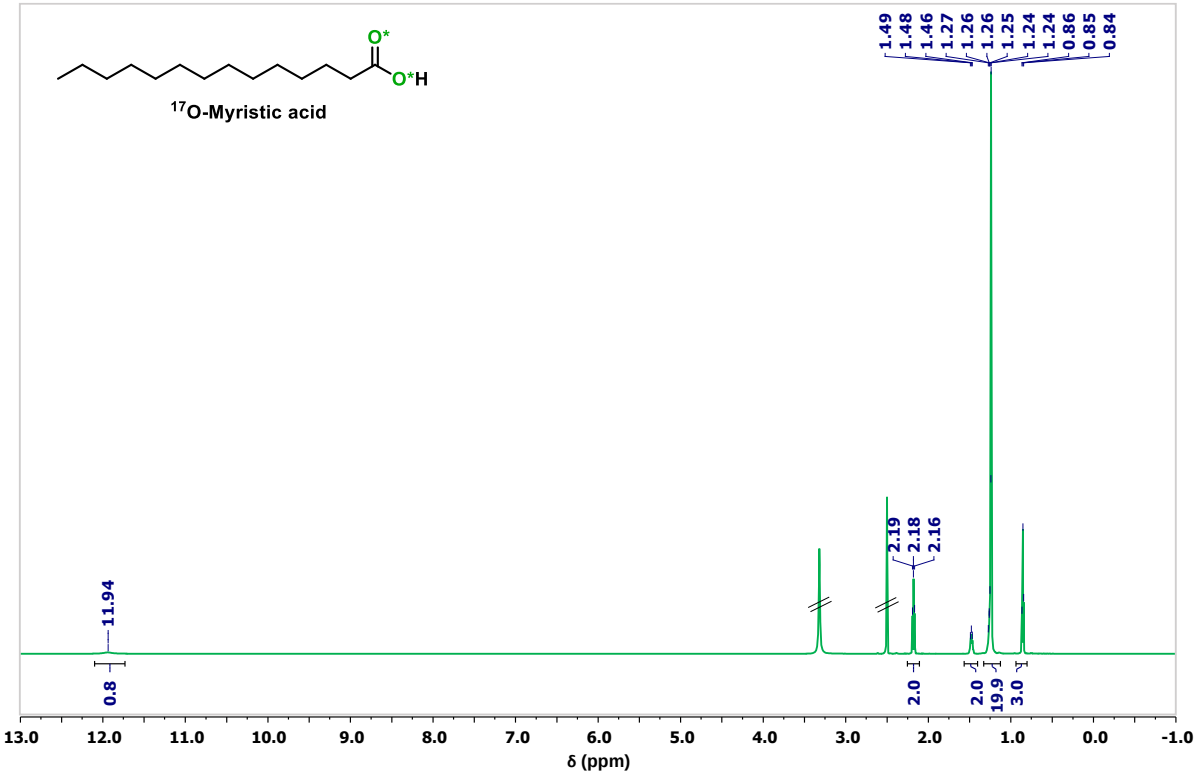

Figure B2-11: ^{13}C NMR spectra of the non-labeled precursor in comparison to the ^{17}O-enriched product (DMSO-d_6, 600 MHz; solvent peaks are crossed out).

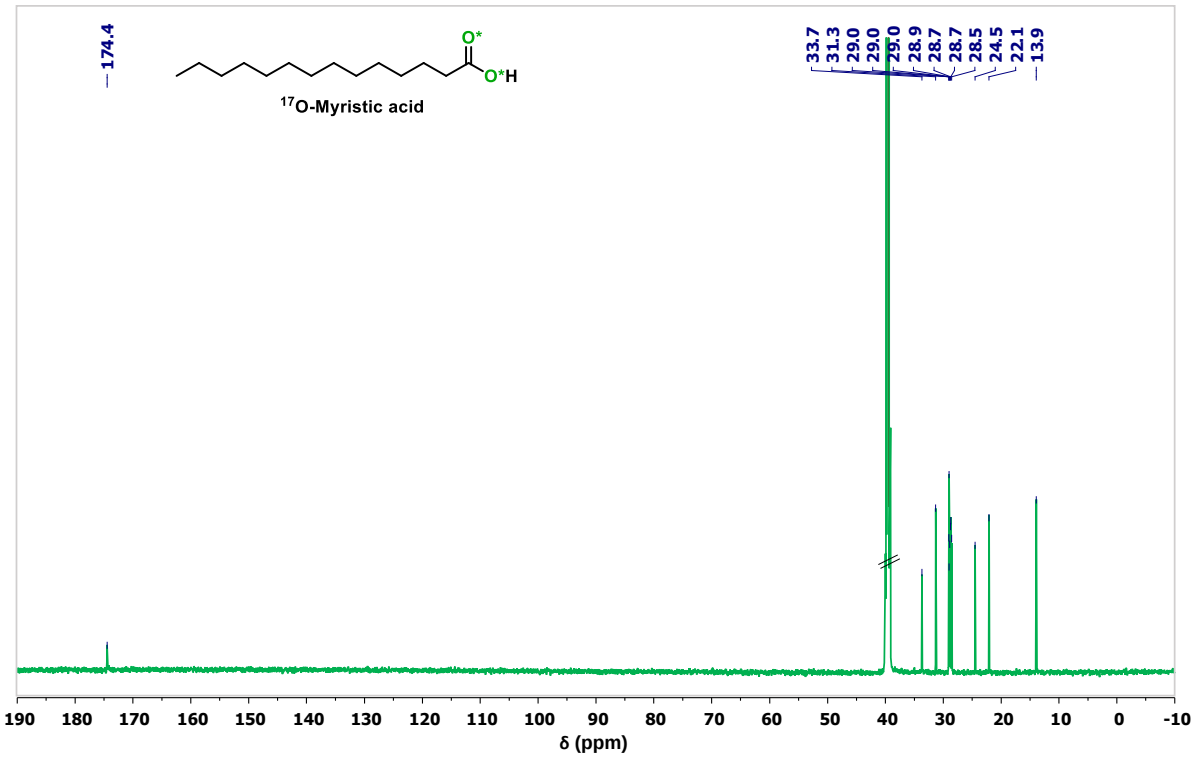

Figure B2-12: XRD powder pattern of the non-labeled precursor in comparison to the ^{17}O-enriched product.

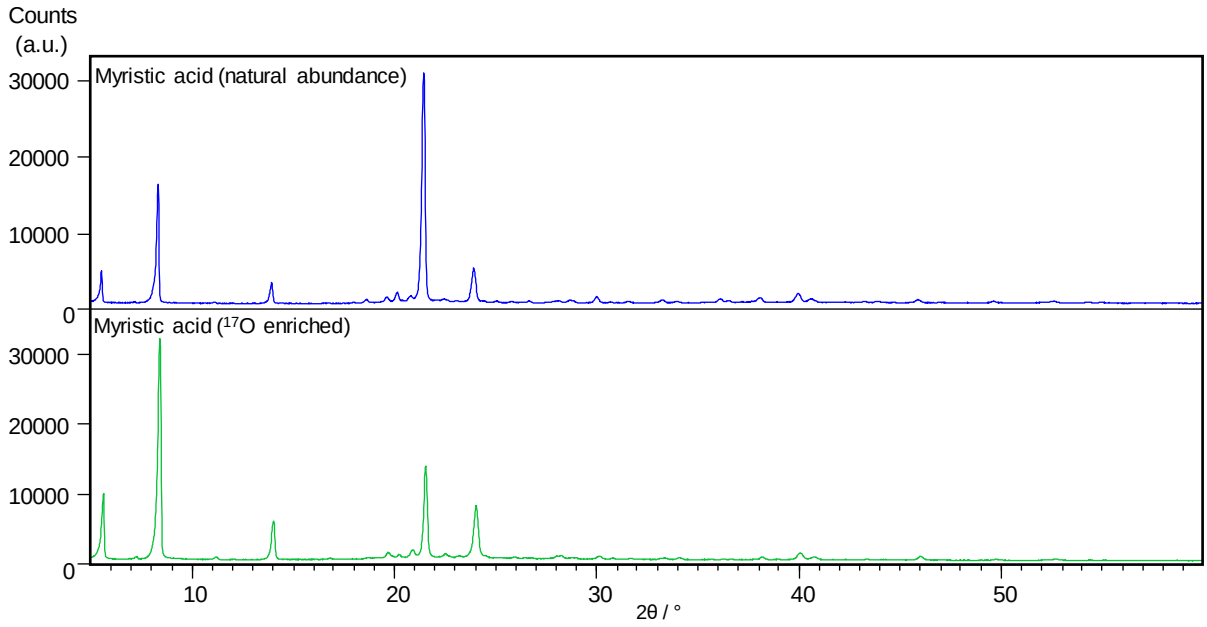

Figure B2-13: ^{17}O MAS NMR spectrum of ^{17}O-labeled MA (black) and its tentative fit (dashed red line), considering the presence of C=O (green) and C-OH (purple) contributions.

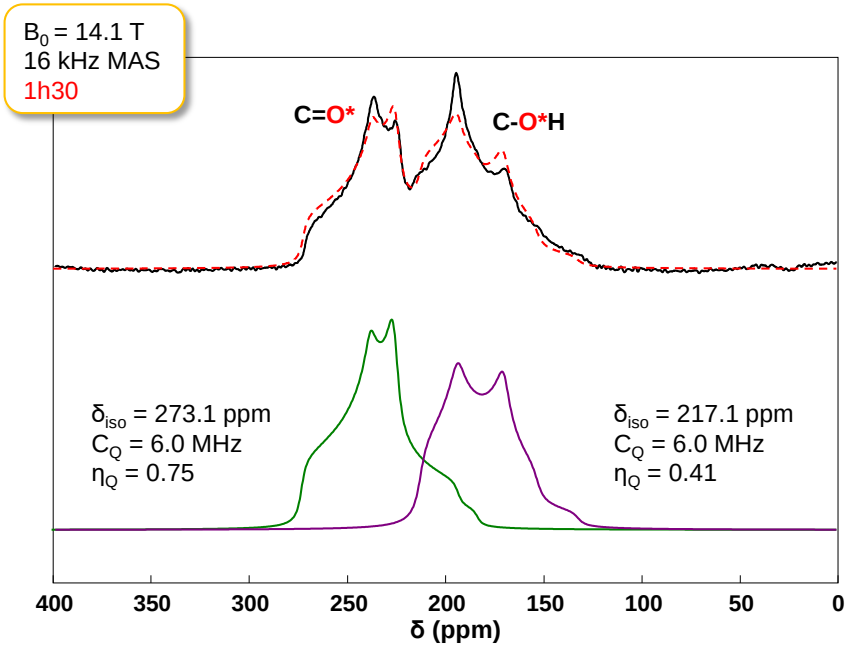

B3) Palmitic acid (PA, $C_{16}H_{32}O_2$)

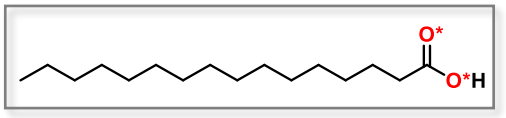

B3-a) Optimized labeling protocol

Palmitic acid (88.5 mg, 0.35 mmol, 1.0 eq) and CDI (61.5 mg, 0.38 mmol, 1.1 eq) were introduced into the stainless-steel grinding jar (10 mL inner volume) containing two stainless-steel balls (10 mm diameter). The jar was closed and subjected to grinding for 30 minutes in the MM400 mixer mill operated at 25 Hz. ^{18}O-labeled water (97.1%, 18.5 µL, 1.03 mmol, 3.0 eq) was then added into the jar, and the mixture was subjected to further grinding for 180 minutes at 30 Hz. To help recover the product, non-labeled water (1 mL) was added into the jar, and the content was subjected to grinding for 2 minutes at 25 Hz. Then, the medium ("milky" solution with a foam on top) was transferred to a beaker (together with sufficient amount of non-labeled water (10-15 mL) used here to rinse the jar), poured into a separatory funnel, diluted and acidified with an aqueous solution of HCl (1M, 15 mL), and finally extracted with ethyl acetate (1x20 mL, 2x10 mL). Combined organic phases were dried over Na_2SO_4, filtered, and finally dried under vacuum to yield the product as white microcrystalline solid. Average yield (n = 3): 78 ± 3 mg, 88 ± 3 %, m. p. 62.0-64.5 °C.

For the ^{17}O-labeling, overall the same reaction/work-up conditions as for ^{18}O-labeling were employed with 90% ^{17}O-enriched water (18.5 µL, 3.0 eq.) used at the hydrolysis step. After addition of ^{17}O-labeled water, the mixture was subjected to grinding for 270 min at 30 Hz. Yield (n = 1): 78 mg, 87 %.

Figure B3-1: ATR-IR analysis of the starting material, reaction intermediates, and final products. The dashed line shows that the C=O stretching frequency of ^{18}O/^{17}O-enriched product is shifted to lower wavenumbers in comparison with non-labeled precursor.

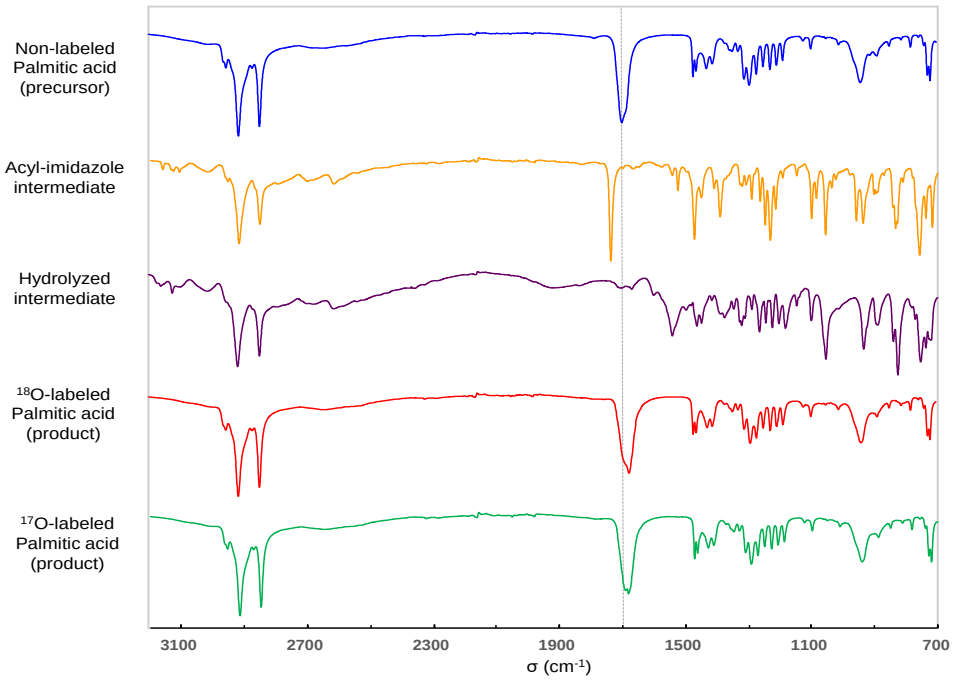

B3-b) Characterization of the ^{18}O-labeled PA

Figure B3-2: MS analyses of the non-labeled precursor in comparison to the ^{18}O-enriched product. Average enrichment per carboxylic oxygen determined by MS: 46.9 ± 0.2 % (n = 3), enrichment yield: ~ 98 %.

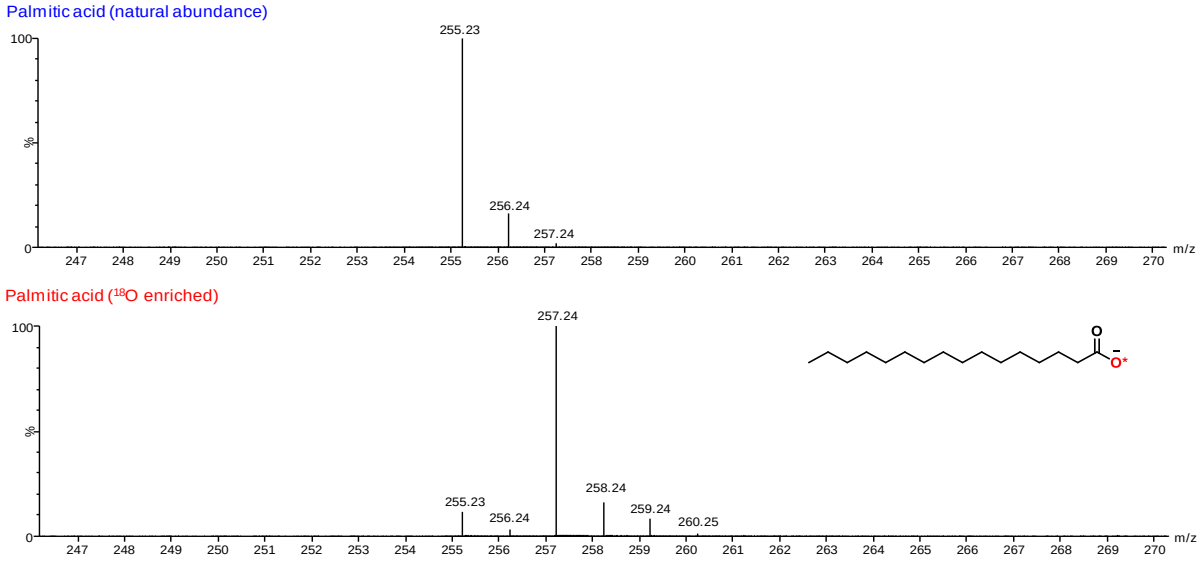

Figure B3-3: LC analyses of the non-labeled precursor in comparison to the ^{18}O-enriched product.

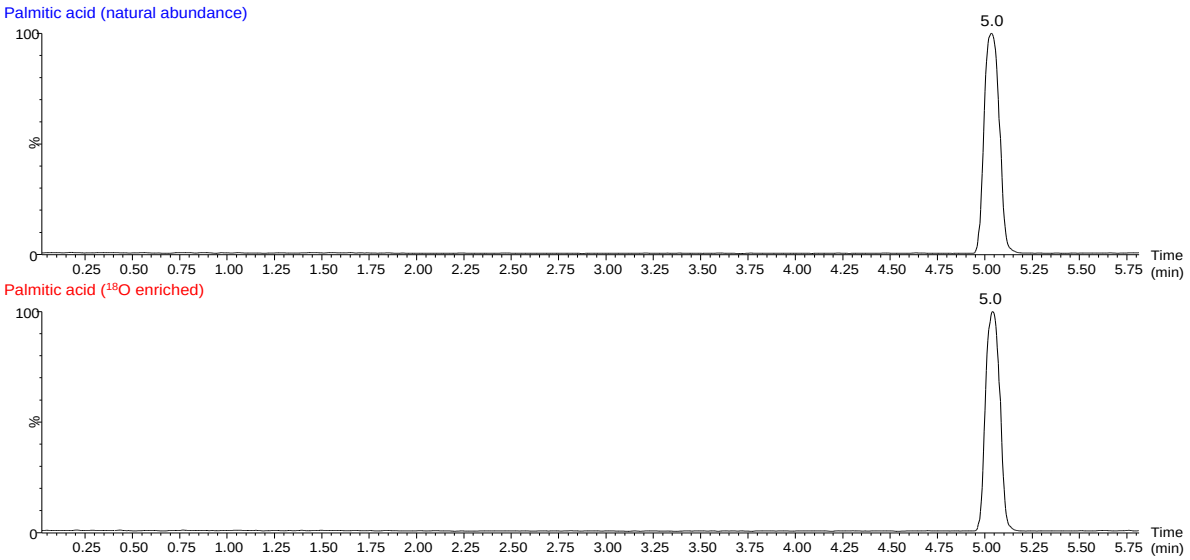

Figure B3-4: ^{1}H NMR spectra of the non-labeled precursor in comparison to the ^{18}O-enriched product (DMSO-d_6, 500 MHz; solvent peaks are crossed out).

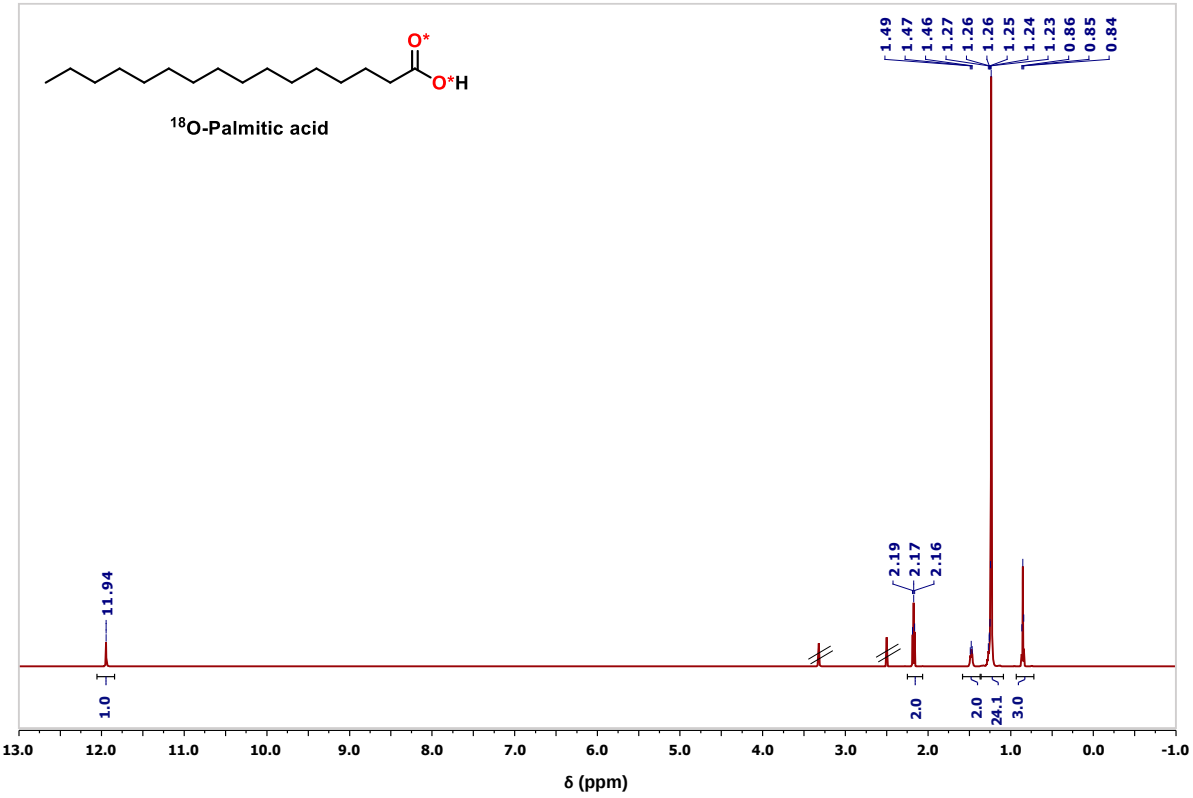

Figure B3-5: ^{13}C NMR spectra of the non-labeled precursor in comparison to the ^{18}O-enriched product (DMSO-d_6, 500 MHz; solvent peaks are crossed out).

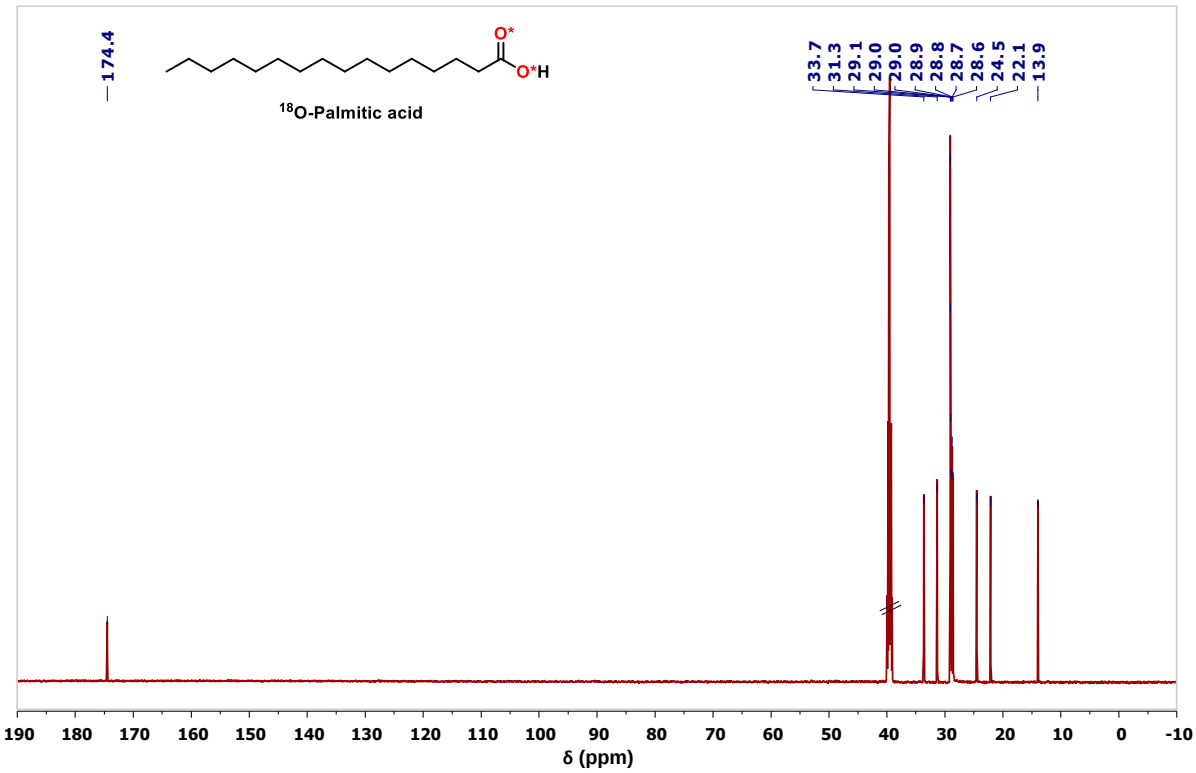

Figure B3-6: XRD powder pattern of the non-labeled precursor in comparison to the ^{18}O-enriched product.

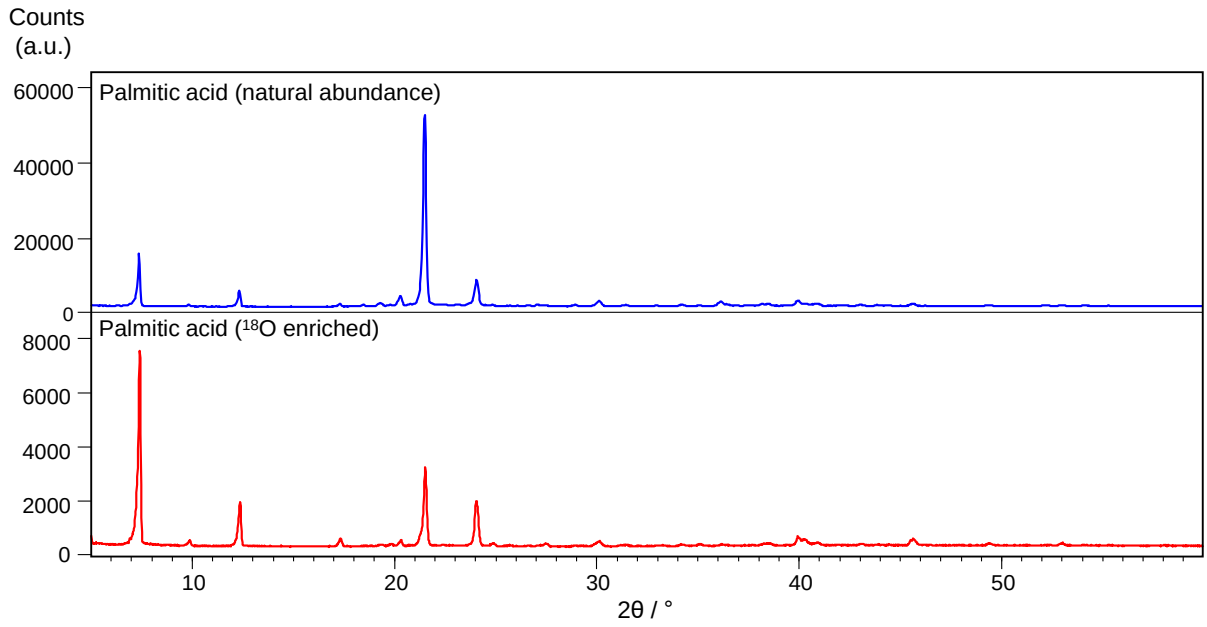

Figure B3-7: ^{13}C NMR study of ^{18}O-isotope effect on the ^{13}C-carboxylic resonance in solution NMR. The non-labeled precursor is compared to the ^{18}O-enriched product, both having been mixed in different ratios, as indicated above each spectrum (DMSO-d_6, 600 MHz).

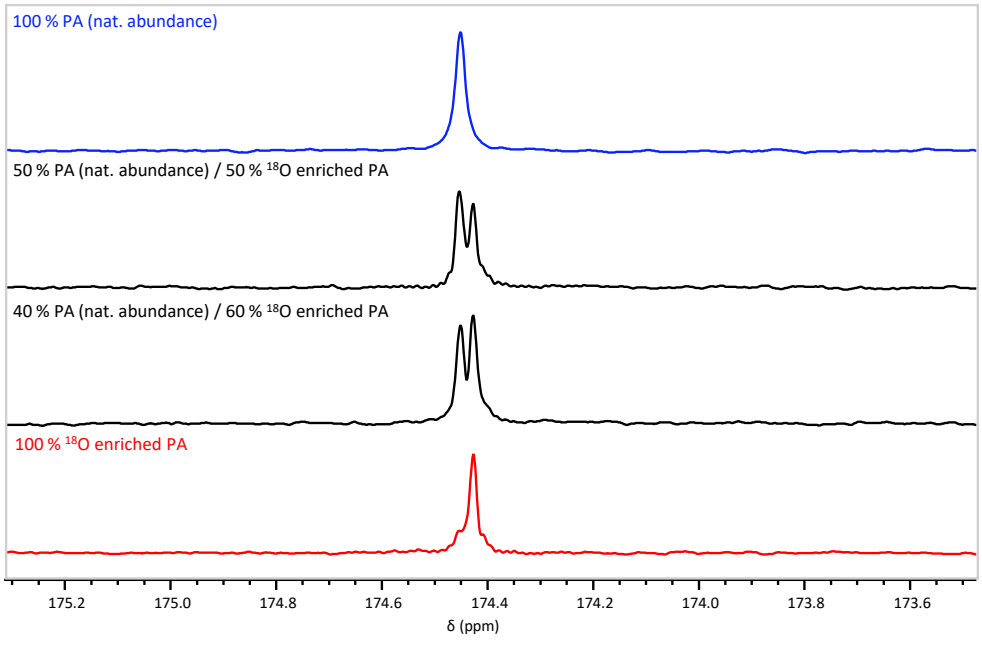

B3-c) Characterization of the ^{17}O-labeled PA

Figure B3-8: MS analyses of the non-labeled precursor in comparison to the ^{17}O-enriched product. Average enrichment per carboxylic oxygen determined by MS: 43 % (n = 1).

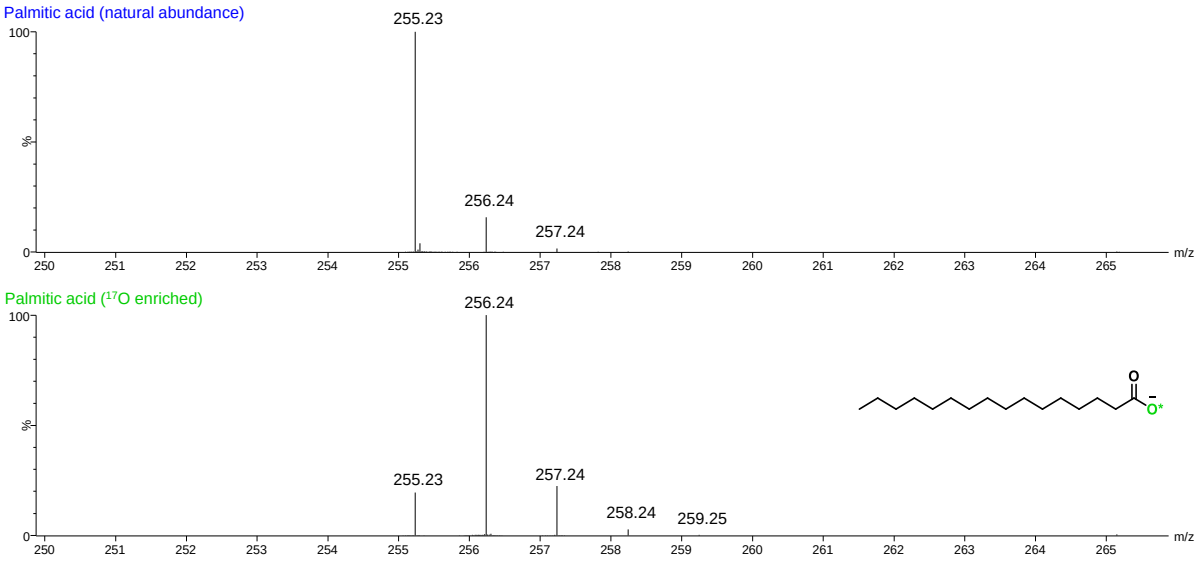

Figure B3-9: LC analyses of the non-labeled precursor in comparison to the ^{17}O-enriched product.

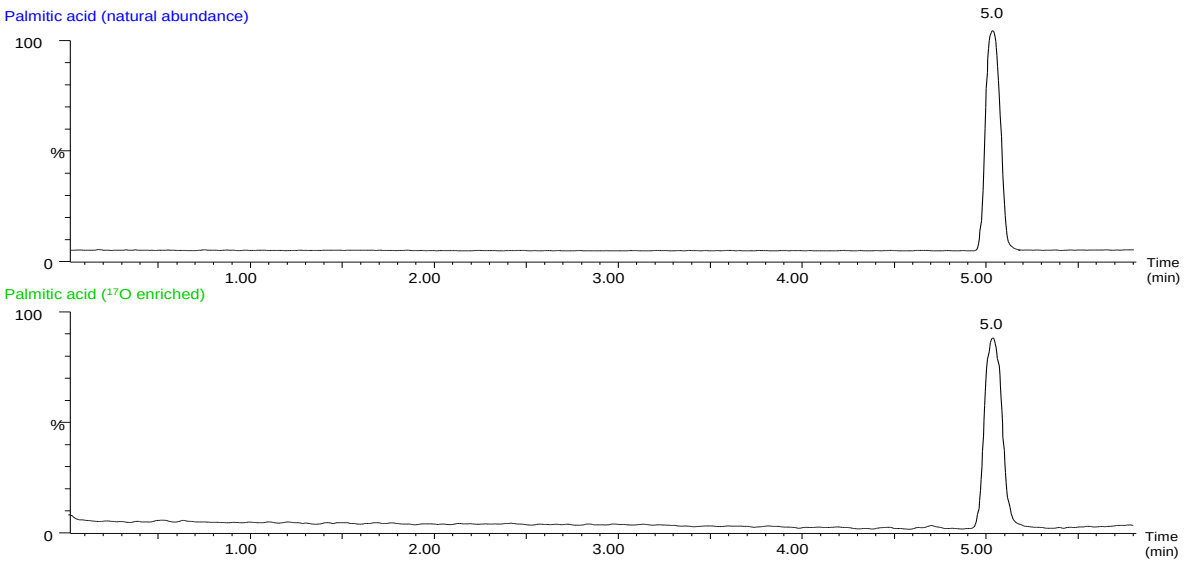

Figure B3-10: ^{1}H NMR spectra of the non-labeled precursor in comparison to the ^{17}O-enriched product (DMSO-d_6, 500 MHz; solvent peaks are crossed out).

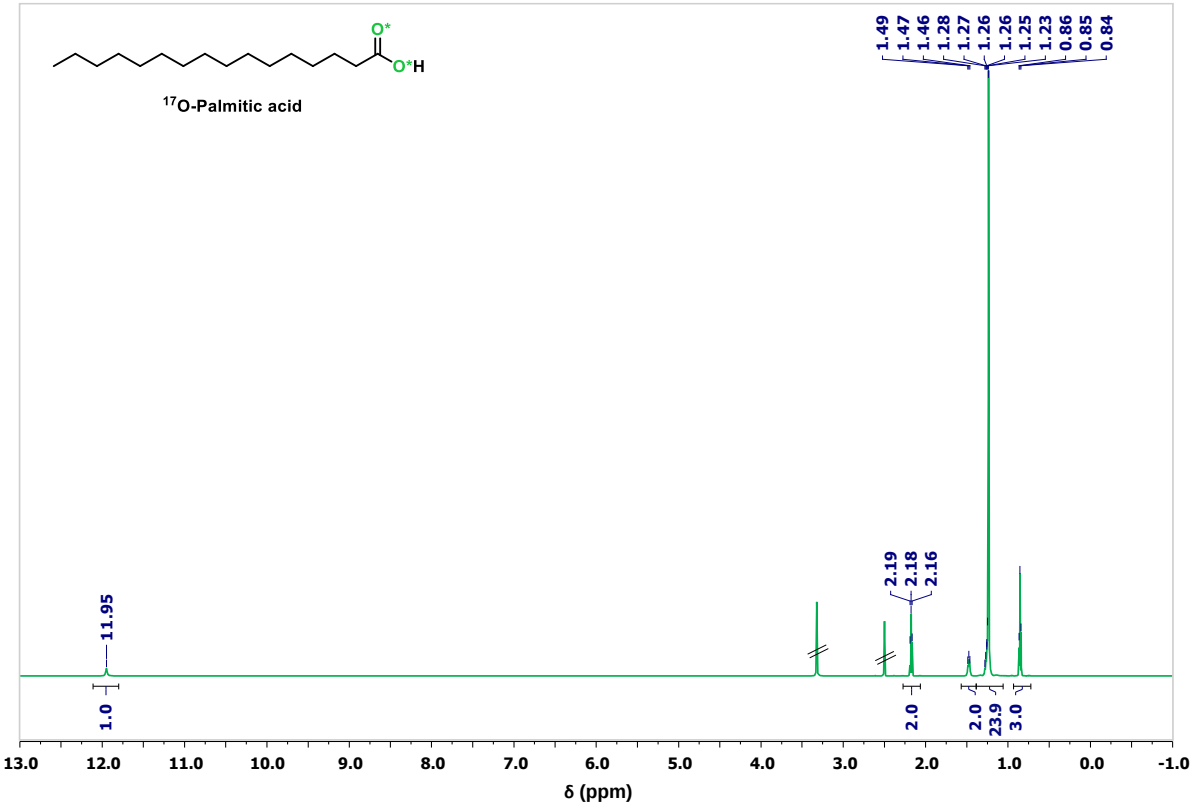

Figure B3-11: ^{13}C NMR spectra of the non-labeled precursor in comparison to the ^{17}O-enriched product (DMSO-d_6, 500 MHz; solvent peaks are crossed out).

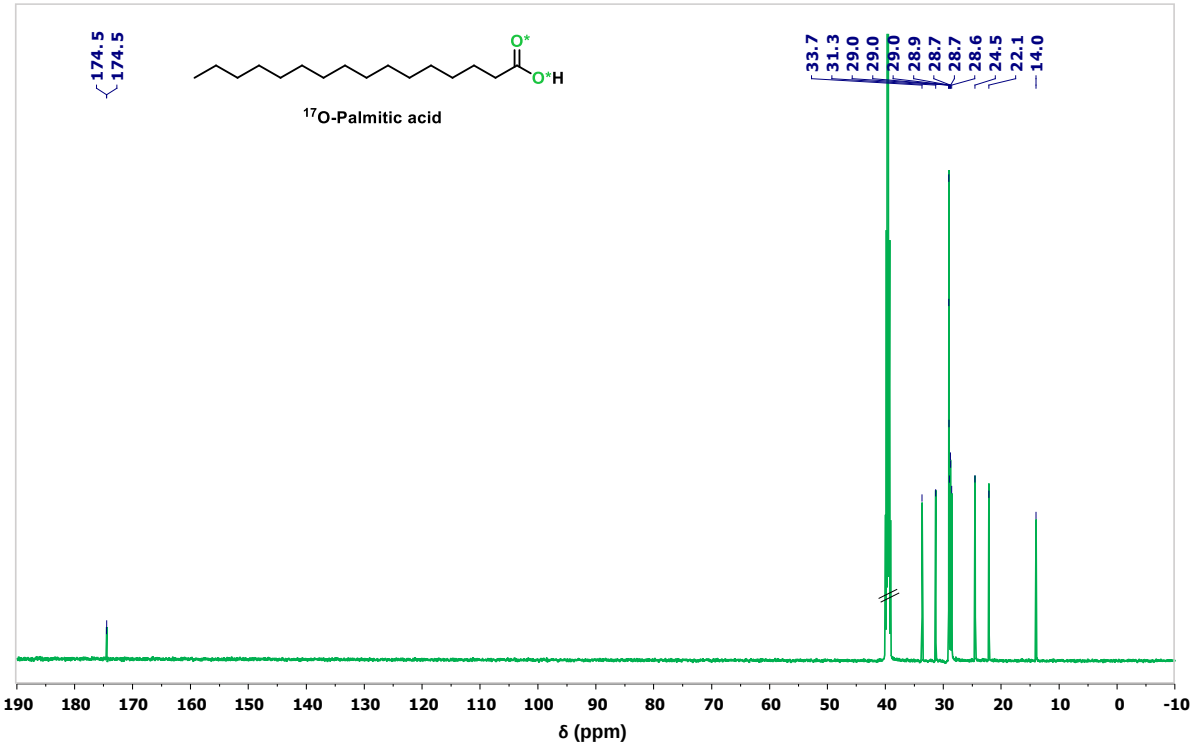

Figure B3-12: XRD powder pattern of the non-labeled precursor in comparison to the ^{17}O-enriched product.

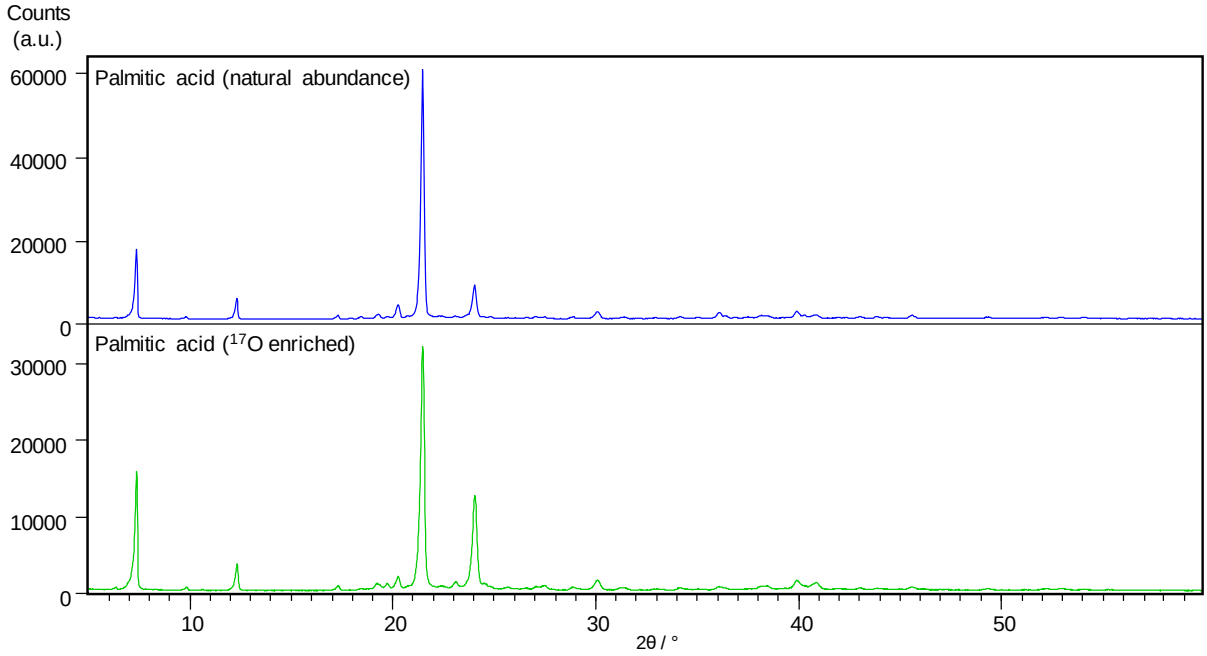

Figure B3-13: ^{17}O MAS NMR spectrum of ^{17}O-labeled PA (black) and its fit (dashed red line), considering the presence of C=O (green) and C-OH (purple) contributions.

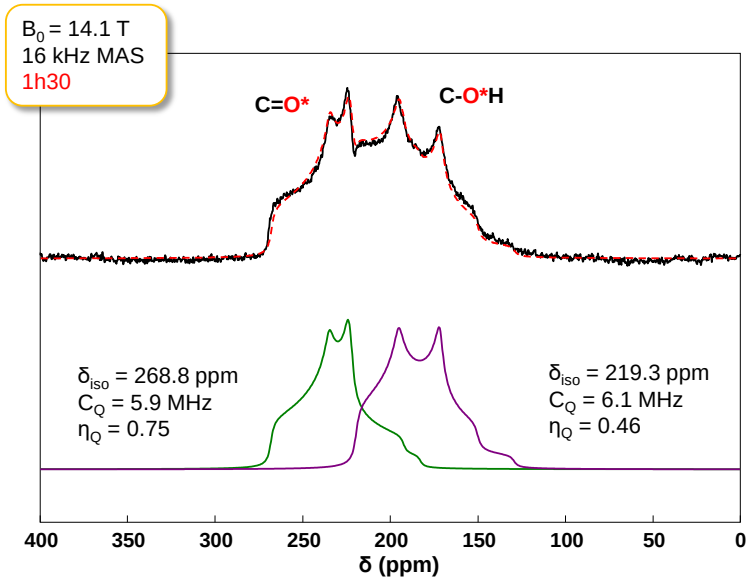

Figure B3-14: SEM/EDX analyses of ^{17}O-labeled PA.

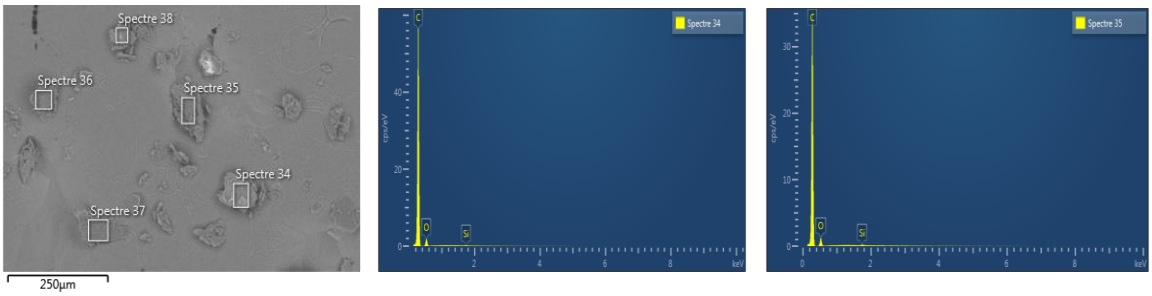

B4) Linoleic acid (LA, $C_{18}H_{32}O_2$)

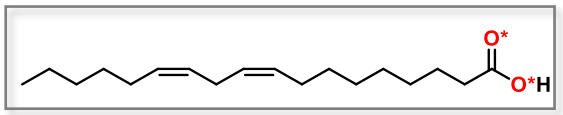

B4-a) Optimized labeling protocol

Linoleic acid (46 mg, 0.16 mmol, 1.0 eq) and CDI (29 mg, 0.18 mmol, 1.1 eq) were introduced into the PTFE grinding jar (5 mL inner volume) containing one PTFE ball (10 mm diameter). The jar was closed and subjected to grinding for 20 minutes in the P23 ball-mill operated at 25 Hz. ^{18}O-labeled water (97.1%, 6 µL, 0.33 mmol, 2.0 eq) was then added into the jar, and the mixture was subjected to further grinding for 3x30 minutes at 25 Hz. In order to enable complete hydrolysis, the jar was opened after each 30 min of grinding and material stuck at the inner edge was scratched into the jar. To help recover the product, non-labeled water (1 mL) was added into the jar, and the content was subjected to grinding for 1 minute at 25 Hz. Then, the colorless emulsion was transferred to a beaker (together with sufficient amount of non-labeled water (6-8 mL) used here to rinse the jar). The medium was acidified to pH ~ 1 with an aqueous solution of HCl (6M, 9-10 drops) and extracted with ethyl acetate (1x10 mL, 3x6 mL). Combined organic phases were dried over Na_2SO_4, filtered and finally dried under vacuum giving the product as a colorless oil. Average yield (n = 2): 42 ± 1 mg, 90 ± 3 %.

For the ^{17}O-labeling, exactly the same reaction/work-up conditions as for ^{18}O-labeling were employed with 90% ^{17}O-enriched water (6 µL, 2.0 eq.) used at the hydrolysis step. Yield (n = 1): 41 mg, 90 %.

Figure B4-1: ATR-IR analysis of the starting material, reaction intermediates, and final products. The dashed line shows that the C=O stretching frequency of ^{18}O/^{17}O-enriched product is shifted to lower wavenumbers in comparison with non-labeled precursor.

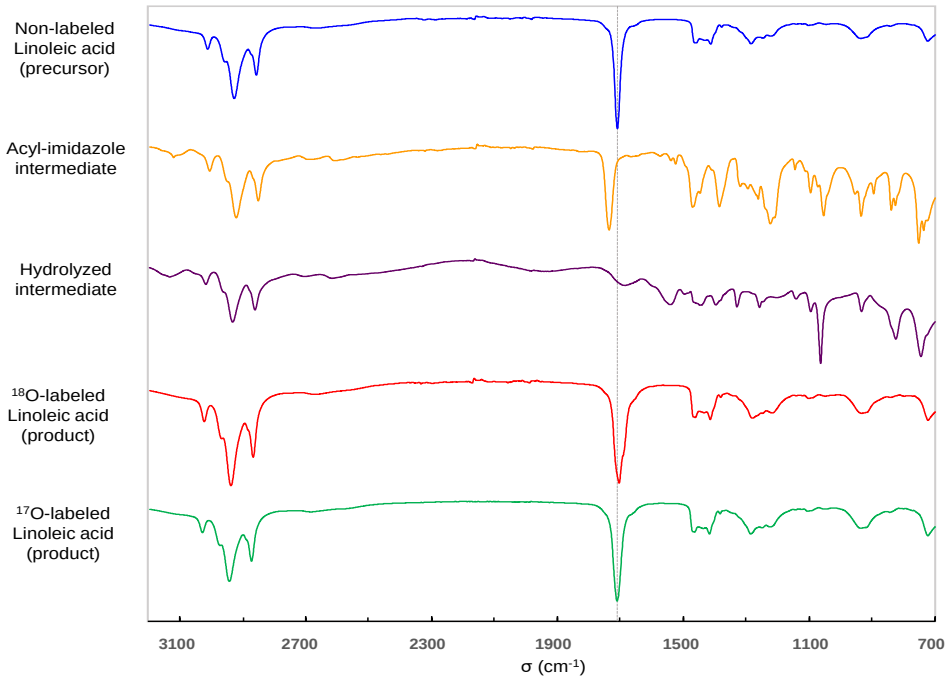

B4-b) Characterization of the ^{18}O-labeled LA

Figure B4-2: MS analyses of the non-labeled precursor in comparison to the ^{18}O-enriched product. Average enrichment per carboxylic oxygen determined by MS: 41.3 ± 0.4 % (n = 2), enrichment yield: ~ 82 %.

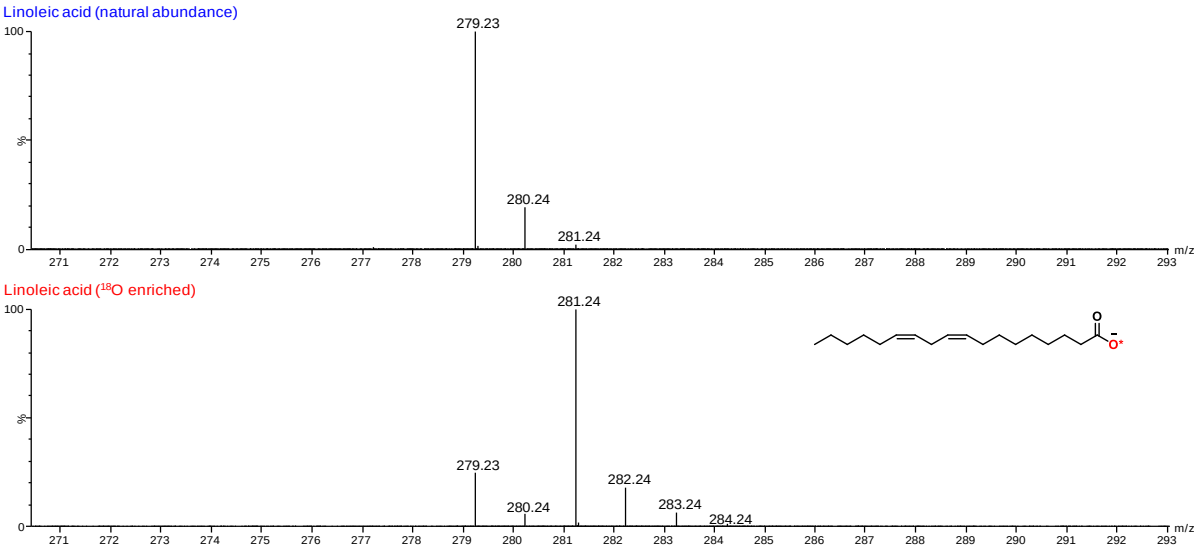

Figure B4-3: LC analyses of the non-labeled precursor in comparison to the ^{18}O-enriched product.

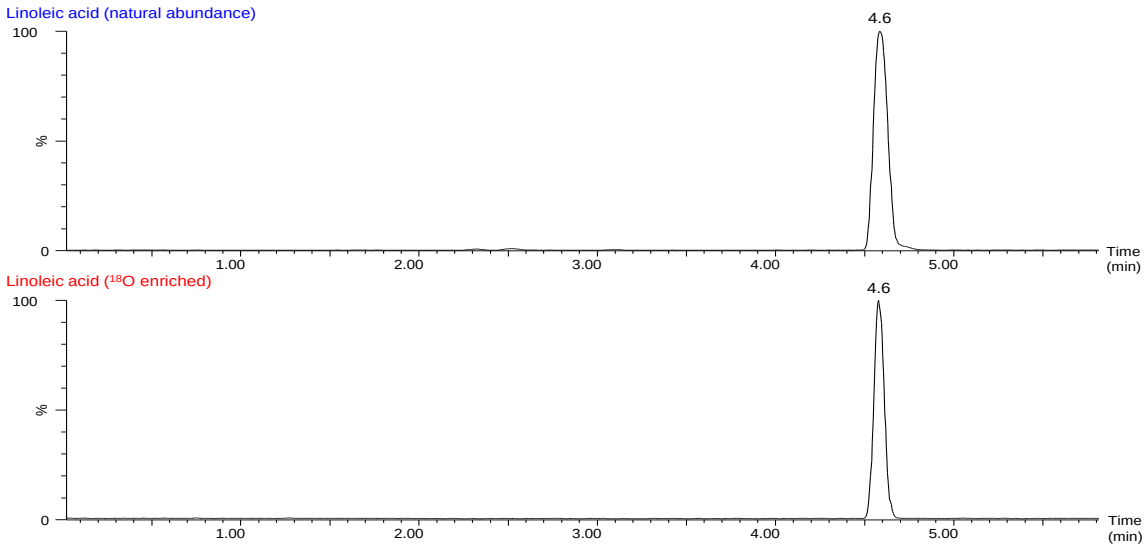

Figure B4-4: ^{1}H NMR spectra of the non-labeled precursor in comparison to the ^{18}O-enriched product (DMSO-d_6, 600 MHz; solvent peaks are crossed out).

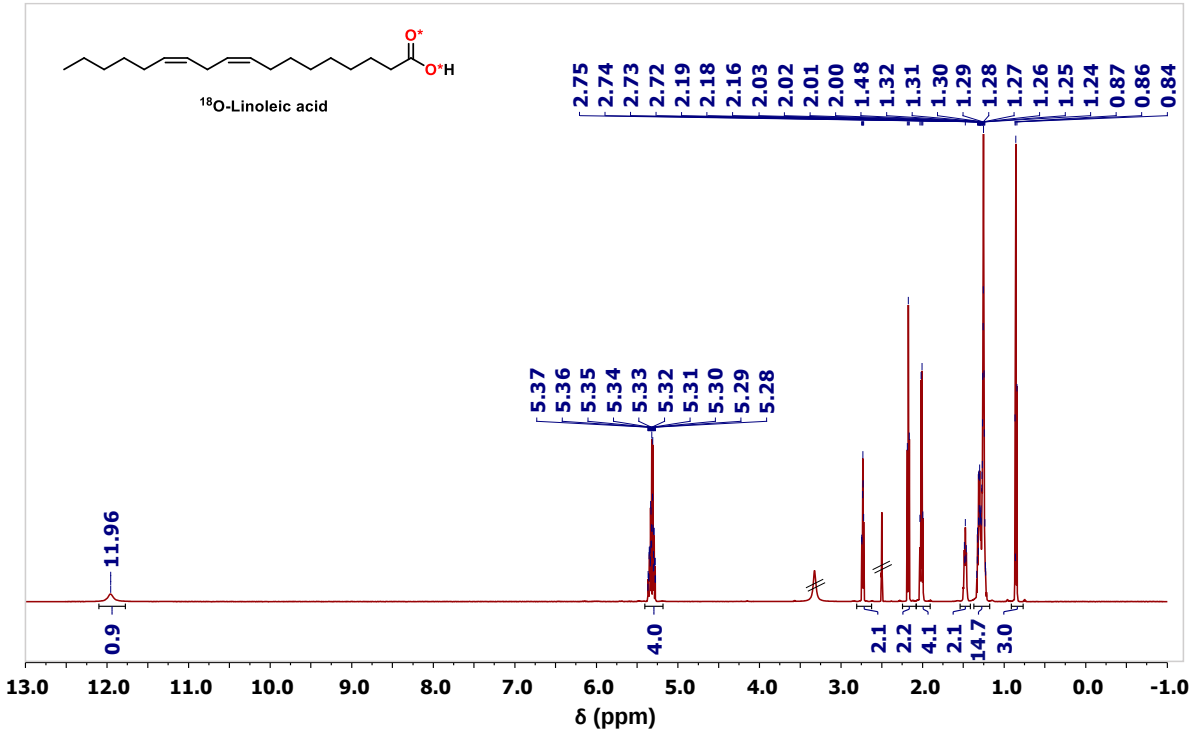

Figure B4-5: ^{13}C NMR spectra of the non-labeled precursor in comparison to the ^{18}O-enriched product (DMSO-d_6, 600 MHz; solvent peaks are crossed out).

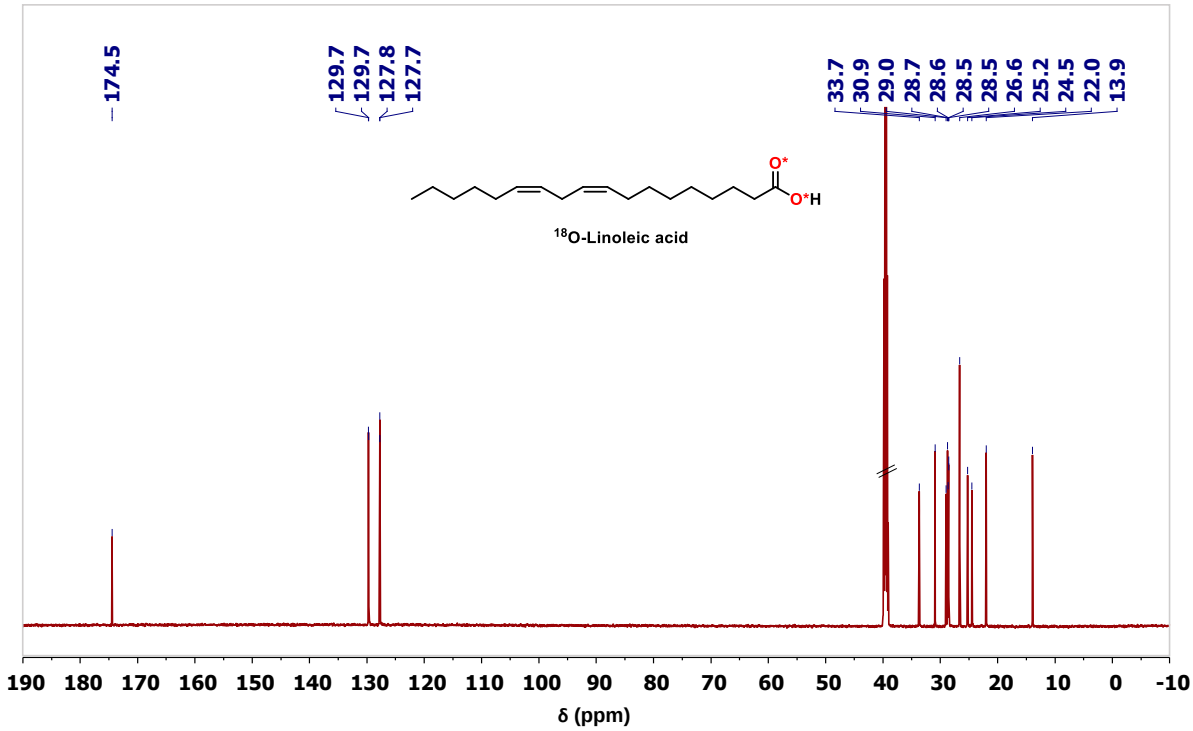

Figure B4-6: ^{13}C NMR **s**tudy of ^{18}O-isotope effect on the ^{13}C-carboxylic resonance in solution NMR. The non-labeled precursor is compared to the ^{18}O-enriched product, both having been mixed in different ratios, as indicated above each spectrum (DMSO-d_6, 600 MHz).

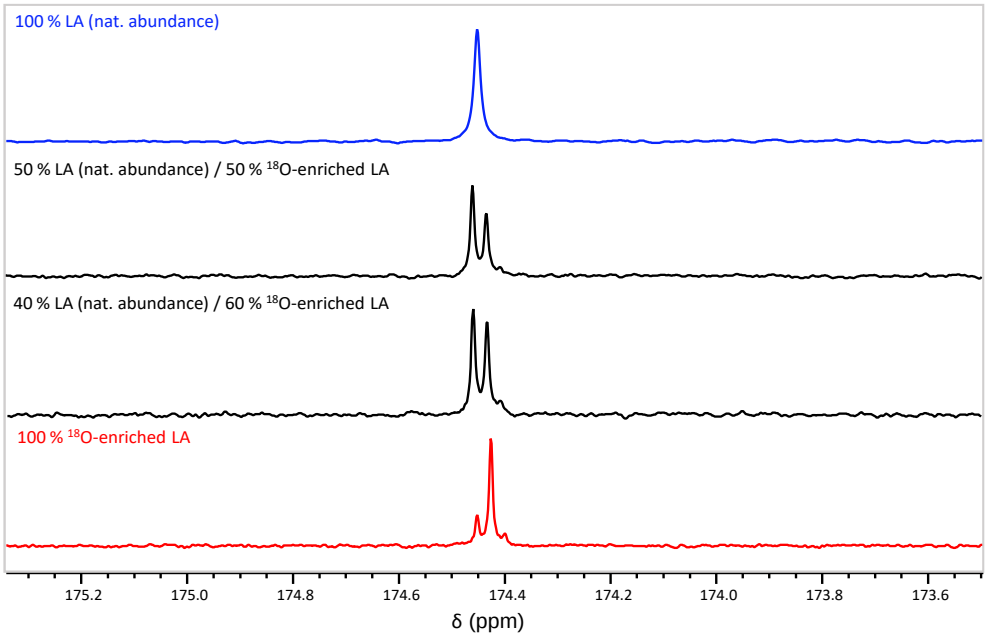

B4-c) Characterization of the ^{17}O-labeled LA

Figure B4-7: MS analyses of the non-labeled precursor in comparison to the ^{17}O-enriched product. Average enrichment per carboxylic oxygen determined by MS: 40 % (n = 1).

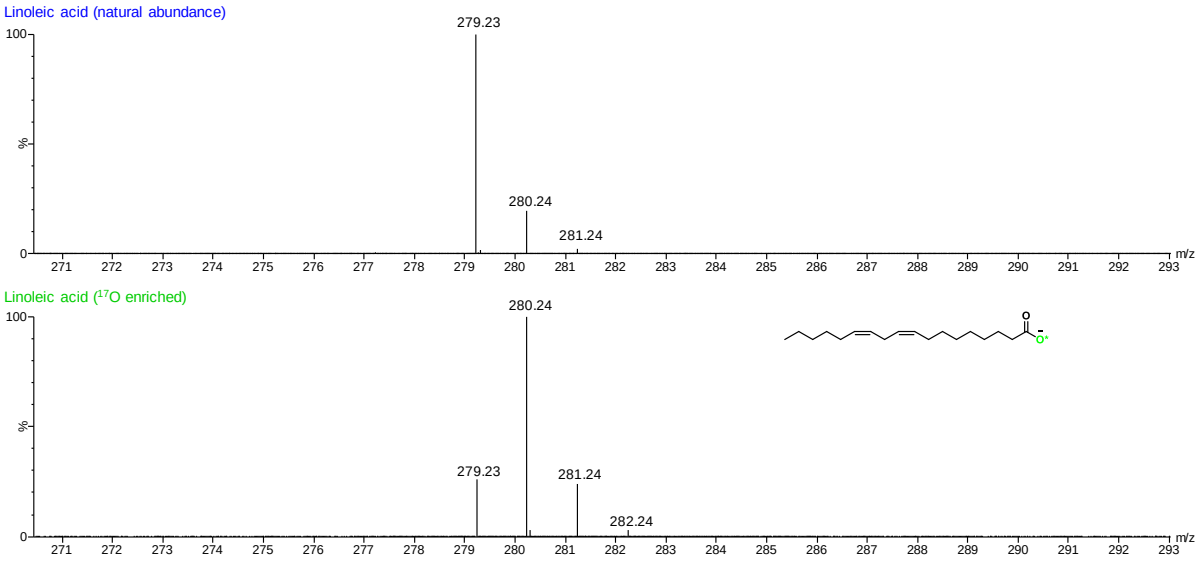

Figure B4-8: LC analyses of the non-labeled precursor in comparison to the ^{17}O-enriched product. The small difference in elution times is caused by slightly different calibration of the instrument.

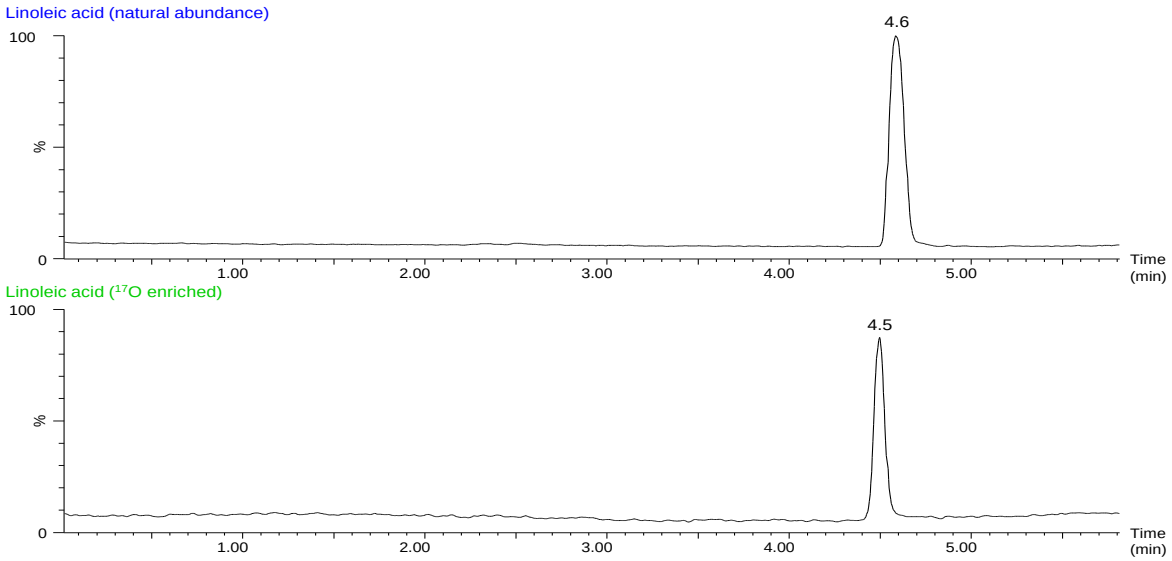

Figure B4-9: ^{1}H NMR spectra of the non-labeled precursor in comparison to the ^{17}O-enriched product (DMSO-d_6, 600 MHz; solvent peaks are crossed out).

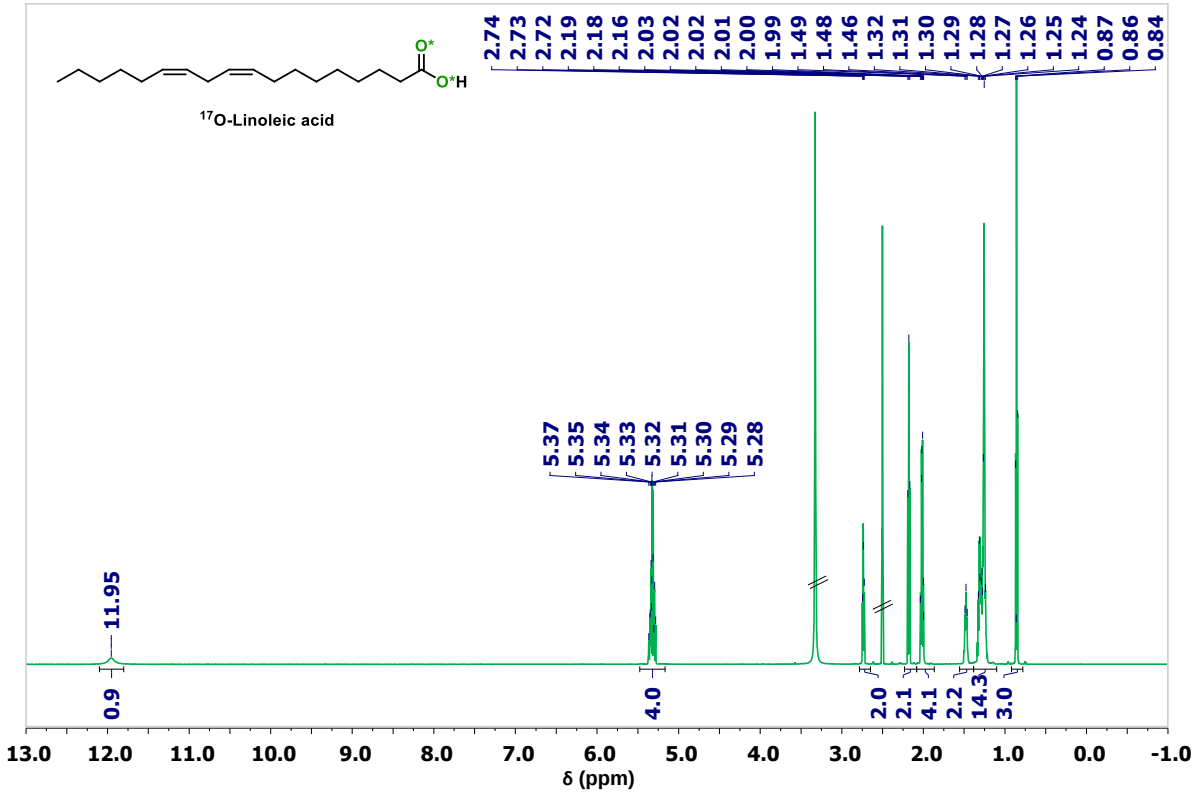

Figure B4-10: ^{13}C NMR spectra of the non-labeled precursor in comparison to the ^{17}O-enriched product (DMSO-d_6, 600 MHz; solvent peaks are crossed out).

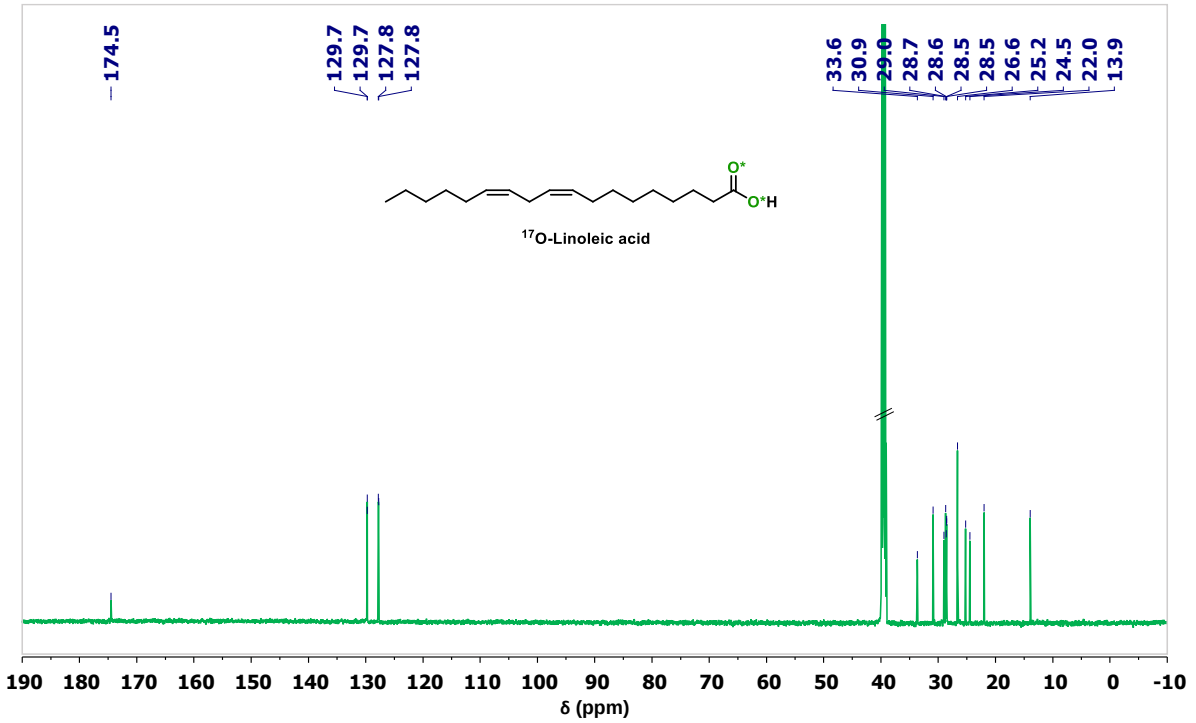

B5) α-Linolenic acid (ALA, $C_{18}H_{30}O_2$)

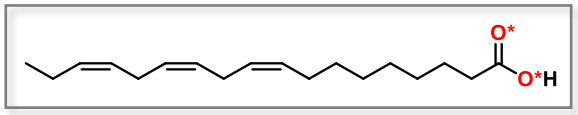

B5-a) Optimized labeling protocol

α-Linolenic acid (46 mg, 0.16 mmol, 1.0 eq) and CDI (29 mg, 0.18 mmol, 1.1 eq) were introduced into the PTFE grinding jar (5 mL inner volume) containing one PTFE ball (10 mm diameter). The jar was closed and subjected to grinding for 20 minutes in the P23 ball-mill operated at 25 Hz. ^{18}O-labeled water (97.1%, 6 µL, 0.33 mmol, 2.0 eq) was then added into the jar, and the mixture was subjected to further grinding for 3x30 minutes at 25 Hz. In order to enable complete hydrolysis, the jar was opened after each 30 min of grinding and material stuck at the inner edge was scratched into the jar). To help recover the product, non-labeled water (1 mL) was added into the jar, and the content was subjected to grinding for 1 minute at 25 Hz. Then, the yellow emulsion was transferred to a beaker (together with sufficient amount of non-labeled water (7-8 mL) used here to rinse the jar). The medium was acidified to pH ~ 1 with an aqueous solution of HCl (6M, 9-12 drops), leading to a cloudy mixture which was extracted with ethyl acetate (1x10 mL, 2x6 mL). Aqueous phase was diluted with brine and extracted with ethyl acetate (6 mL) one more time. Combined organic phases were dried over Na_2SO_4, filtered and finally dried under vacuum giving the product as a yellow oil. Average yield (n = 2): 40 ± 3 mg, 87 ± 7 %.

For the ^{17}O-labeling, exactly the same reaction/work-up conditions as for ^{18}O-labeling were employed with 90% ^{17}O-enriched water (6 µL, 2.0 eq.) used at the hydrolysis step. Yield (n = 1): 41 mg, 89 %.

Figure B5-1: ATR-IR analysis of the starting material, reaction intermediates, and final products. The dashed line shows that the C=O stretching frequency of ^{18}O/^{17}O-enriched product is shifted to lower wavenumbers in comparison with non-labeled precursor.

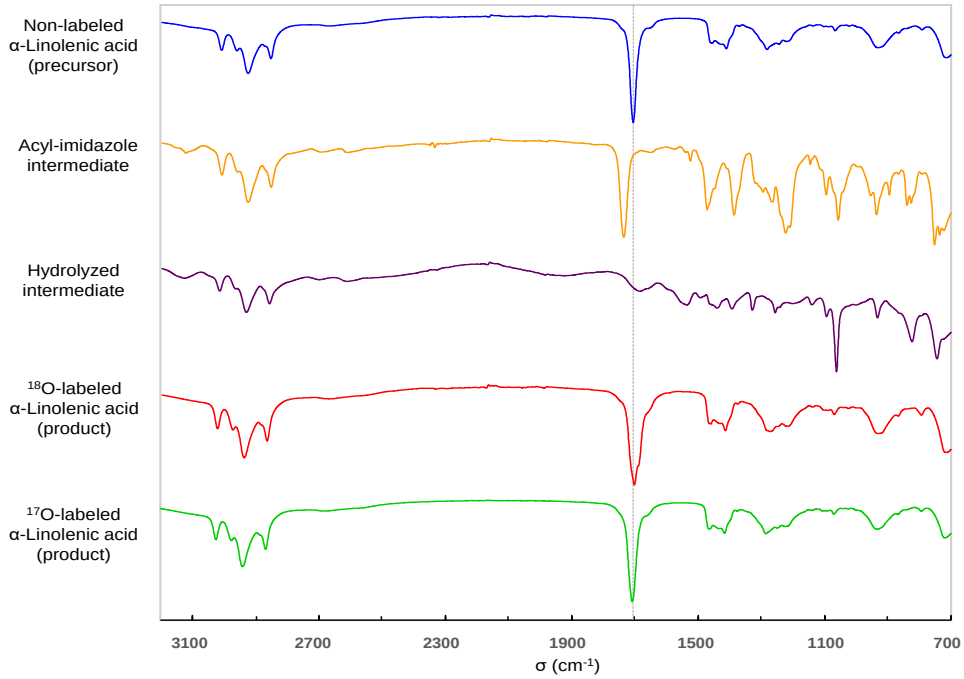

B5-b) Characterization of the ^{18}O-labeled ALA

Figure B5-2: MS analyses of the non-labeled precursor in comparison to the ^{18}O-enriched product. Average enrichment per carboxylic oxygen determined by MS: 42.5 ± 0.3 % (n = 2), enrichment yield: ~ 88 %.

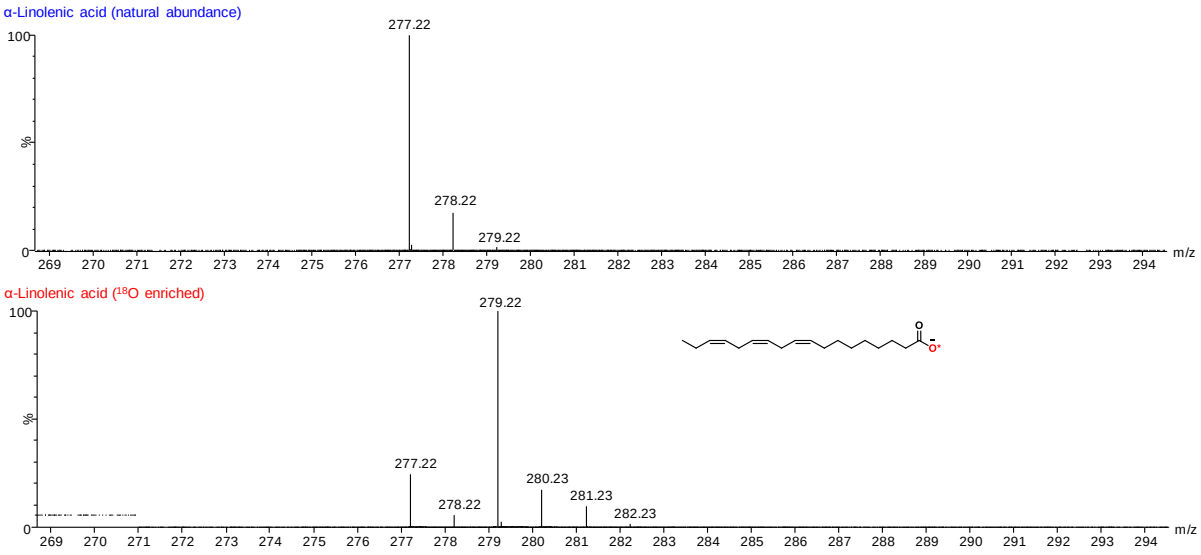

Figure B5-3: LC analyses of the non-labeled precursor in comparison to the ^{18}O-enriched product.

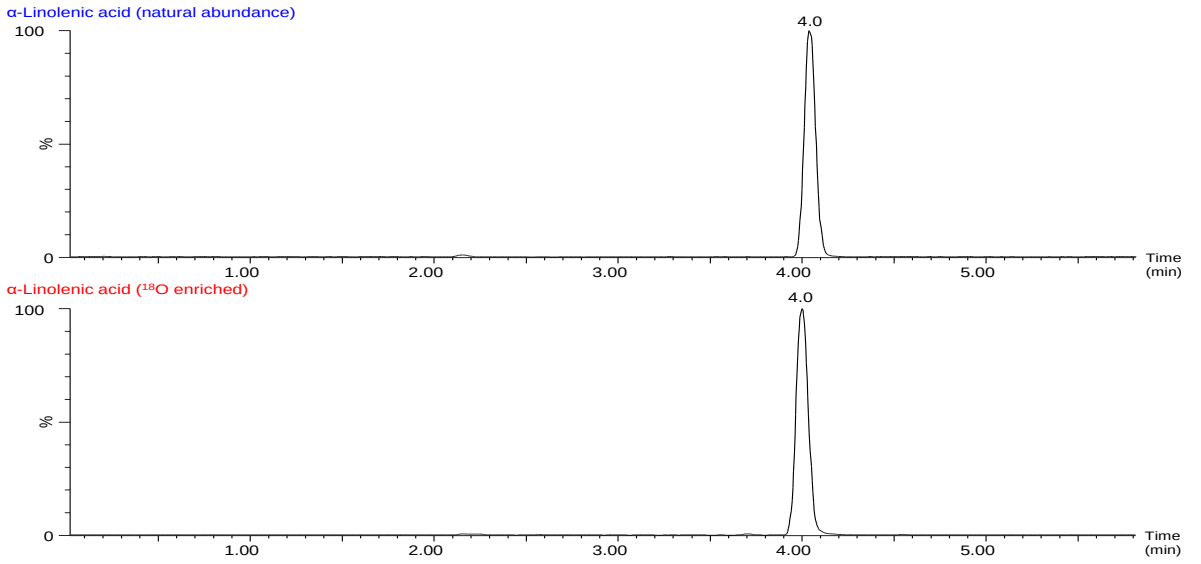

Figure B5-4: ^{1}H NMR spectra of non-labeled precursor in comparison to the ^{18}O-enriched product (DMSO-d_6, 600 MHz; solvent peaks are crossed out).

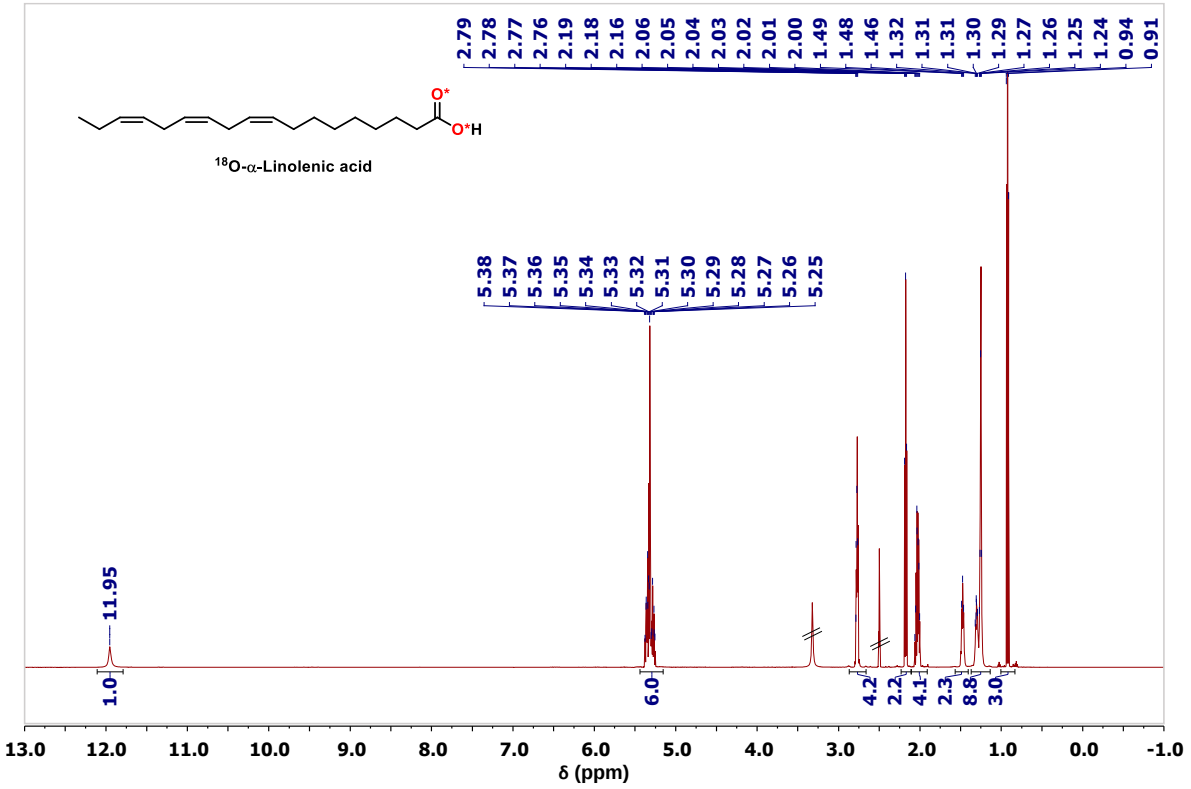

Figure B5-5: ^{13}C NMR spectra of the non-labeled precursor in comparison to the ^{18}O-enriched product (DMSO-d_6, 600 MHz; solvent peaks are crossed out).

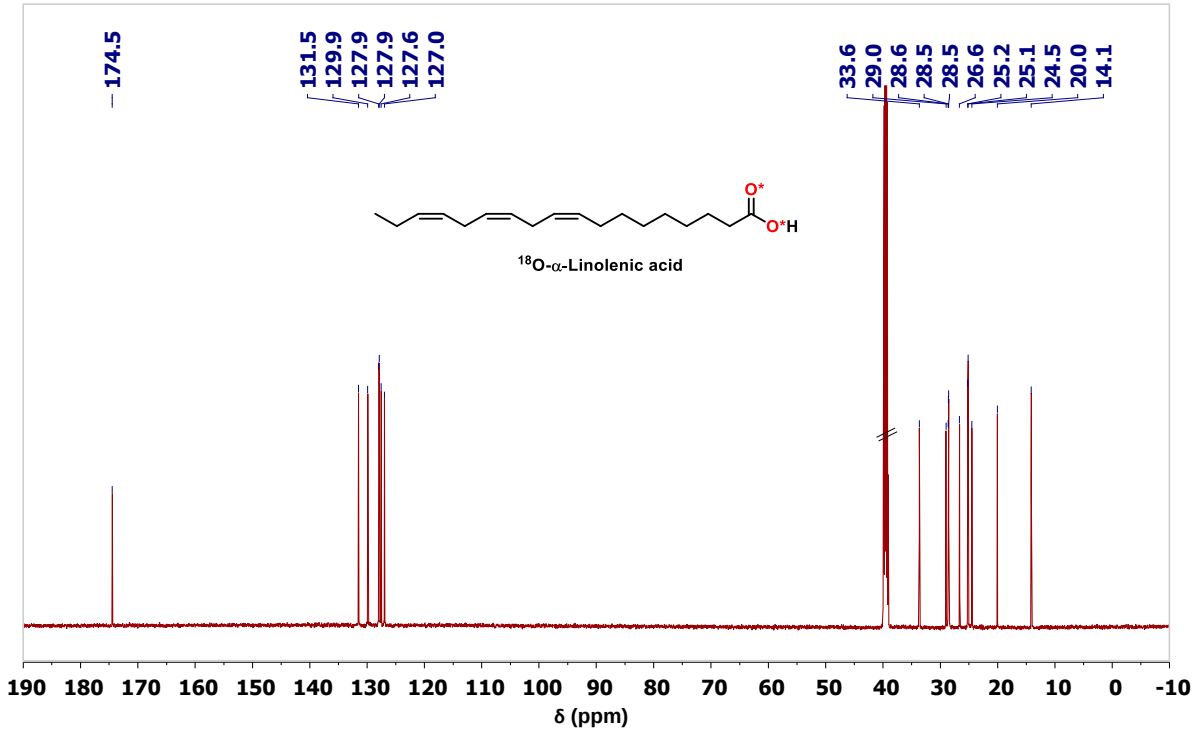

Figure B5-6: ^{13}C NMR **s**tudy of ^{18}O-isotope effect on the ^{13}C-carboxylic resonance in solution NMR. The non-labeled precursor is compared to the ^{18}O-enriched product, both having been mixed in different ratios, as indicated above each spectrum (DMSO-d_6, 600 MHz).

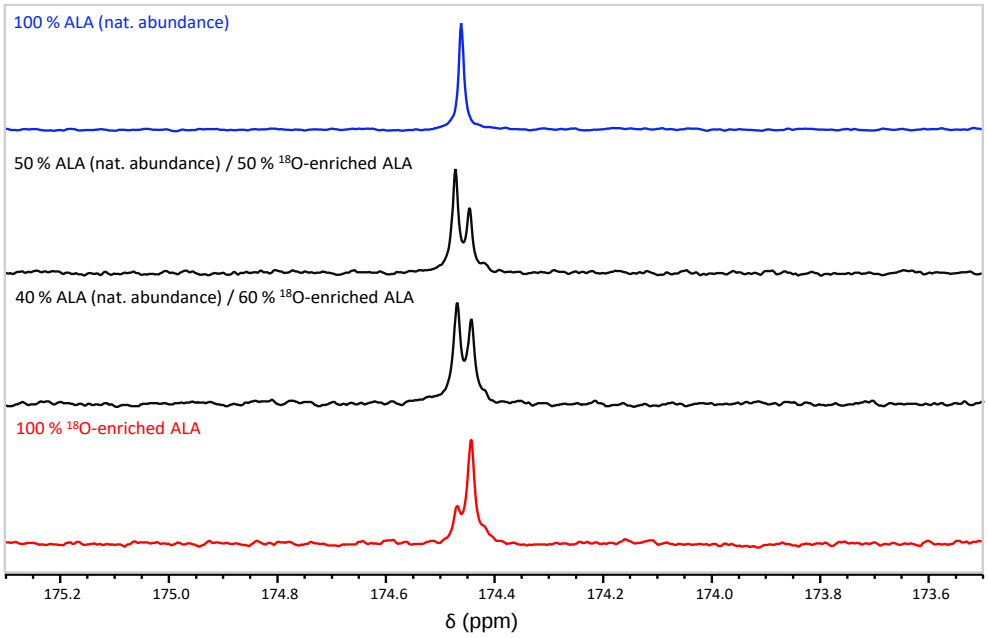

B5-c) Characterization of the ^{17}O-labeled ALA

Figure B5-7: MS analyses of the non-labeled precursor in comparison to the ^{17}O-enriched product. Average enrichment per carboxylic oxygen determined by MS: 40 % (n = 1).

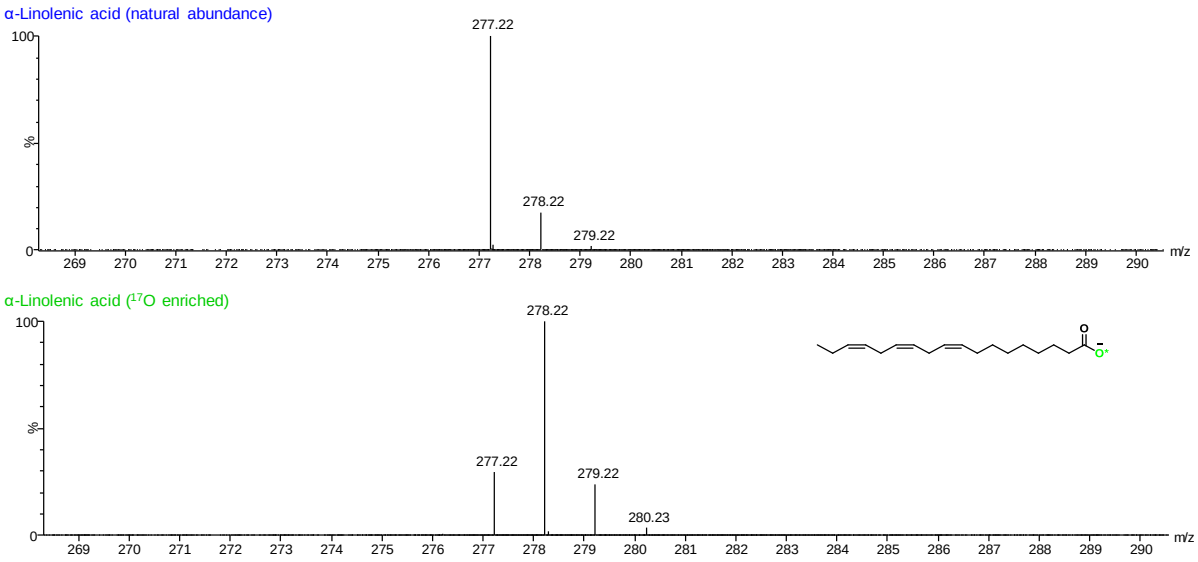

Figure B5-8: LC analyses of the non-labeled precursor in comparison to the ^{17}O-enriched product.

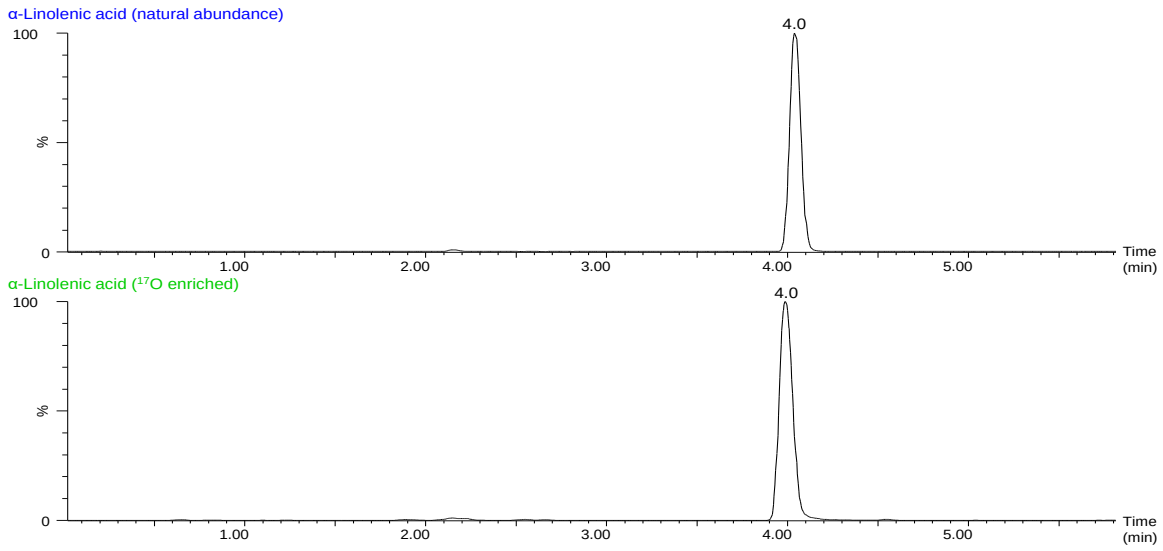

Figure B5-9: ^{1}H NMR spectra of the non-labeled precursor in comparison to the ^{17}O-enriched product (DMSO-d_6, 600 MHz; solvent peaks are crossed out).

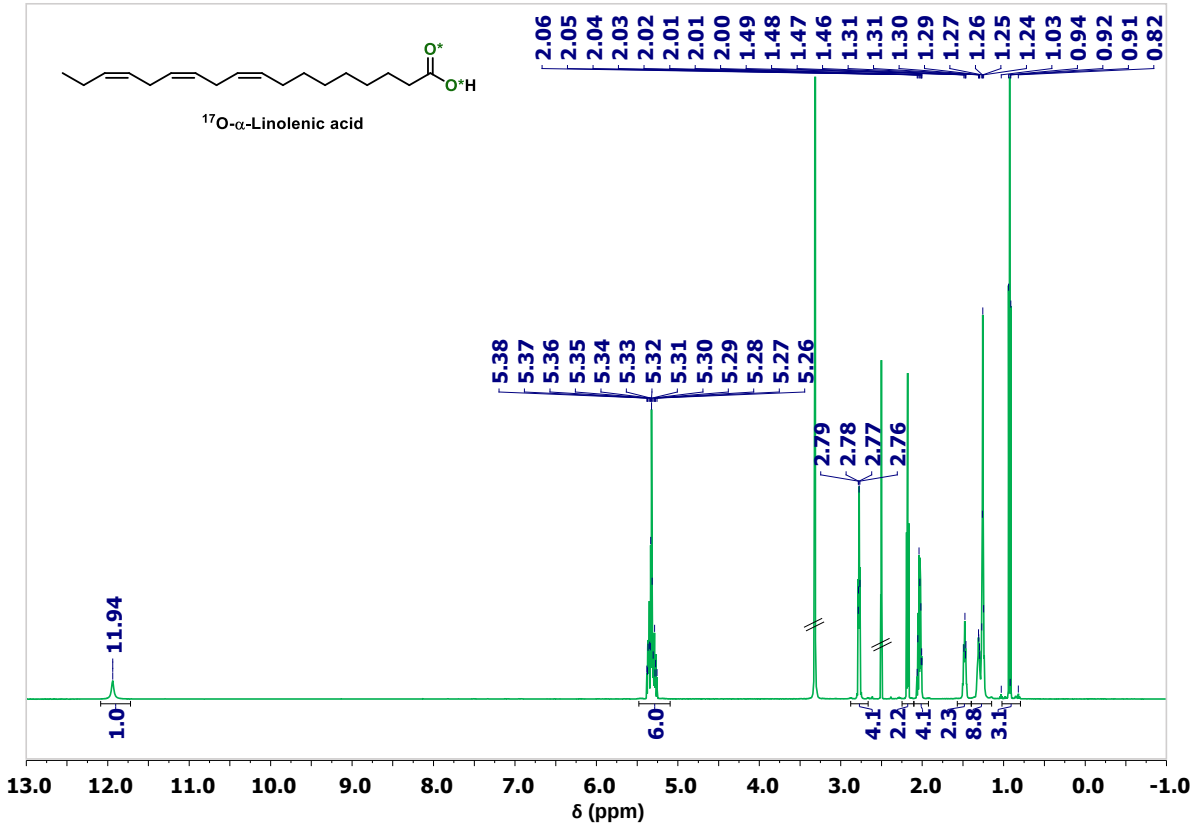

Figure B5-10: ^{13}C NMR spectra of the non-labeled precursor in comparison to the ^{17}O-enriched product (DMSO-d_6, 600 MHz; solvent peaks are crossed out).

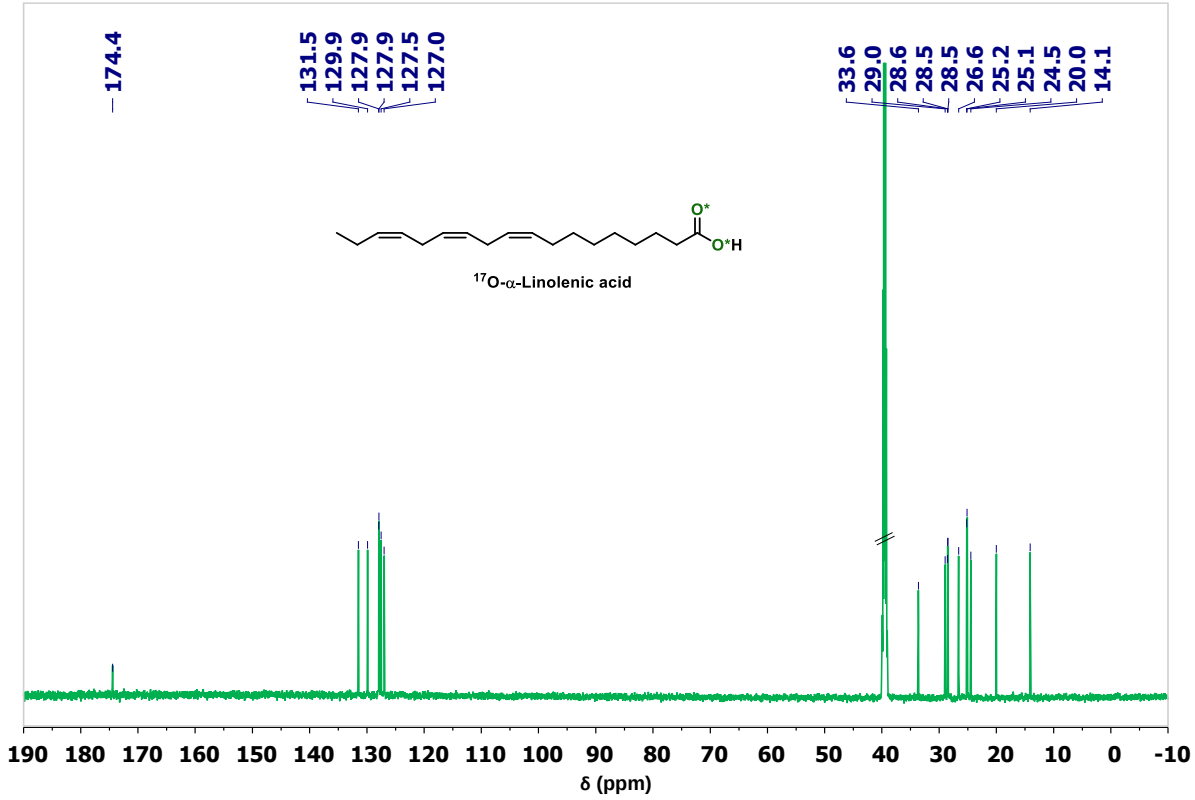

B6) Arachidonic acid (AA, $C_{20}H_{32}O_2$)

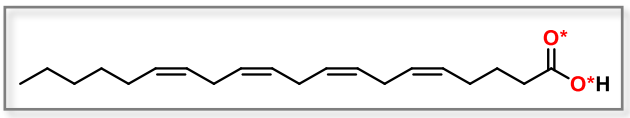

B6-a) Optimized labeling protocol

Arachidonic acid (47 mg, 0.15 mmol, 1.0 eq) and CDI (28 mg, 0.17 mmol, 1.1 eq) were introduced into the PTFE grinding jar (5 mL inner volume) containing one PTFE ball (10 mm diameter). The jar was closed and subjected to grinding for 20 minutes in the P23 ball-mill operated at 25 Hz. ^{18}O-labeled water (97.1%, 5.75 µL, 0.32 mmol, 2.0 eq) was then added into the jar, and the mixture was subjected to further grinding for 3x30 minutes at 25 Hz. In order to enable complete hydrolysis, the jar was opened after each 30 min of grinding and material stuck at the inner edge was scratched into the reactor). To help recover the product, non-labeled water (1 mL) was added into the jar, and the content was subjected to grinding for 1 minute at 25 Hz. Then, the yellow emulsion was transferred to a beaker (together with sufficient amount of non-labeled water (6-7 mL) used here to rinse the jar). The medium was acidified to pH ~ 1 with an aqueous solution of HCl (6M, 7-9 drops), leading to a cloudy mixture, which was diluted with brine (10 mL) and then extracted with ethyl acetate (1x10 mL, 3x6 mL). Combined organic phases were dried over Na_2SO_4, filtered and finally dried under vacuum giving the product as a yellow oil. Average yield (n = 3): 44 ± 1 mg, 90 ± 2 %.

For the ^{17}O-labeling, exactly the same reaction/work-up conditions as for ^{18}O-labeling were employed with 90% ^{17}O-enriched water (5.75 µL, 2.0 eq.) used at the hydrolysis step. Yield (n = 1): 42 mg, 88 %.

Figure B6-1: ATR-IR analysis of the starting material, reaction intermediates, and final products. The dashed line shows that the C=O stretching frequency of ^{18}O/^{17}O-enriched product is shifted to lower wavenumbers in comparison with non-labeled precursor.

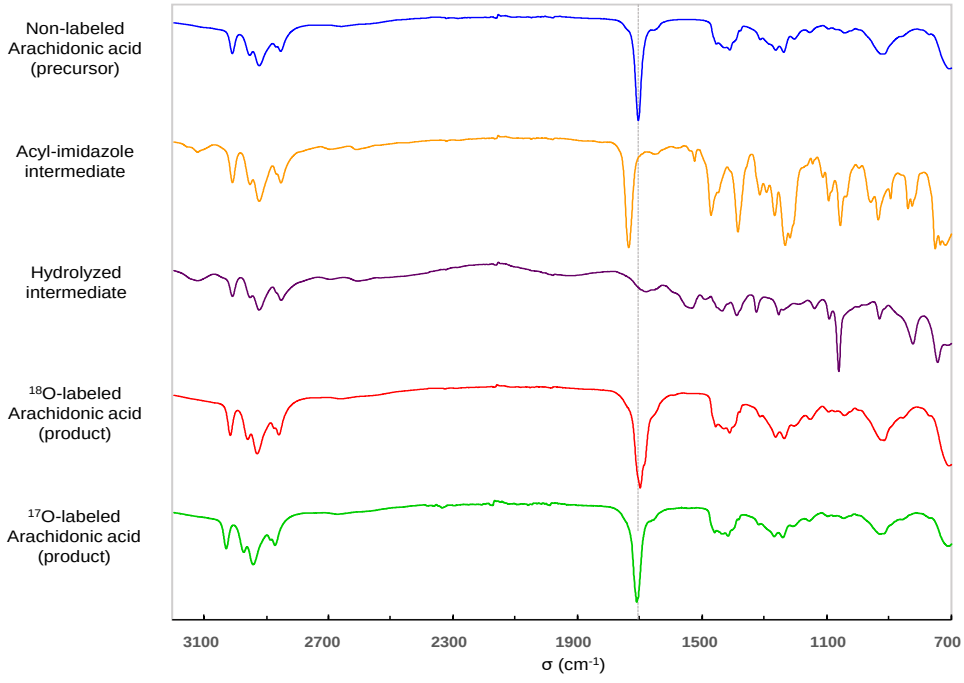

B6-b) Characterization of the ^{18}O-labeled AA

Figure B6-2: MS analyses of the non-labeled precursor in comparison to the ^{18}O-enriched product. Average enrichment per carboxylic oxygen determined by MS: 38.8 ± 1.5 % (n = 3), enrichment yield: ~ 84 %.

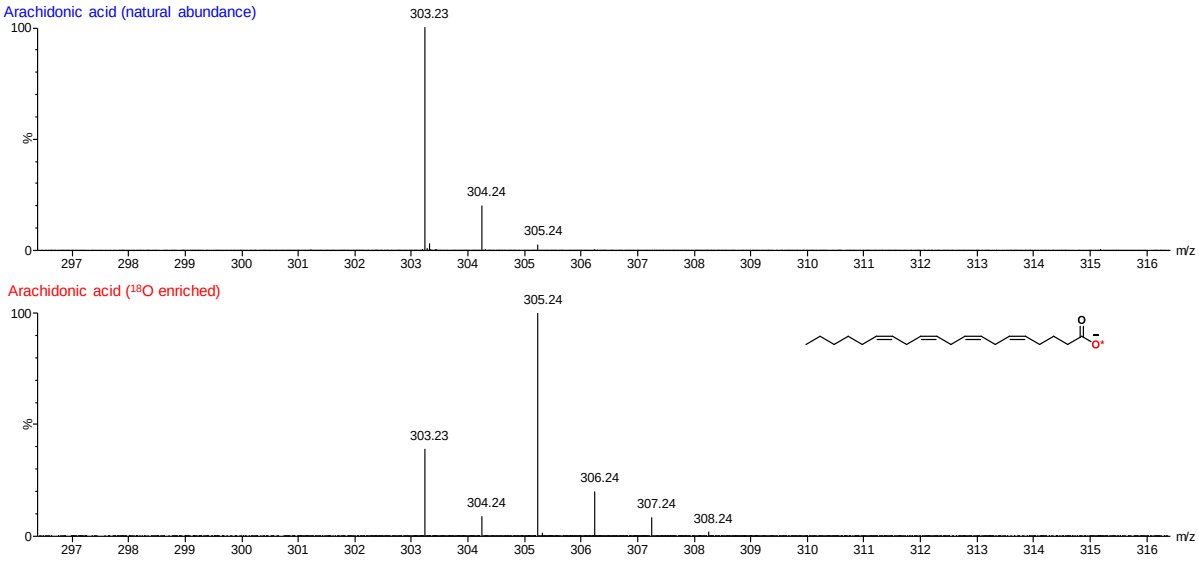

Figure B6-3: LC analyses of the non-labeled precursor in comparison to the ^{18}O-enriched product.

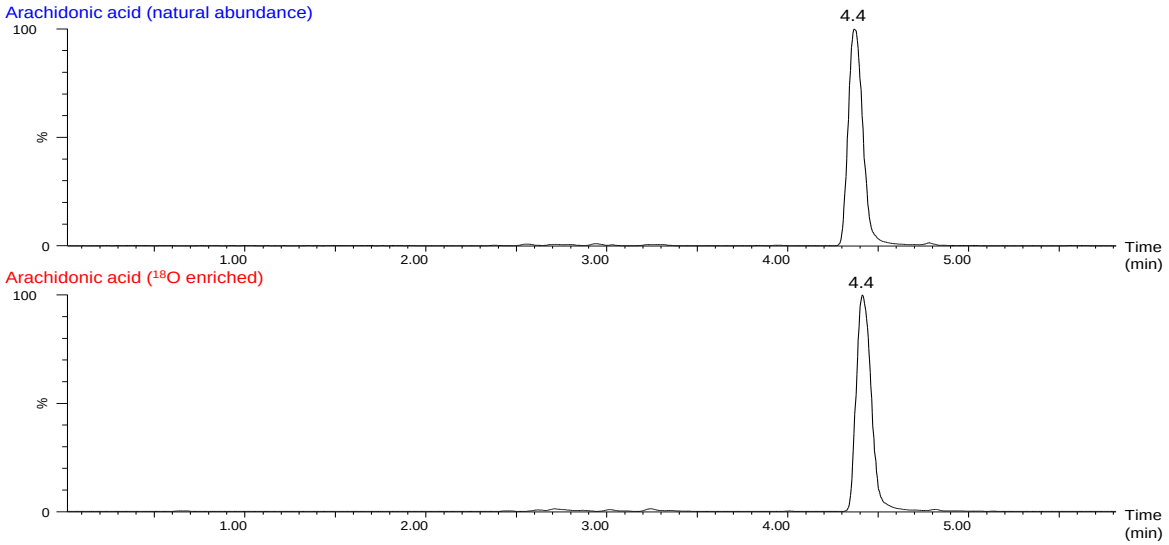

Figure B6-4: ^{1}H NMR spectra of the non-labeled precursor in comparison to the ^{18}O-enriched product (DMSO-d_6, 600 MHz; solvent peaks are crossed out).

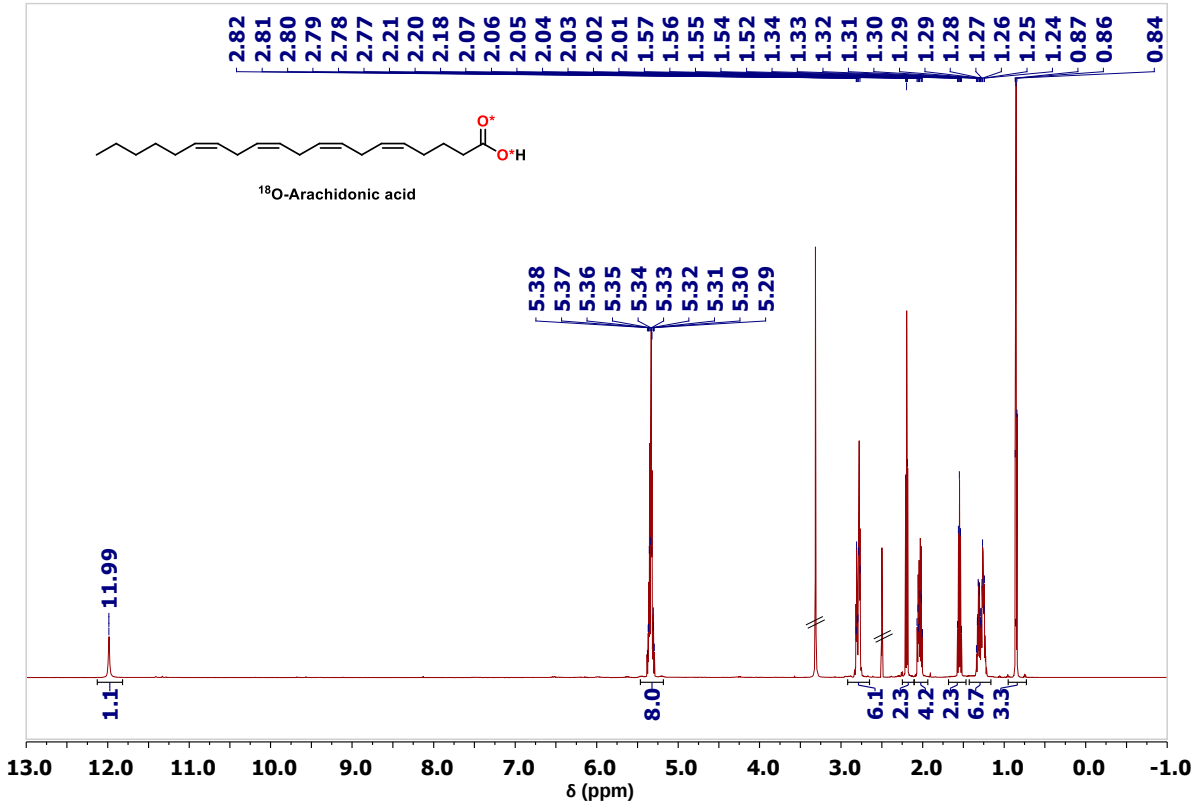

Figure B6-5: ^{13}C NMR spectra of the non-labeled precursor in comparison to the ^{18}O-enriched product (DMSO-d_6, 600 MHz; solvent peaks are crossed out).

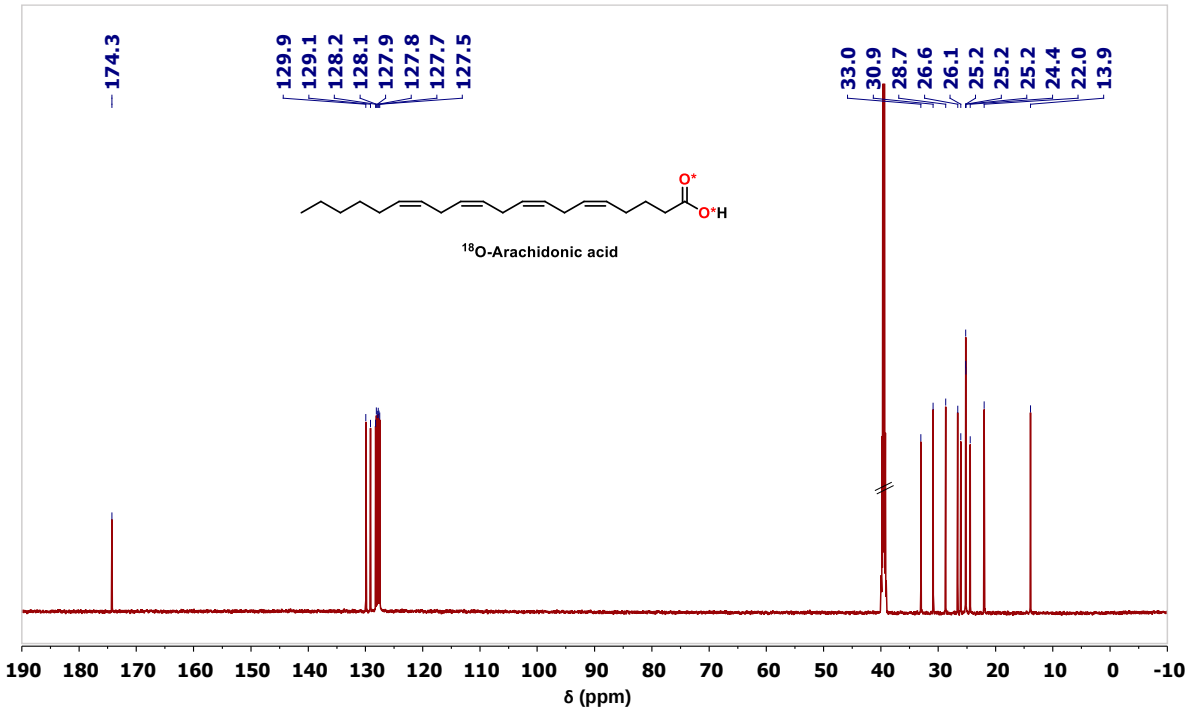

Figure B6-6: ^{13}C NMR study of ^{18}O-isotope effect on the ^{13}C-carboxylic resonance in solution NMR. The non-labeled precursor is compared to the ^{18}O-enriched product, both having been mixed in different ratios, as indicated above each spectrum (DMSO-d_6, 600 MHz).

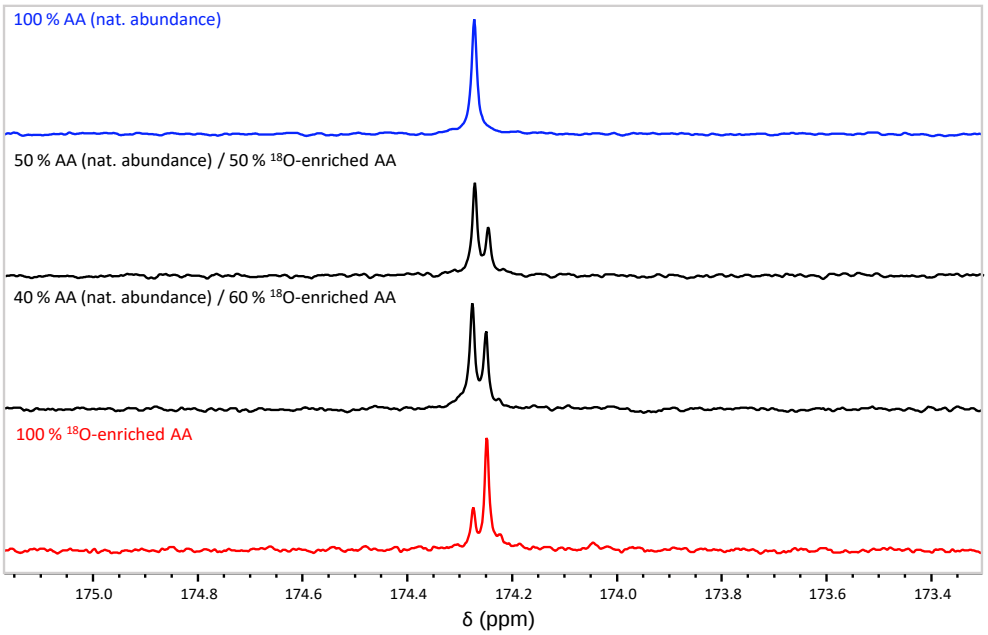

B6-c) Characterization of the ^{17}O-labeled AA

Figure B6-7: MS analyses of the non-labeled precursor in comparison to the ^{17}O-enriched product. Average enrichment per carboxylic oxygen determined by MS: 37 % (n = 1).

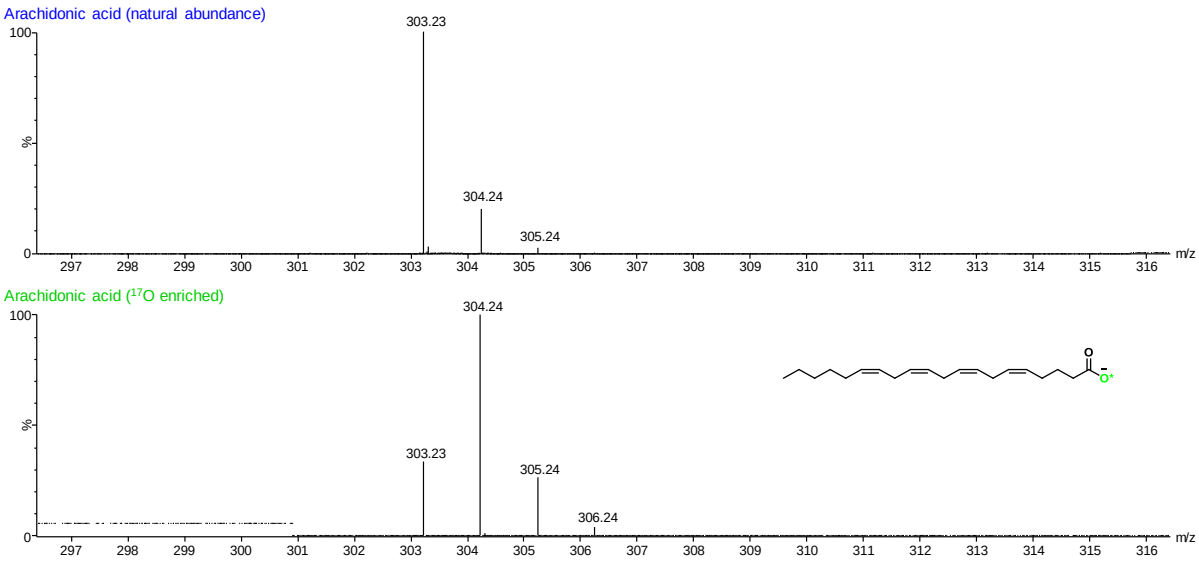

Figure B6-8: LC analyses of the non-labeled precursor in comparison to the ^{17}O-enriched product.

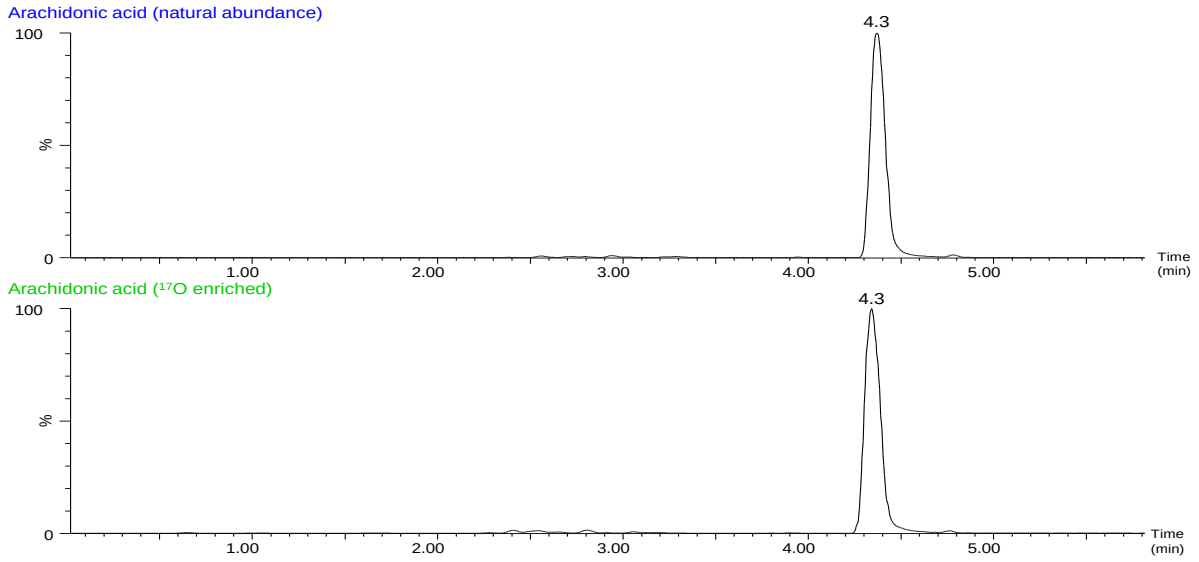

Figure B6-9: ^{1}H NMR spectra of the non-labeled precursor in comparison to the ^{17}O-enriched product (DMSO-d_6, 600 MHz; solvent peaks crossed out).

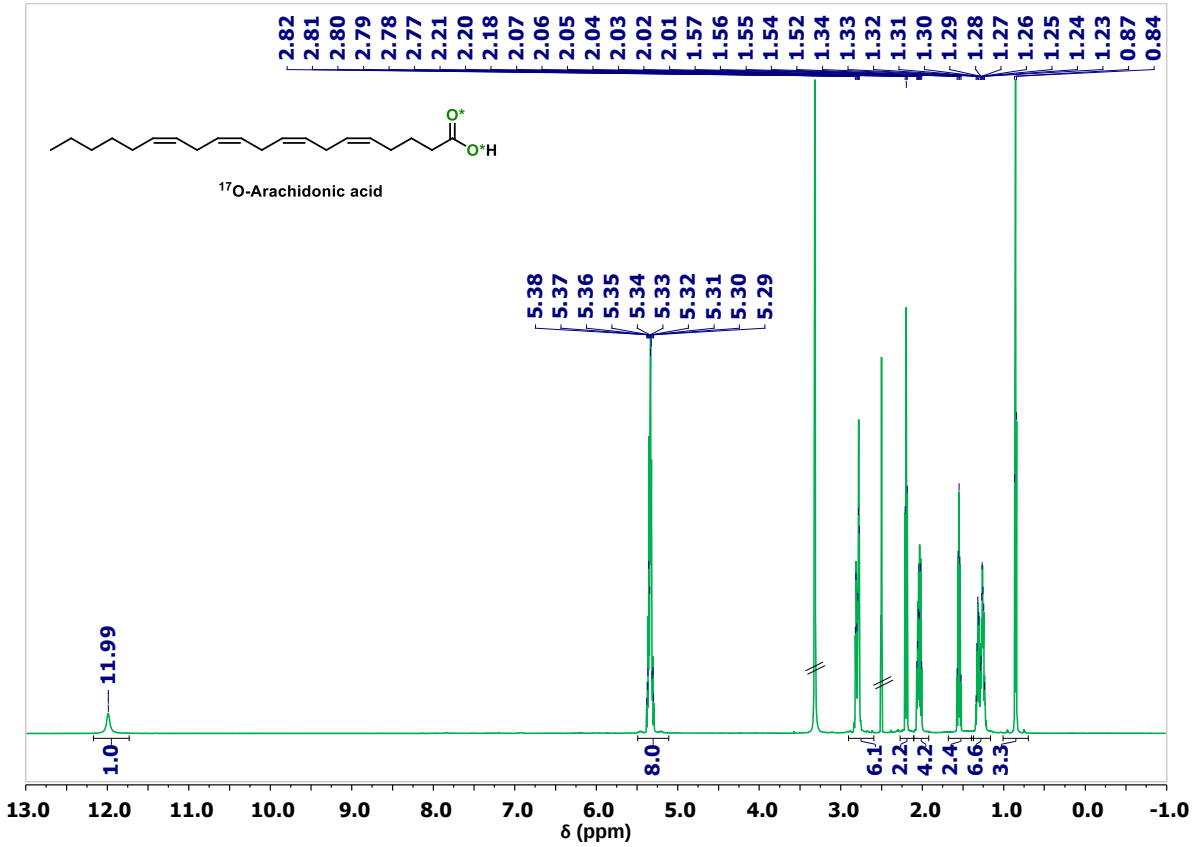

Figure B6-10: ^{13}C NMR spectra of the non-labeled precursor in comparison to the ^{17}O-enriched product (DMSO-d_6, 600 MHz; solvent peaks crossed out).

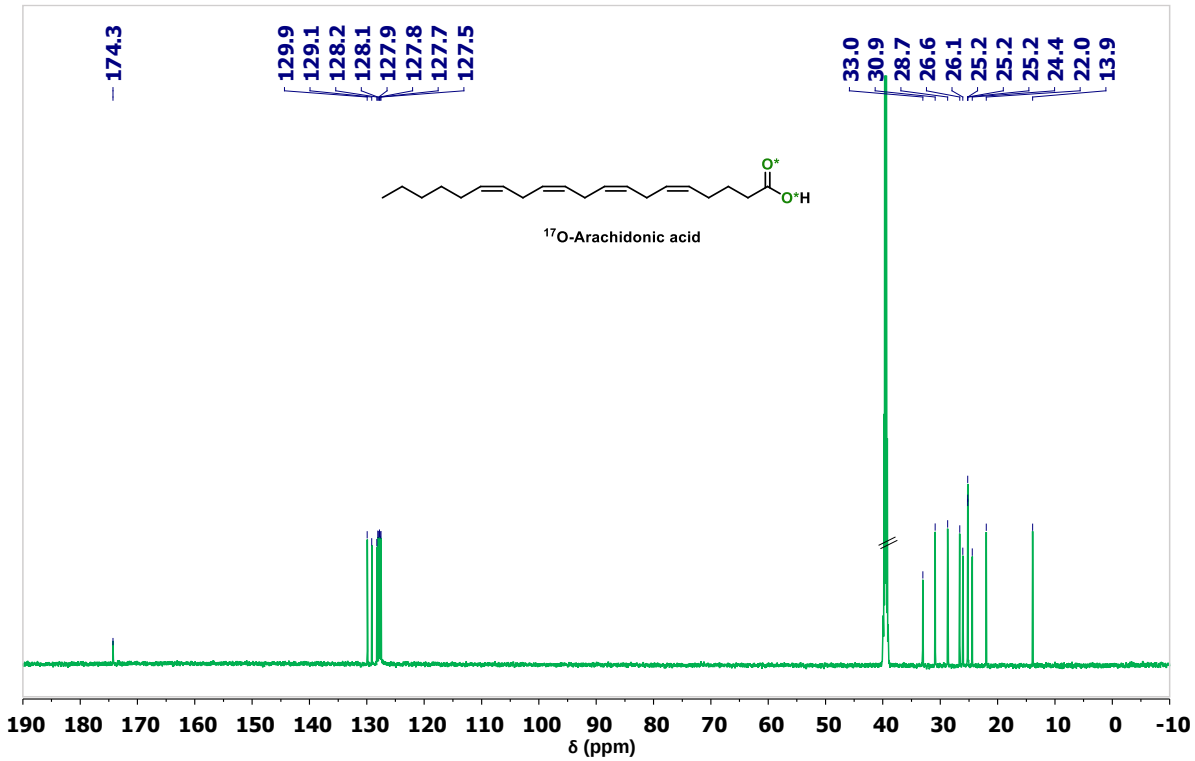

C) SYNTHESES AND CHARACTERIZATIONS OF ^{17}O AND ^{18}O-LABELED COMPOUNDS PREPARED VIA SAPONIFICATION

C1) α-Linolenic acid (ALA, $C_{18}H_{30}O_2$)

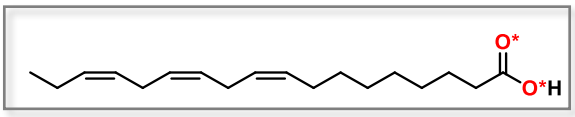

C1-a) Optimized labeling protocol

Ethyl linolenate (56 mg, 0.18 mmol, 1.0 eq), ^{18}O-labeled water (97.1%, 9.5 µL, 0.52 mmol, 3.0 eq) and sodium ethoxide (19 mg, 0.27 mmol, 1.5 eq) were introduced successively into the stainless steel grinding jar (5 mL inner volume) containing two stainless steel balls (7 mm diameter). The jar was closed and subjected to grinding for 30 minutes in the MM400 mixer mill operated at 25 Hz. To help recover the product, non-labeled water (1 mL) was added into the jar, and the content was subjected to grinding for 2 minutes at 25 Hz. Then, the yellow solution (with foam-like texture) was transferred to a beaker (together with sufficient amount of non-labeled water (3-5 mL) used here to rinse the jar). The medium was acidified to pH ~ 1 with an aqueous solution of HCl (6M, 8-9 drops), leading to a cloudy suspension, which was diluted with brine and extracted with ethyl acetate (1x10 mL, 3x6 mL). Combined organic phases were dried over Na_2SO_4, filtered and finally dried under vacuum giving the product as a yellow oil. Average yield (n = 2): 48 ± 1 mg, 96 ± 1 %.

For the ^{17}O-labeling, overall the same reaction/work-up conditions as for ^{18}O-labeling were employed with 90% ^{17}O-enriched water (9.75 µL, 3.0 eq) used at the hydrolysis step. After addition of ^{17}O-labeled water, the mixture was subjected to grinding for 45 min at 25 Hz. Yield (n = 1): 47 mg, 95 %.

Figure C1-1: ATR-IR analysis of the starting material, reaction intermediate, and final products. The dashed line shows that the C=O stretching frequency of $^{18}O/^{17}O$-enriched product is shifted to lower wavenumbers in comparison with non-labeled precursor.

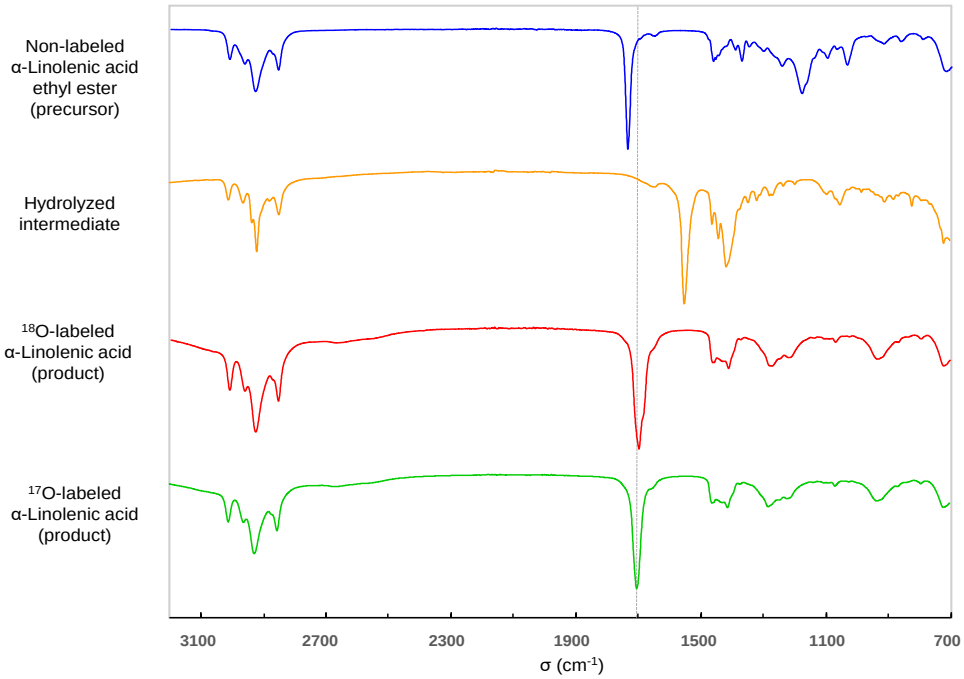

C1-b) Characterization of the ^{18}O-labeled ALA

Figure C1-2: MS analyses of the non-labeled acid in comparison to the ^{18}O-enriched product. Average enrichment per carboxylic oxygen determined by MS: 44.5 ± 1.0 % (n = 2), enrichment yield: ~ 91 %.

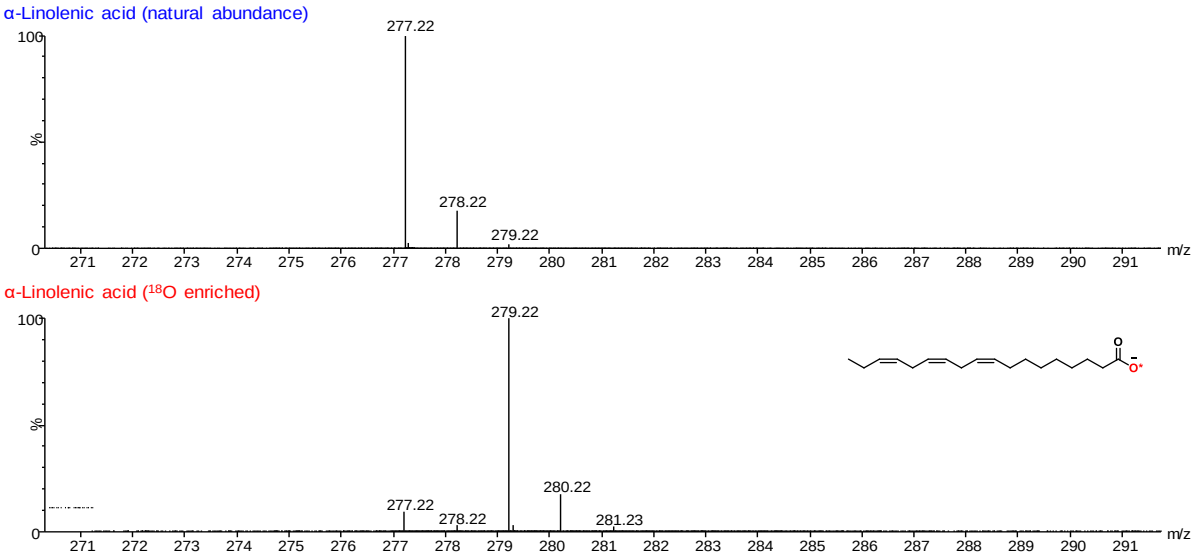

Figure C1-3: LC analyses of the non-labeled precursor in comparison to the ^{18}O-enriched product. Small impurities in the labeled compound are coming from the impurities already present in the precursor.

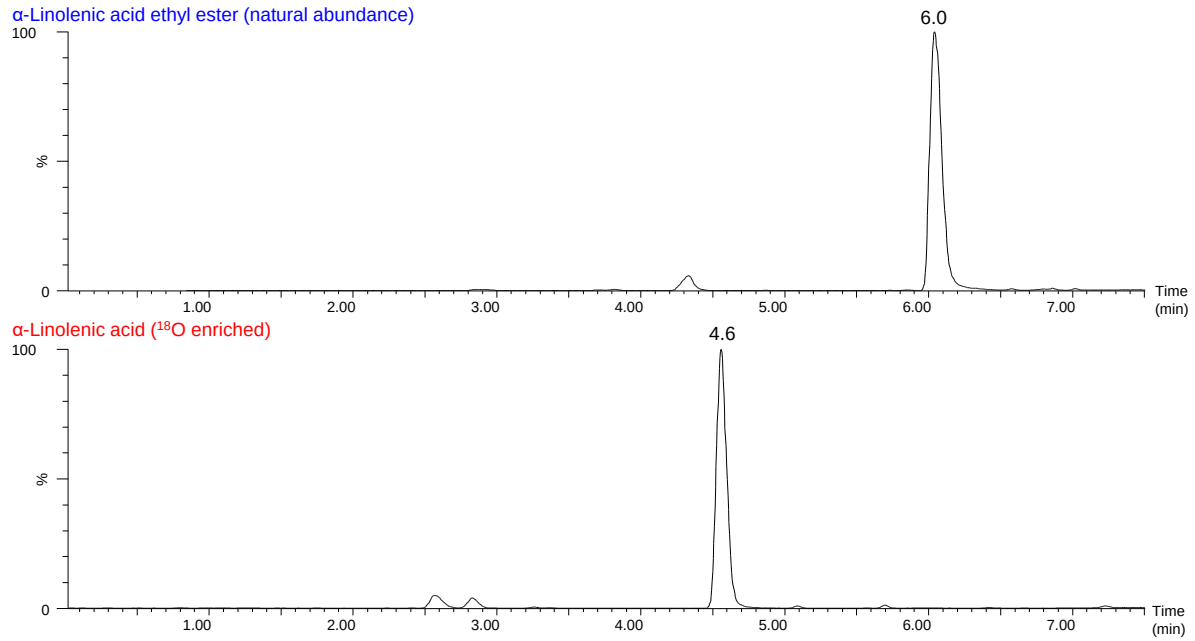

Figure C1-4: ^{1}H NMR spectra of the non-labeled precursor in comparison to the ^{18}O-enriched product (DMSO-d_6, 600 MHz; solvent peaks are crossed out).

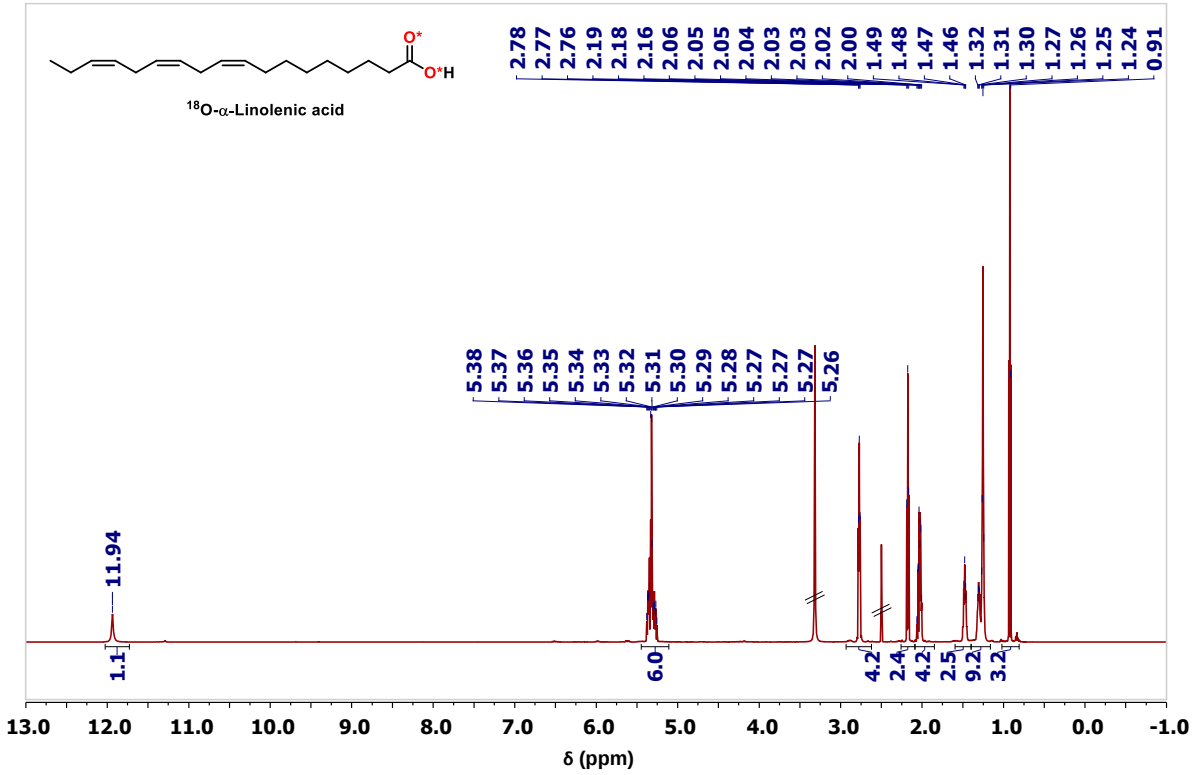

Figure C1-5: ^{13}C NMR spectra of the non-labeled precursor in comparison to the ^{18}O-enriched product (DMSO-d_6, 600 MHz; solvent peaks are crossed out).

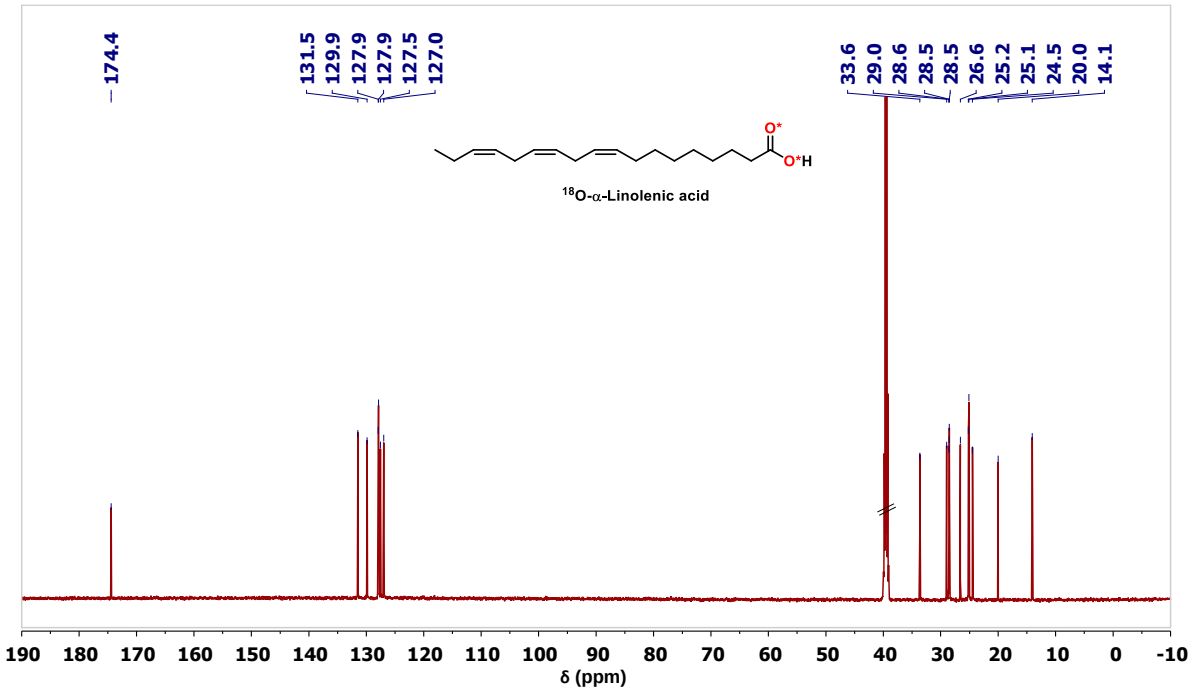

Figure C1-6: ^{13}C NMR **s**tudy of ^{18}O-isotope effect on the ^{13}C-carboxylic resonance in solution NMR. The non-labeled precursor is compared to the ^{18}O-enriched product, both having been mixed in different ratios, as indicated above each spectrum (DMSO-d_6, 600 MHz).

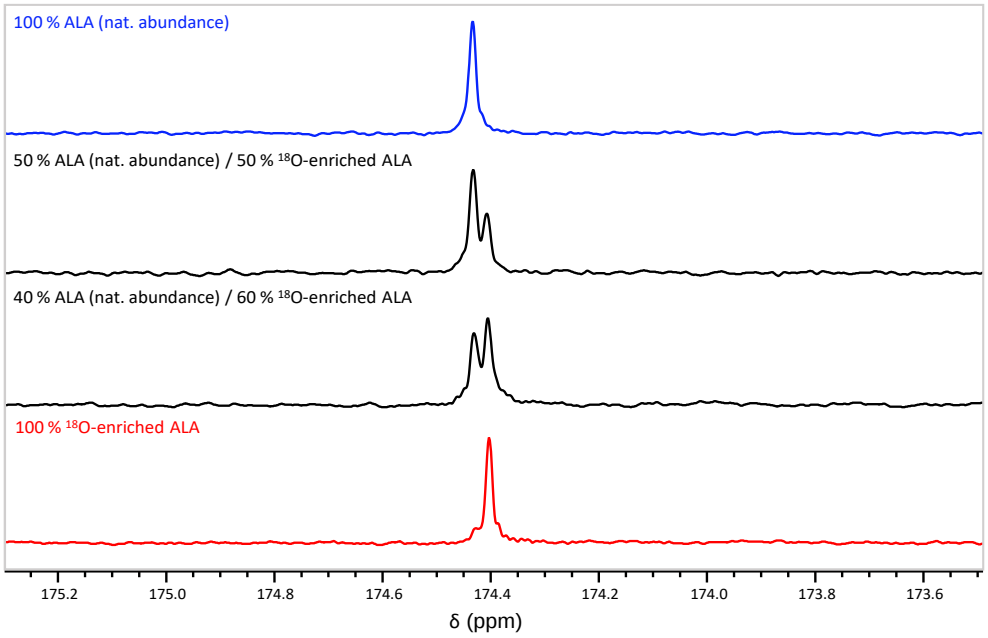

C1-c) Characterization of the ^{17}O-labeled ALA

Figure C1-7: MS analyses of the non-labeled acid in comparison to the ^{17}O-enriched product. Average enrichment per carboxylic oxygen determined by MS: 42 % (n = 1).

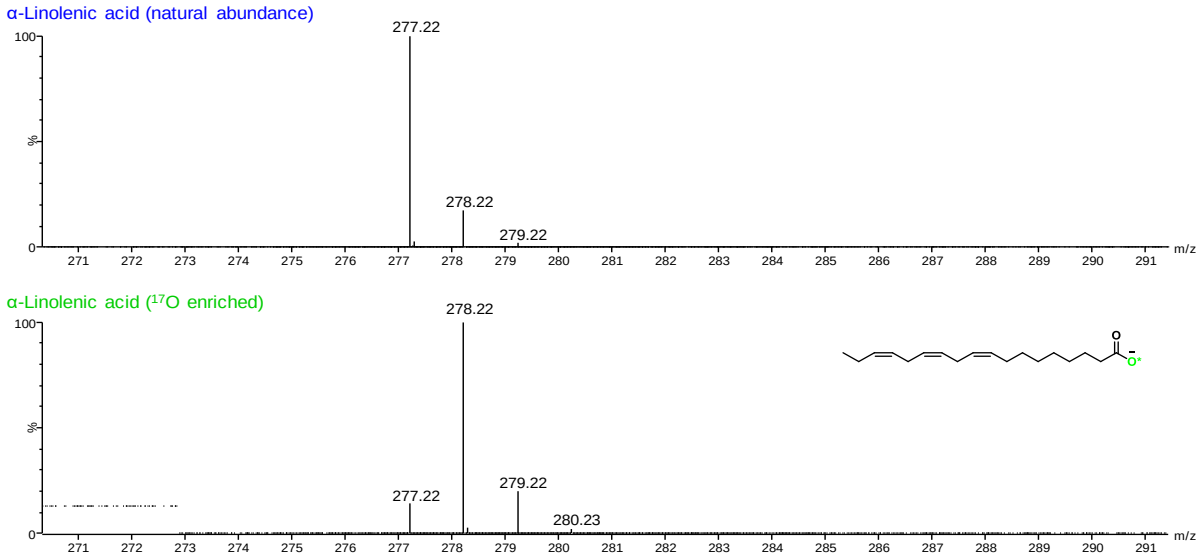

Figure C1-8: LC analyses of the non-labeled precursor in comparison to the ^{17}O-enriched product. Small impurities in the labeled compound are coming from the impurities already present in the precursor.

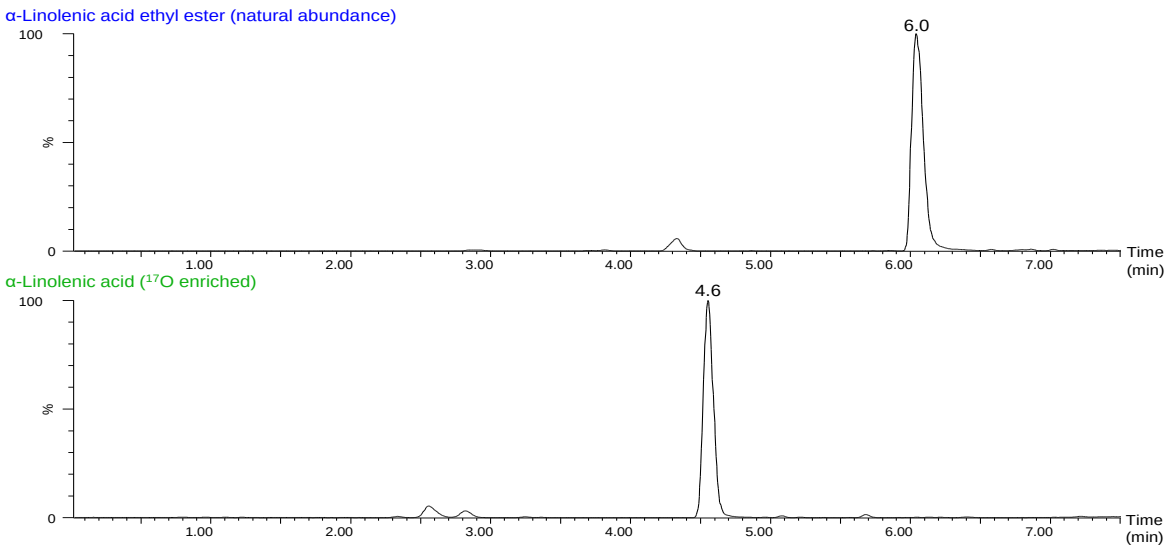

Figure C1-9: ^{1}H NMR spectra of the non-labeled precursor in comparison to the ^{17}O-enriched product (DMSO-d_6, 600 MHz; solvent peaks are crossed out).

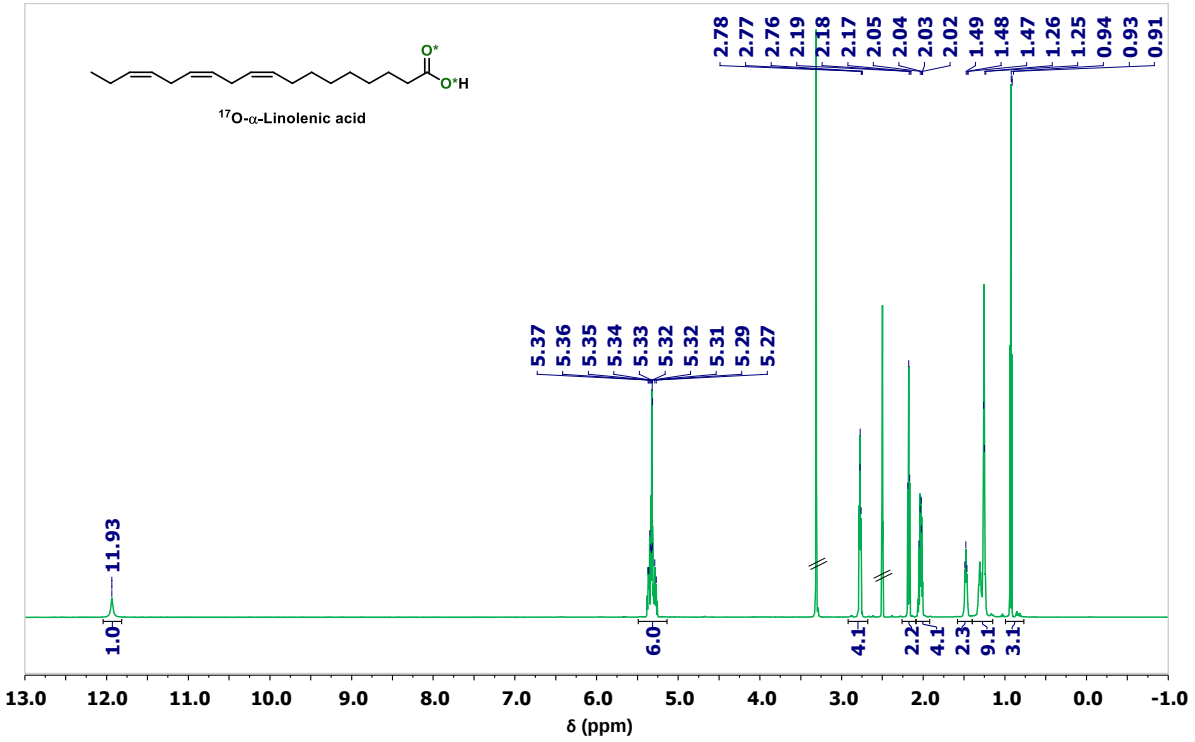

Figure C1-10: ^{13}C NMR spectra of the non-labeled precursor in comparison to the ^{17}O-enriched product (DMSO-d_6, 600 MHz; solvent peaks are crossed out).

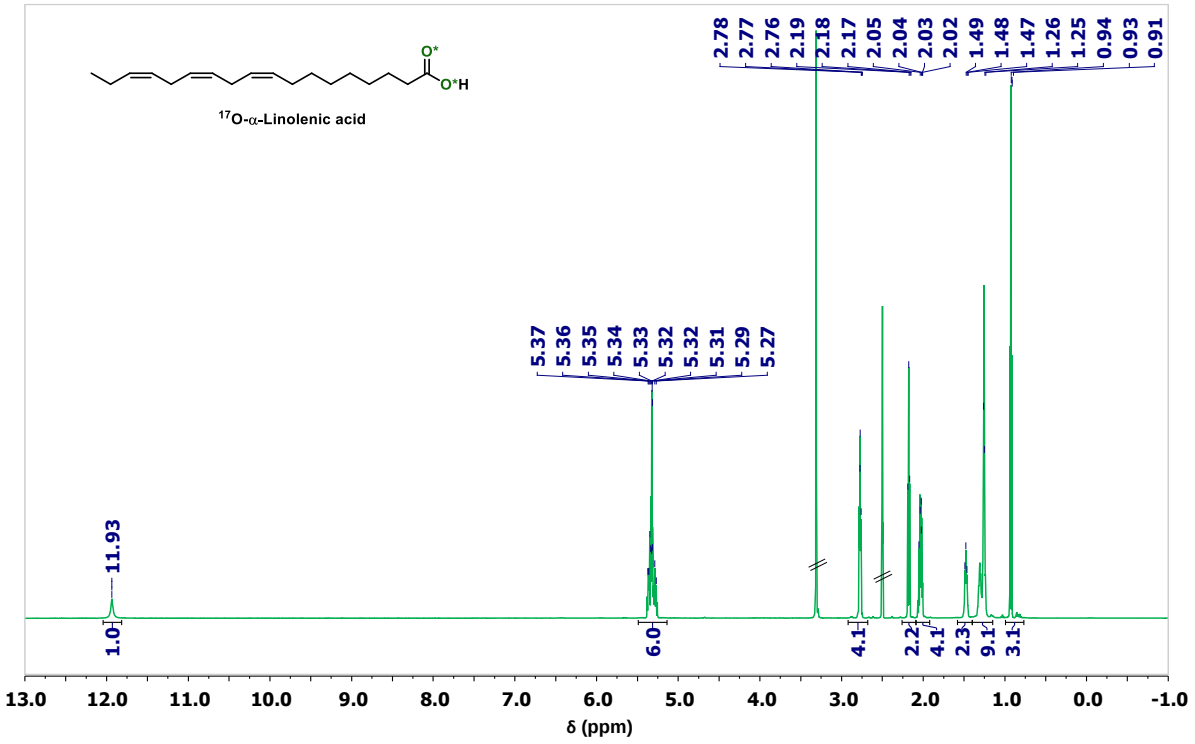

C2) Eicosapentaeonic acid (EPA, $C_{20}H_{30}O_2$)

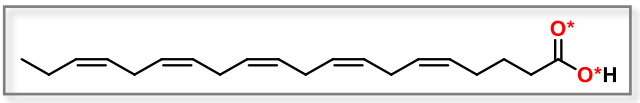

C2-a) Optimized labeling protocol

Ethyl eicosapentaeonate (57 mg, 0.17 mmol, 1.0 eq), ^{18}O-labeled water (97.1%, 9 µL, 0.50 mmol, 3.0 eq) and sodium ethoxide (18 mg, 0.26 mmol, 1.5 eq) were introduced successively into the stainless steel grinding jar (5 mL inner volume) containing two stainless steel balls (7 mm diameter). The jar was closed and subjected to grinding for 30 minutes in the MM400 mixer mill operated at 25 Hz. To help recover the product, non-labeled water (1 mL) was added into the jar, and the content was subjected to grinding for 2 minutes at 25 Hz. Then, the yellow solution (with a foam-like texture) was transferred to a beaker (together with sufficient amount of non-labeled water (4 mL) used here to rinse the jar). The medium was acidified to pH ~ 1 with an aqueous solution of HCl (6M, 9 drops), leading to a cloudy suspension, which was diluted with brine and extracted with ethyl acetate (1x10 mL). Combined organic phases were dried over Na_2SO_4, filtered and finally dried under vacuum giving the product as a yellow oil. Average yield (n = 2): 48 ± 1 mg, 94 ± 1 %.

For the ^{17}O-labeling, exactly the same reaction/work-up conditions as for ^{18}O-labeling were employed with 90% ^{17}O-enriched water (9.25 µL, 3.0 eq) used at the hydrolysis step. Yield (n = 1): 51 mg, 99 %.

Figure C2-1: ATR-IR analysis of the starting material, reaction intermediate, and final products. The dashed line shows that the C=O stretching frequency of ^{18}O/^{17}O-enriched product is shifted to lower wavenumbers in comparison with non-labeled precursor.

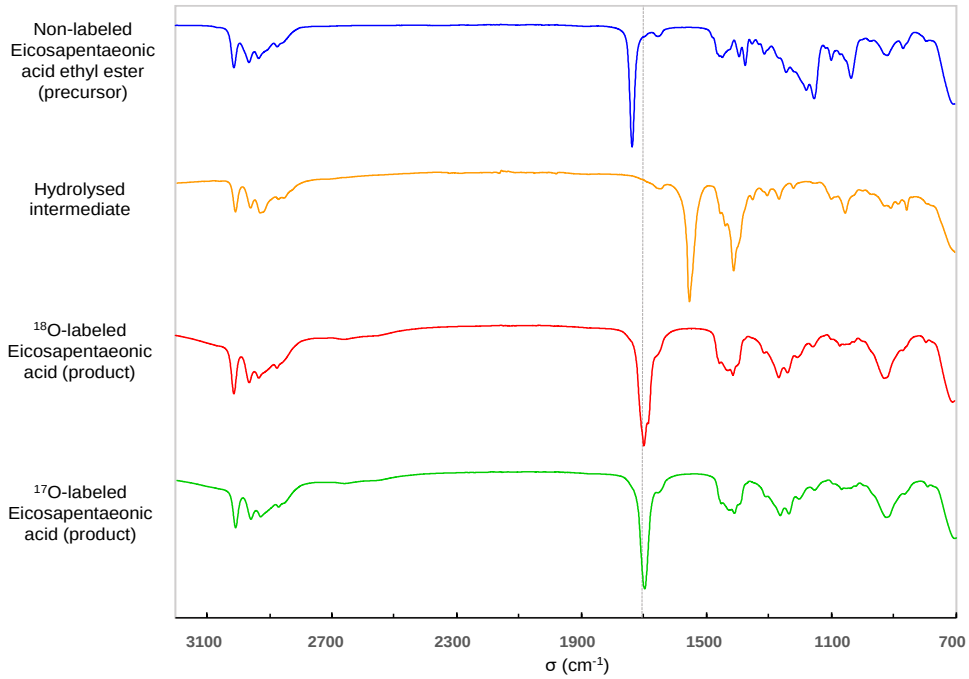

C2-b) Characterization of the ^{18}O-labeled EPA

Figure C2-2: MS analyses of the non-labeled acid in comparison to the ^{18}O-enriched product. Average enrichment per carboxylic oxygen determined by MS: 44.7 ± 1.2 % (n = 2), enrichment yield: ~ 92 %.

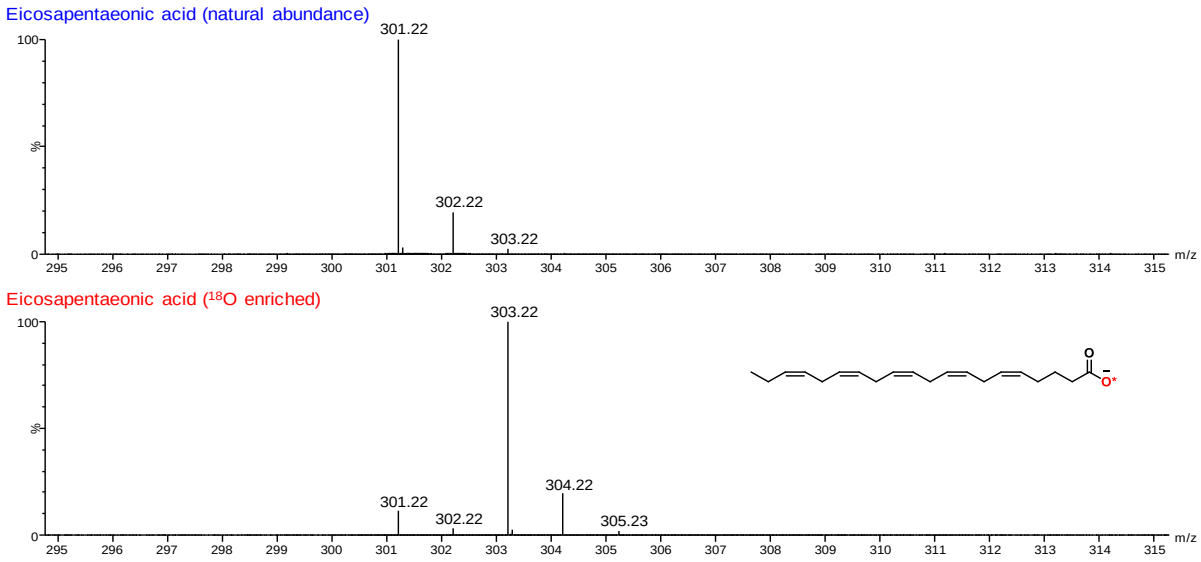

Figure C2-3: LC analyses of the non-labeled precursor in comparison to the ^{18}O-enriched product. Small impurities in the labeled compound are coming from the impurities already present in the precursor.

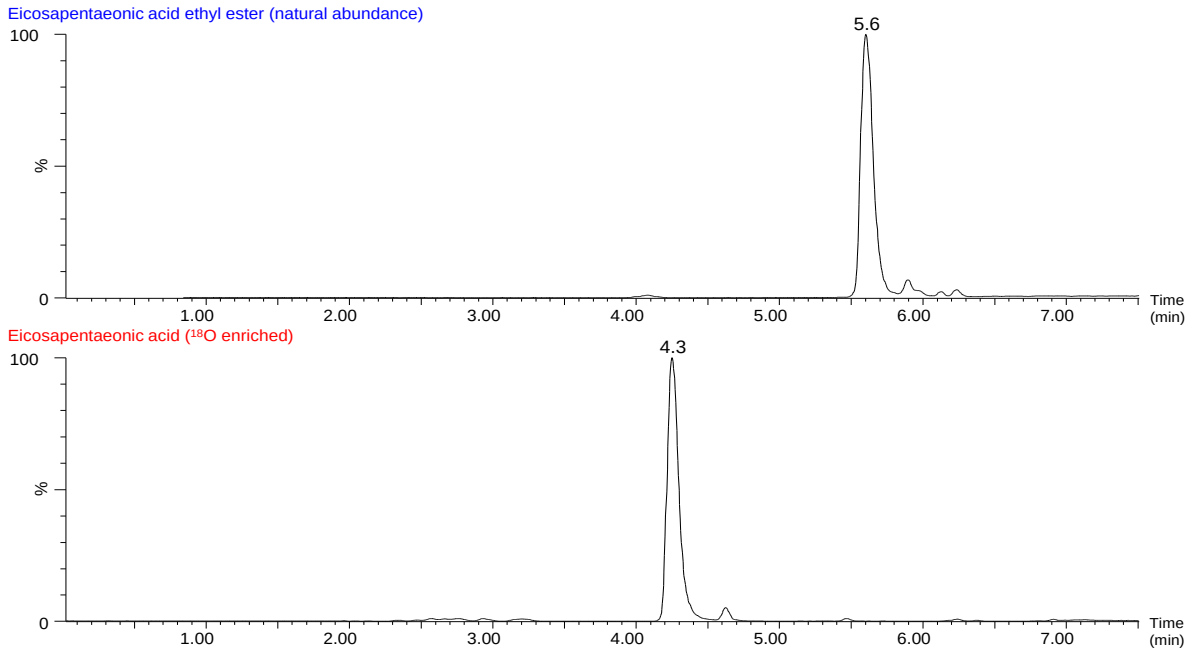

Figure C2-4: ^{1}H NMR spectra of the non-labeled precursor in comparison to the ^{18}O-enriched product (DMSO-d_6, 600 MHz; solvent peaks are crossed out).

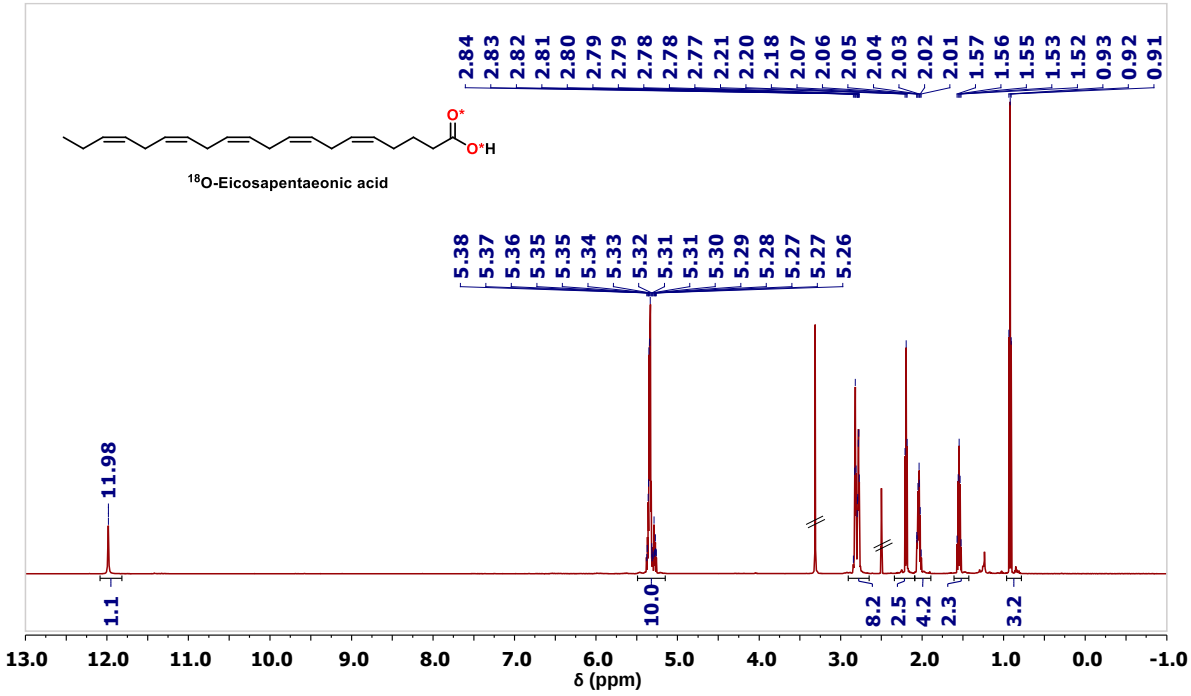

Figure C2-5: ^{13}C NMR spectra of the non-labeled precursor in comparison to the ^{18}O-enriched product (DMSO-d_6, 600 MHz; residual peaks are crossed out).

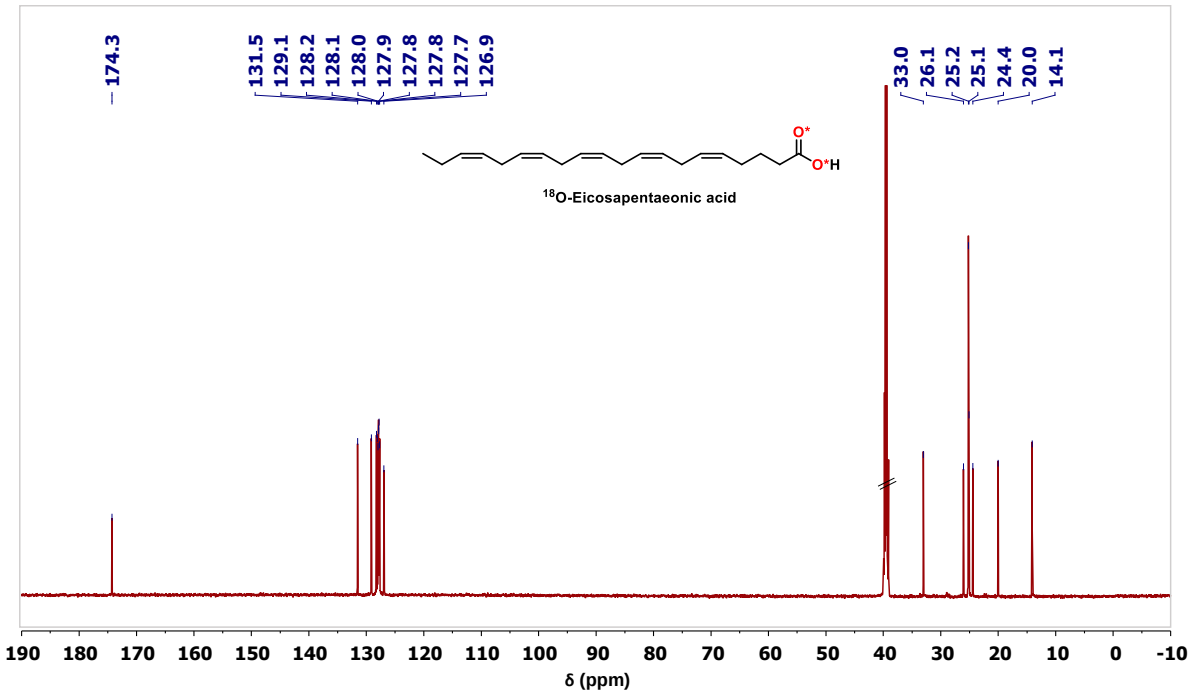

Figure C2-6: ^{13}C NMR **s**tudy of ^{18}O-isotope effect on the ^{13}C-carboxylic resonance in solution NMR. The non-labeled precursor is compared to the ^{18}O-enriched product, both having been mixed in different ratios, as indicated above each spectrum (DMSO-d_6, 600 MHz).

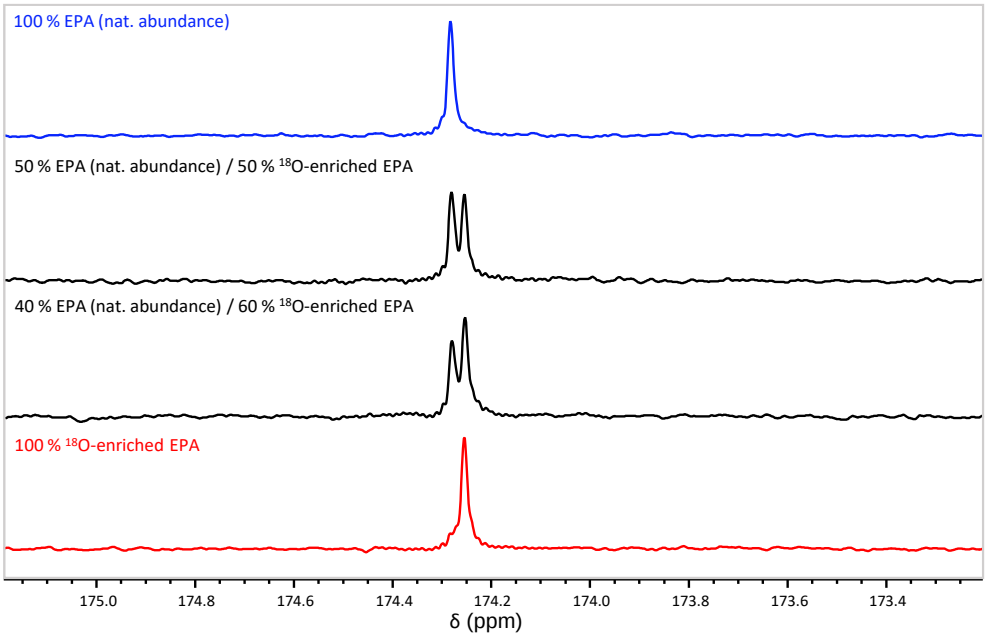

C2-c) Characterization of the ^{17}O-labeled EPA

Figure C2-7: MS analyses of the non-labeled acid in comparison to the ^{17}O-enriched product. Average enrichment per carboxylic oxygen determined by MS: 42 % (n = 1).

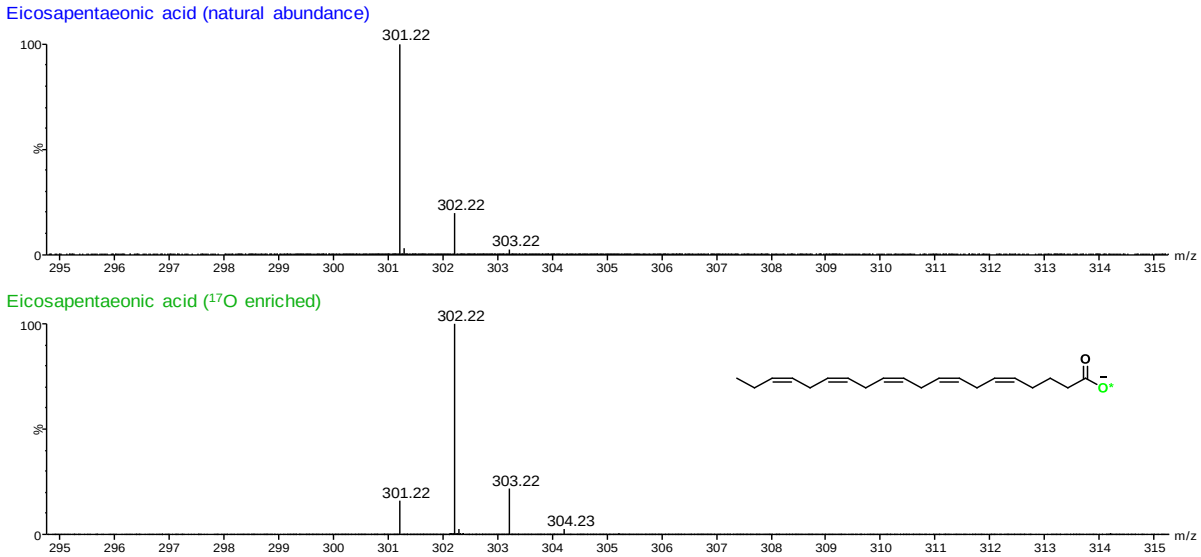

Figure C2-8: LC analyses of the non-labeled precursor in comparison to the ^{17}O-enriched product. Small impurities in the labeled compound are coming from the impurities already present in the precursor.

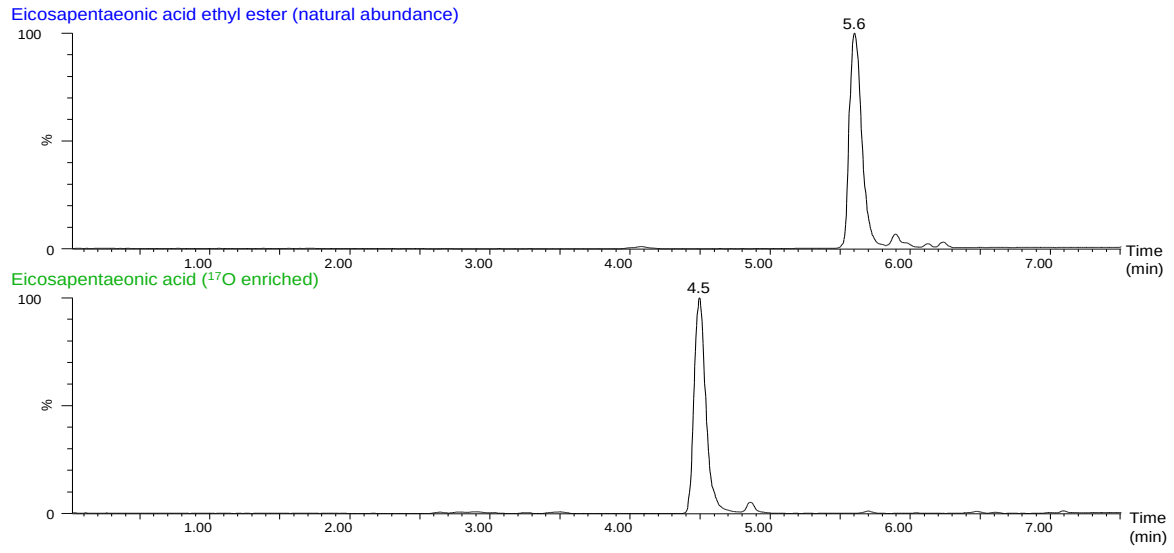

Figure C2-9: ^{1}H NMR spectra of the non-labeled precursor in comparison to the ^{17}O-enriched product (DMSO-d_6, 600 MHz; solvent peaks are crossed out).

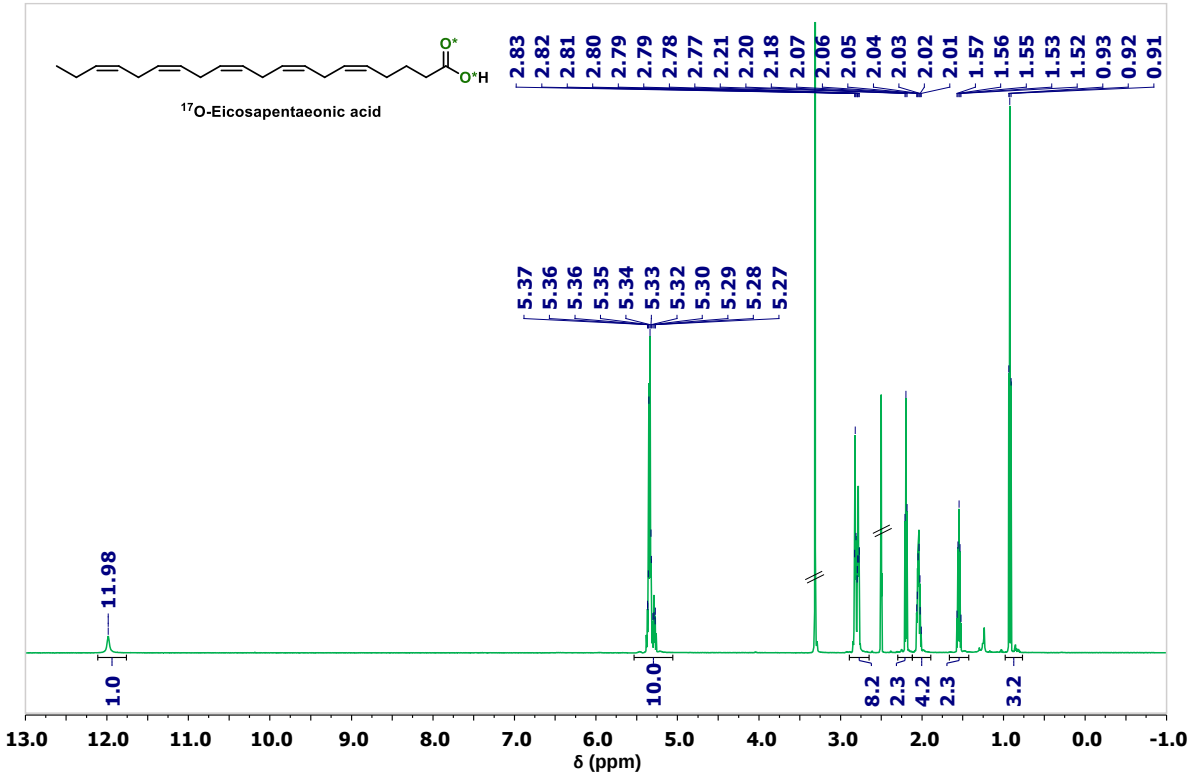

Figure C2-10: ^{13}C NMR spectra of the non-labeled precursor in comparison to the ^{17}O-enriched product (DMSO-d_6, 600 MHz; solvent peaks are crossed out).

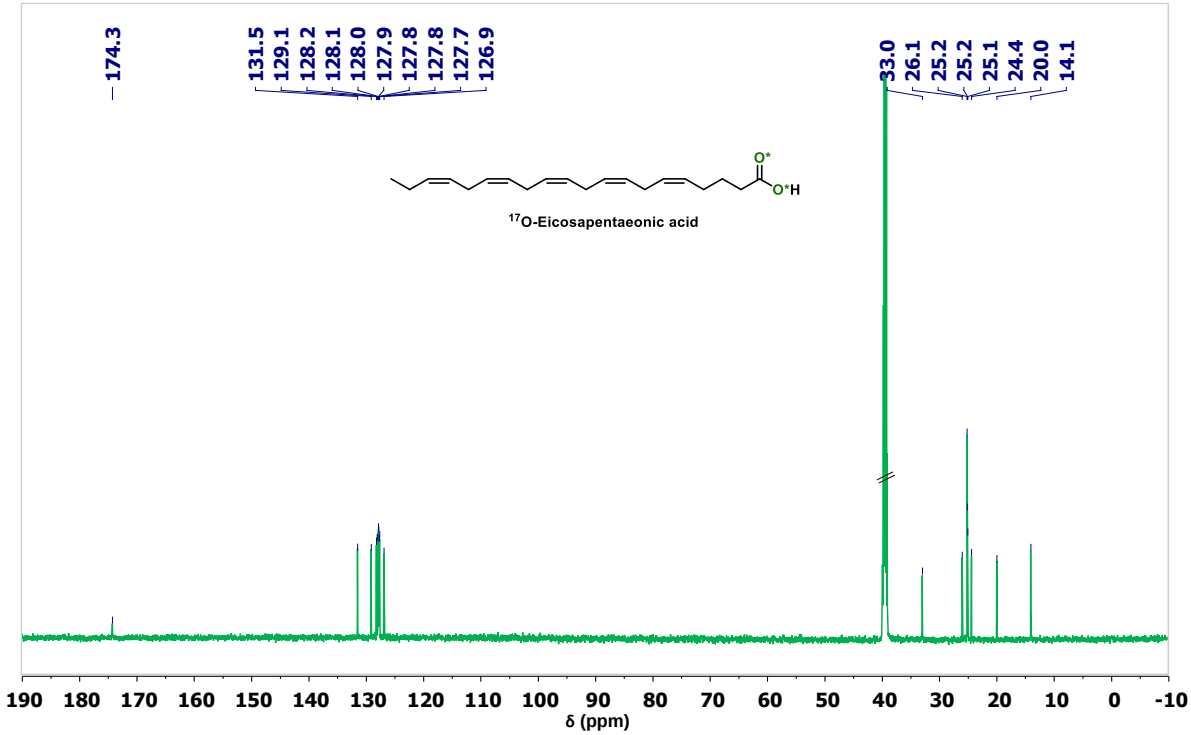

C3) Docosahexaeonic (DHA, $C_{22}H_{32}O_2$)

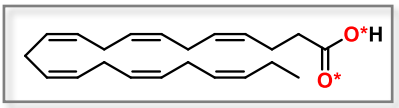

C3-a) Optimized labeling protocol

Ethyl docosahexaeonate (58 mg, 0.16 mmol, 1.0 eq), ^{18}O-labeled water (97.1%, 8.75 µL, 0.49 mmol, 3.0 eq) and sodium ethoxide (17 mg, 0.25 mmol, 1.5 eq) were introduced successively into the stainless steel grinding jar (5 mL inner volume) containing two stainless steel balls (7 mm diameter). The jar was closed and subjected to grinding for 30 minutes in the MM400 mixer mill operated at 25 Hz. To help recover the product, non-labeled water (1 mL) was added into the jar, and the content was subjected to grinding for 2 minutes at 25 Hz. Then, the yellow solution (with a foam-like aspect) was transferred to a beaker (together with sufficient amount of non-labeled water (4 mL) used here to rinse the jar). The medium was acidified to pH ~ 1 with an aqueous solution of HCl (6M, 9 drops), and the cloudy suspension was diluted with brine and extracted with ethyl acetate (1x10 mL). Combined organic phases were dried over Na_2SO_4, filtered and finally dried under vacuum giving the product as a yellow oil. Average yield (n = 2): 50 ± 1 mg, 95 ± 1 %.

For the ^{17}O-labeling, exactly the same reaction/work-up conditions as for ^{18}O-labeling were employed with 90% ^{17}O-enriched water (8.75 µL, 3.0 eq) used at the hydrolysis step. Yield (n = 1): 48 mg, 90 %.

Figure C3-1: ATR-IR analysis of the starting material, reaction intermediate, and final products. The dashed line shows that the C=O stretching frequency of ^{18}O/^{17}O-enriched product is shifted to lower wavenumbers in comparison with non-labeled precursor.

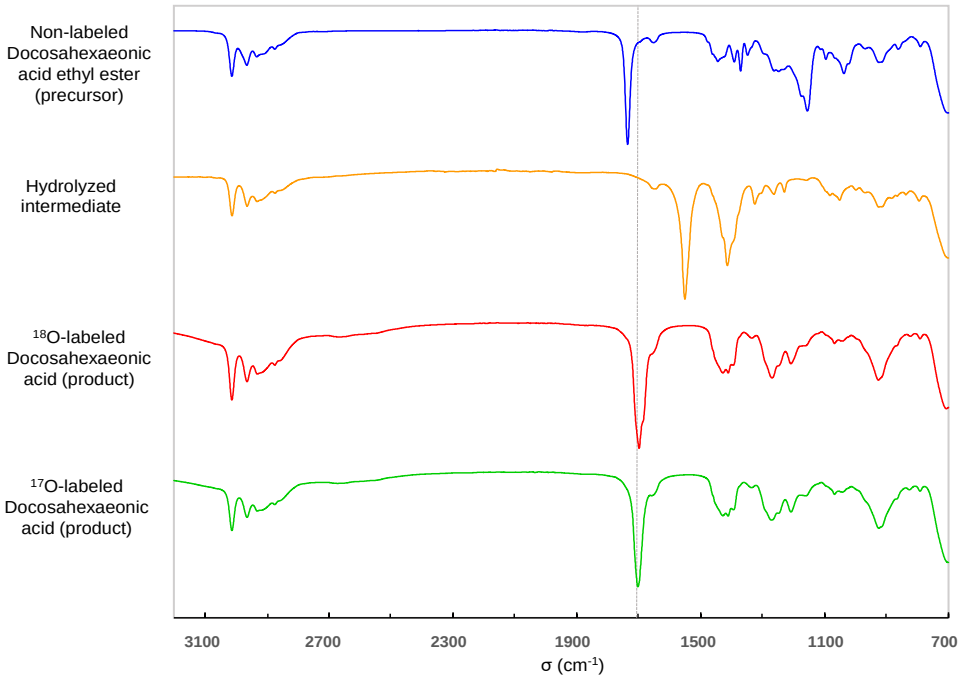

C3-b) Characterization of the ^{18}O-labeled DHA

Figure C3-2: MS analyses of the non-labeled acid in comparison to the ^{18}O-enriched product. Average enrichment per carboxylic oxygen determined by MS: 44.5 ± 0.9 % (n = 2), enrichment yield: ~ 91 %.

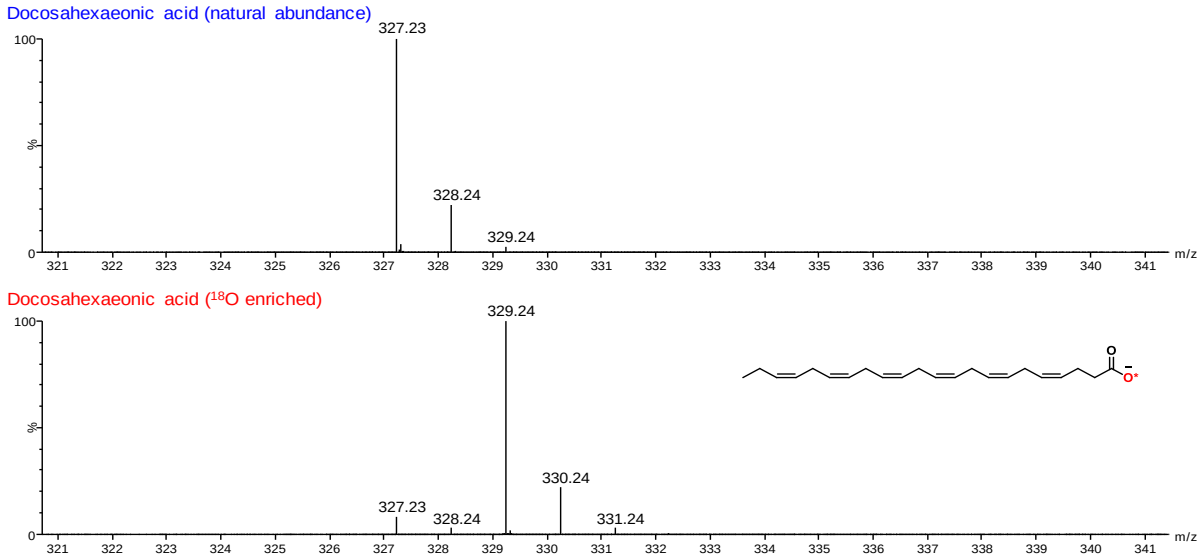

Figure C3-3: LC analyses of the non-labeled precursor in comparison to the ^{18}O-enriched product. Small impurities in the labeled compound are coming from the impurities already present in the precursor.

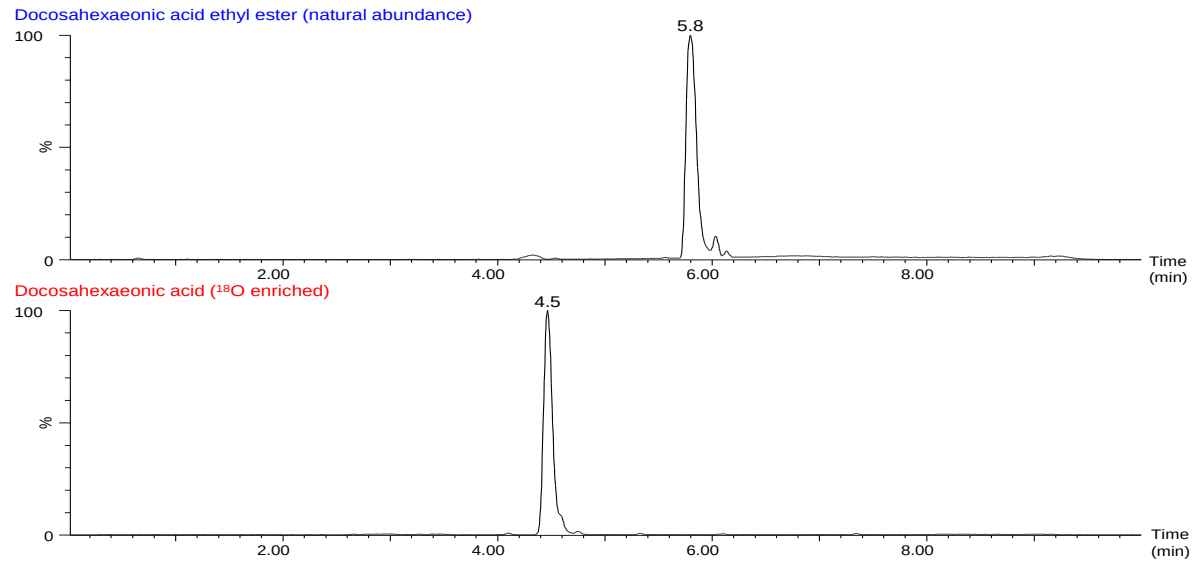

Figure C3-4: ^{1}H NMR spectra of the non-labeled precursor in comparison to the ^{18}O-enriched product (DMSO-d_6, 600 MHz; solvent peaks are crossed out).

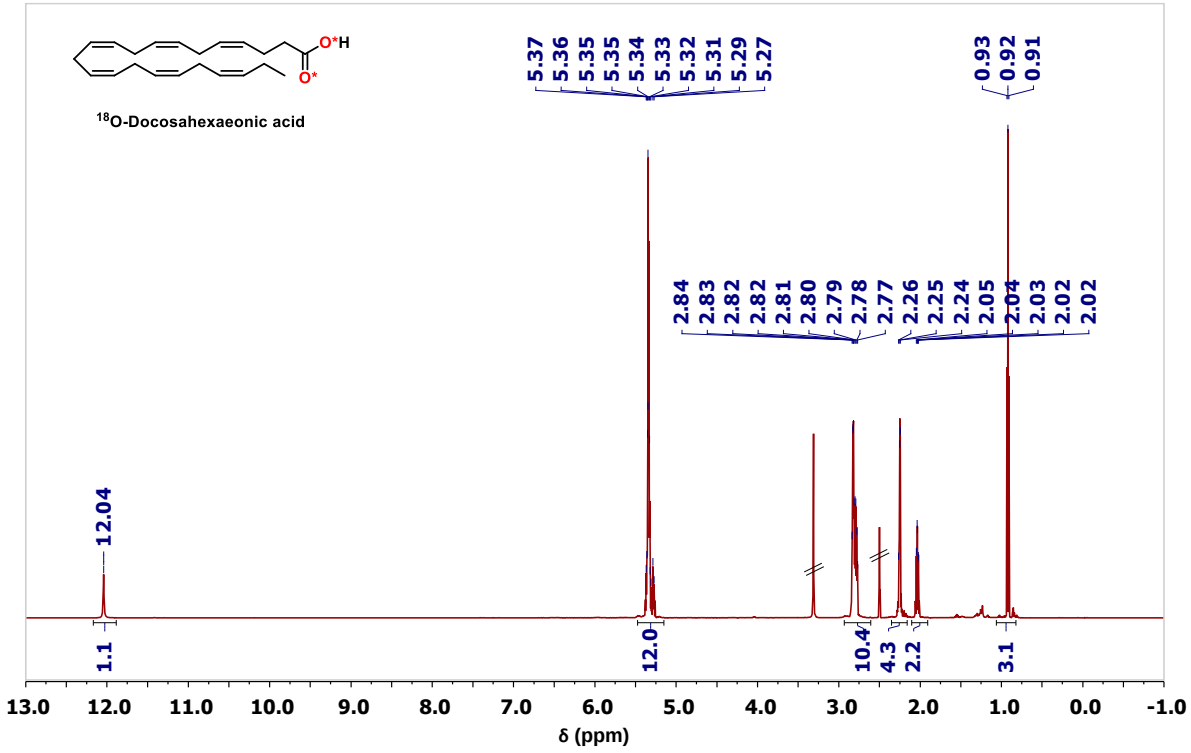

Figure C3-5: ^{13}C NMR spectra of the non-labeled precursor in comparison to the ^{18}O-enriched product (DMSO-d_6, 600 MHz; solvent peaks are crossed out).

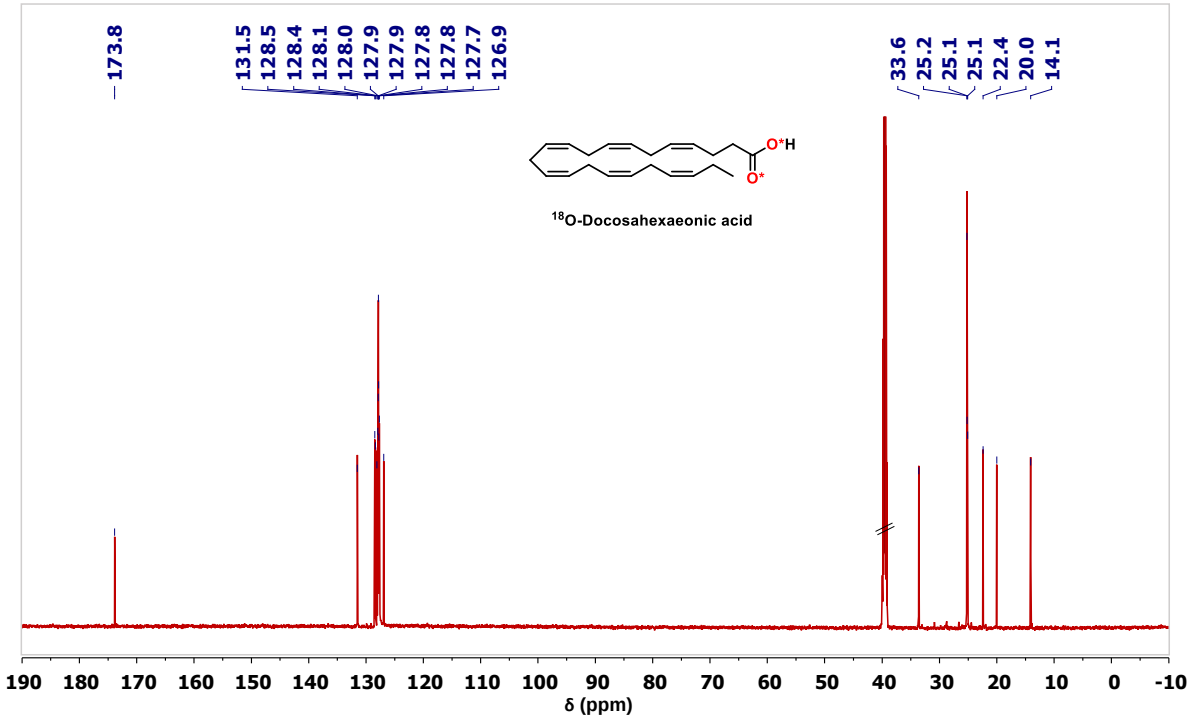

Figure C3-6: ^{13}C NMR **s**tudy of ^{18}O-isotope effect on the ^{13}C-carboxylic resonance in solution NMR. The non-labeled precursor is compared to the ^{18}O-enriched product, both having been mixed in different ratios, as indicated above each spectrum (DMSO-d_6, 600 MHz).

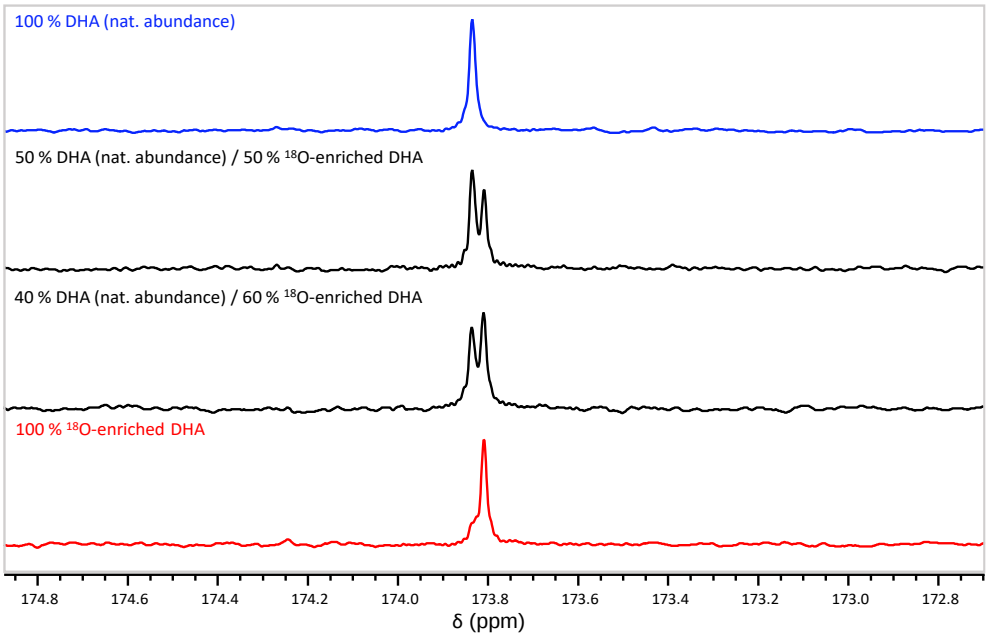

C3-c) Characterization of the ^{17}O-labeled DHA

Figure C3-7: MS analyses of the non-labeled acid in comparison to the ^{17}O-enriched product. Average enrichment per carboxylic oxygen determined by MS: 41 % (n = 1).

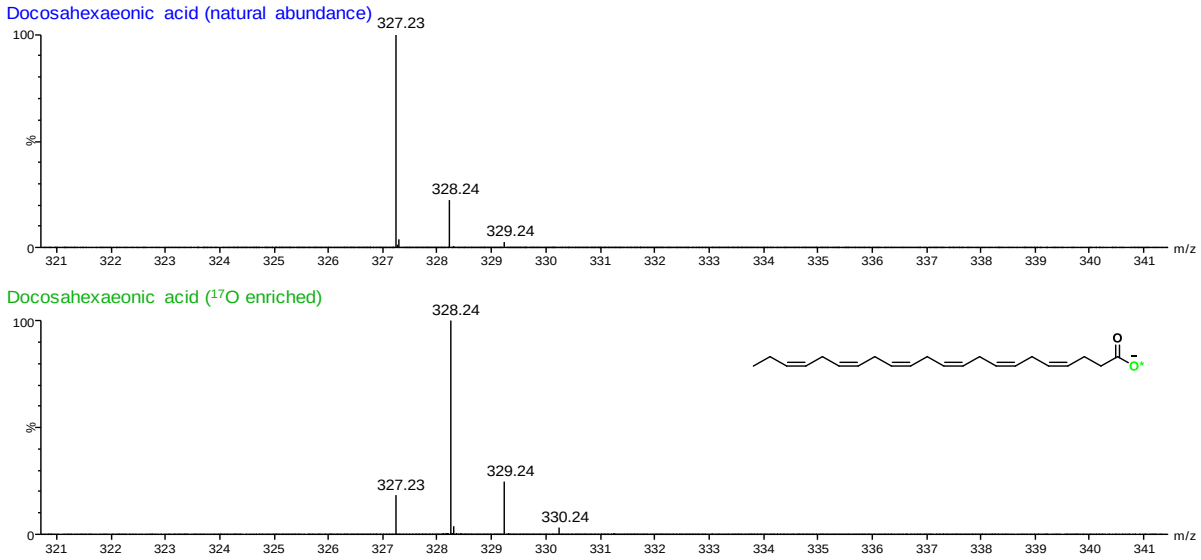

Figure C3-8: LC analyses of the non-labeled precursor in comparison to the ^{17}O-enriched product. Small impurities in the labeled compound are coming from the impurities already present in the precursor.

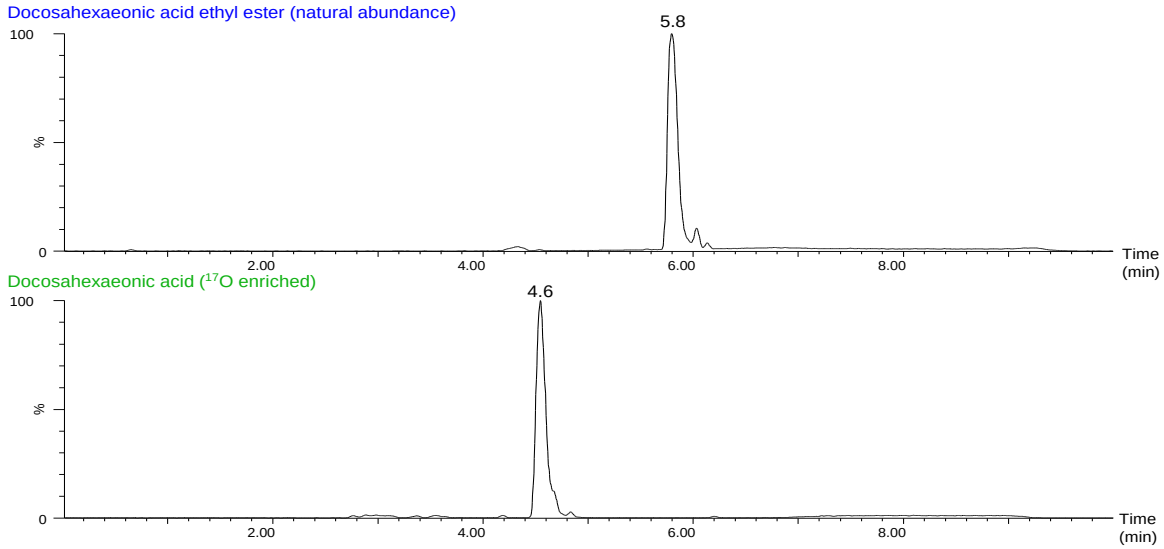

Figure C3-9: ^{1}H NMR spectra of the non-labeled precursor in comparison to the ^{17}O-enriched product (DMSO-d_6, 600 MHz; solvent peaks are crossed out).

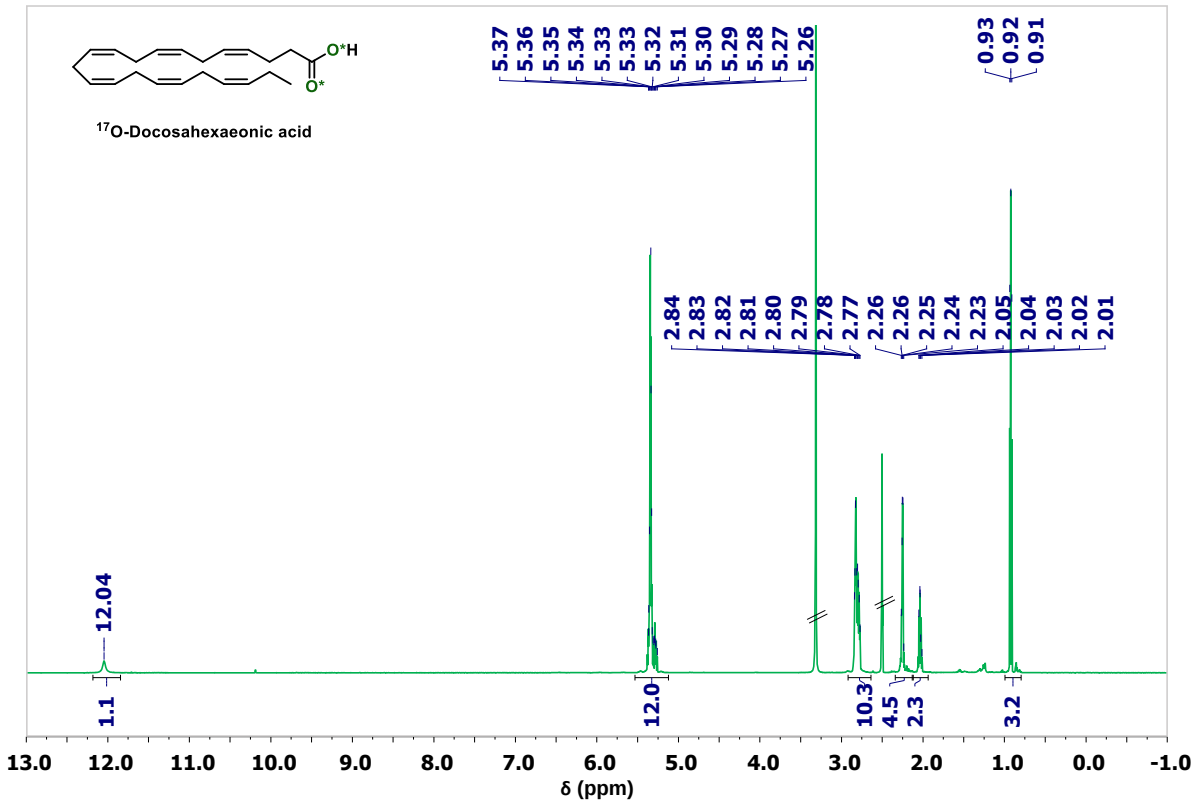

Figure C3-10: ^{13}C NMR spectra of the non-labeled precursor in comparison to the ^{17}O-enriched product (DMSO-d_6, 600 MHz; solvent peaks are crossed out).

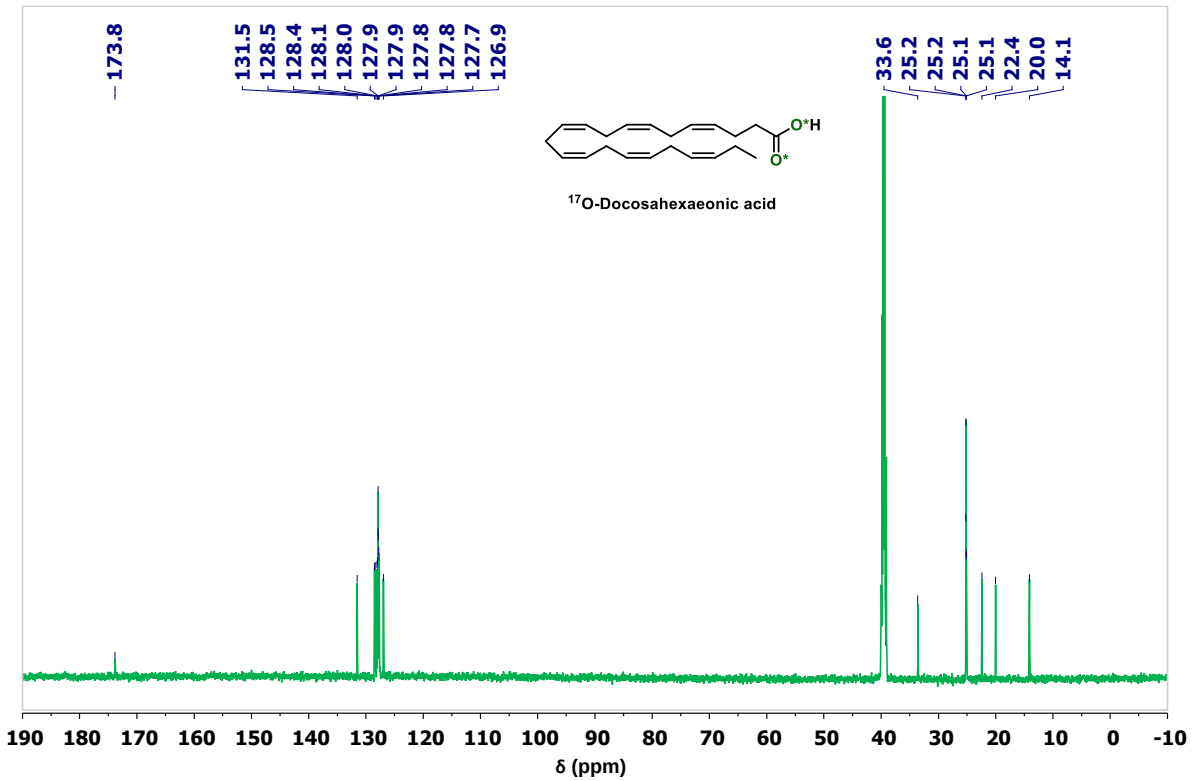

D) ADDITIONAL TABLES AND FIGURES

Table D-1: Summary of $^{17}O/^{18}O$-labeled fatty acids enriched using mechanochemical protocols (CDI-activation or saponification) Average synthetic yields and enrichment level with including error bars were calculated from repeated experiments (where nx = average of x repetitions). Synthetic protocols and characterizations of SA were published elsewhere.[3]

Entry	Product	Enrichment procedure	Isolated yield [%]	^{18}O-Enrich. level [%]	^{17}O-Enrich. level [%]
Saturated fatty acids					
1	Lauric acid (LauA, C12)	CDI-activation	82 ± 10 (n4)	46.9 ± 0.5 (n3)	44 (n1)
2	Myristic acid (MA, C14)	CDI-activation	80 ± 6 (n4)	46.4 ± 0.8 (n3)	44 (n1)
3	Palmitic acid (PA, C16)	CDI-activation	88 ± 2 (n4)	46.9 ± 0.2 (n3)	43 (n1)
4	Stearic acid (SA, C18)	CDI-activation	84 ± 2 (n4)	44.1 ± 1.1 (n3)	42 (n1)
Unsaturated fatty acids					
5	Linoleic acid (LA, C18:2)	CDI-activation	90 ± 2 (n3)	41.3 ± 0.4 (n2)	40 (n1)
6	α-Linolenic acid (ALA, C18:3)	CDI-activation	88 ± 5 (n3)	42.5 ± 0.3 (n2)	40 (n1)
7	α-Linolenic acid (ALA, C18:3)	Saponification	96 ± 1 (n3)	44.5 ± 1.0 (n2)	42 (n1)
8	Arachidonic acid (AA, C20:4)	CDI-activation	89 ± 2 (n4)	38.8 ± 1.5 (n3)	37 (n1)
9	Eisocapentaeonic acid (EPA, C20:5)	Saponification	96 ± 3 (n3)	44.7 ± 1.2 (n2)	42 (n1)
10	Docosahexaeonic acid (DHA, C22:6)	Saponification	93 ± 3 (n3)	44.5 ± 0.9 (n2)	41 (n1)

Table D-2: Measured enrichment levels of $^{17}O/^{18}O$-labeled FAs (n = 1) after 1 year of storage in parafilmed vials in a freezer (average enrichment per carboxylic oxygen, as determined by MS). ^{rt}Samples stored in parafilmed vials at room temperature. 40% ^{17}O-enriched water was used here for PA labeling.

	Enrichment level [%]	
Fatty acid	t_0	t_0 + 1 year
Saturated fatty acids		
Lauric acid-^{18}O	47.4	47.6^{rt}
Lauric acid-^{17}O	44	45
Myristic acid-^{18}O	47.2	46.9
Myristic acid-^{17}O	44	45
Palmitic acid-^{18}O	47.2	47.3^{rt}
Palmitic acid-^{17}O	19.6	19.9^{rt}
Unsaturated fatty acids		
Linoleic acid-^{18}O	41.6	41.4
Linoleic acid-^{17}O	40	41
α-Linolenic acid-^{18}O	42.2	42.2
α-Linolenic acid-^{17}O	40	41
Arachidonic acid-^{18}O	38.0	38.0
Arachidonic acid-^{17}O	37	39
Eicosapentaeonic acid-^{18}O	43.9	43.6
Eicosapentaeonic acid-^{17}O	42	42
Docosahexaeonic acid-^{18}O	45.1	45.1
Docosahexaeonic acid-^{17}O	41	42

^{rt}Samples were stored in parafilmed vials at room temperature.

Table D-3: Melting points of non-labeled saturated FAs and their activated intermediates mixtures, and reaction conditions used for activation and hydrolysis steps.

Substrate	Chemical formula	M.p. [°C]	CDI activation		M.p. (activ. interm.) [°C]	Hydrolysis		
			Time [min]	Frequency [Hz]		H_2O eq.	Time [min]	Frequency [Hz]
Saturated fatty acids		*(n=2)*			*(n =3)*			
LauA	$C_{12}H_{24}O_2$	43.4-46.3	30	25	58.4-62.3	3	60	30
MA	$C_{14}H_{28}O_2$	54.2-56.0	30	25	66.3-70.9	3	150	30
PA	$C_{16}H_{32}O_2$	62.4-64.4	30	25	73.5-78.1	3	180	30
SA	$C_{18}H_{36}O_2$	67.3-71.0	30	25	77.0-82.0	3	180*	30

** hydrolysis complete only using additive K_2CO_3 (1 eq.)*

Table D-4: Study of evolution of enrichment before work-up (i.e. right after hydrolysis by $H_2{}^{18}O$), and after work-up (i.e. recovery, acidification, extraction and drying steps). Average ^{18}O-enrichment levels including error bars were calculated from repeated experiments (where n=x is average of x repetitions).

Fatty acid	^{18}O-EL [%] before work-up	^{18}O-EL [%] after work-up
Palmitic acid (PA, C16)	46.5 ± 0.4 (n=3)	46.8 ± 0.5 (n=3)
α-Linolenic acid (ALA, C18:3)	42.3 ± 2.2 (n=2)	42.4 ± 0.5 (n=2)

Figure D-1: Photos of reactors showing the typical evolution of the physical state of the reaction mixtures before and after hydrolysis; a) starting from solid FAs (LauA, MA, PA) - white powdery mixture is converted to colorless viscous oil only when the hydrolysis step is complete, b) starting from oily FAs (LA, ALA, AA) - white/yellowish suspension is converted to colorless oil when hydrolysis step is complete.

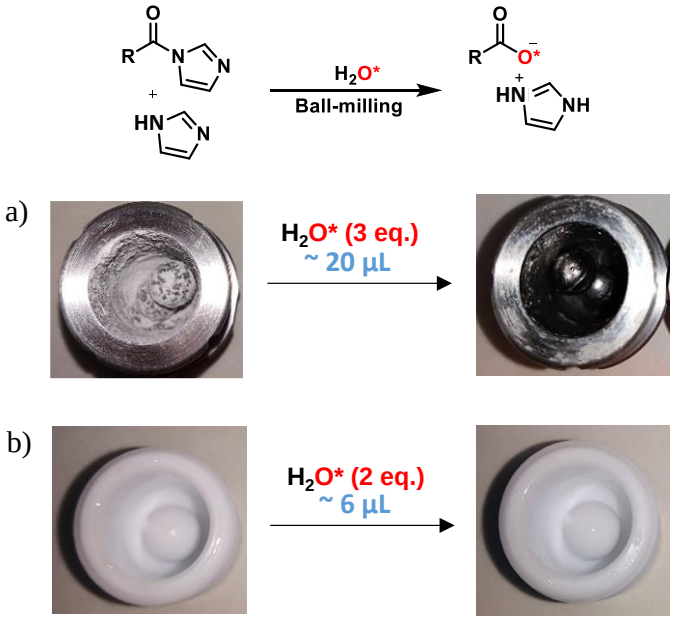

Figure D-2: Photos and a scheme of PTFE (5 mL inner volume, Fritsch) jar used for enrichment of unsaturated FAs (LA, ALA, AA). Due to the beveled edge at the contact planes of both parts of the jar, a gap is created where the two parts of the jar meet. During the milling experiments, small portion of a reaction mixture remains stuck in this gap and cannot interact with the labeled water, thus remains not labeled. During the work-up, this non-labeled portion is included into the final product and very probably causes a decrease of the overall enrichment of isolated products.

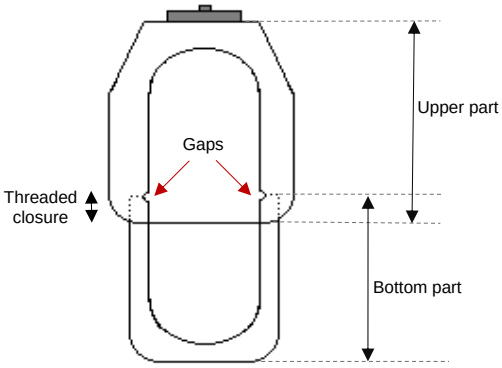

REFERENCES

1. Chen, C.-H.; Gaillard, E.; Mentink-Vigier, F.; Chen, K.; Gan, Z.; Gaveau, P.; Rebière, B.; Berthelot, R.; Florian, P.; Bonhomme, C.; Smith, M. E.; Métro, T.-X.; Alonso, B.; Laurencin, D.; Direct ^{17}O Isotopic Labeling of Oxides Using Mechanochemistry, *Inorg. Chem.* **2020**, *59* (18), 13050–13066.
2. Perras, F. A.; Viger-Gravel, J.; Burgess, K. M.; Bryce, D. L., Signal enhancement in solid-state NMR of quadrupolar nuclei. *Solid State Nucl. Magn. Reson.* **2013,** *51*, 1-15.
3. Špačková, J.; Fabra, C.; Mittelette, S.; Gaillard, E.; Chen, C.-H.; Cazals, G.; Lebrun, A.; Sene, S.; Berthomieu, D.; Chen, K.; Gan, Z.; Gervais, C.; Métro, T.-X.; Laurencin, D., Unveiling the Structure and Reactivity of Fatty-Acid Based (Nano)materials Thanks to Efficient and Scalable ^{17}O and ^{18}O-Isotopic Labeling Schemes. *J. Am. Chem. Soc.* **2020,** *142* (50), 21068-21081.